UNIVERSITA' DEGLI STUDI DI PARMA

Dottorato di ricerca in Scienze Chimiche

Ciclo XXVII (2012-2014)

Evaluation studies of cleaning methods for artworks: from chelating agents on inorganic substrates to *Dry cleaning* treatments on contemporary surfaces.

Coordinatore:
Chiar.mo Prof. Roberto Cammi

Tutor:
Chiar.ma Prof. Antonella Casoli

Dottoranda:
Valentina Emanuela Selva Bonino

2015

"Volli, e volli sempre, e fortissimamente volli"
Vittorio Alfieri, 1783.

Introduction 1

Aim of the research 4

1. Model study of solubility of the constituents of wall painting degradation patinas treated with chelating agents 6

Introduction 6

1.1. Experimental 7

1.1.1. Material and equipments 7

1.1.2. Experimental procedures 8

1.1.2.1. Treatments of calcium salts with chelating agents solutions 8

1.1.2.2. Calculations of the speciation models in solutions 9

1.1.2.3. Characterization of $NaCaC_6H_5O_7$ (NaCaCitr) 10

1.2. Results and discussion 12

1.2.1. Treatments with chelating ligands 12

1.2.1.1. Characterization of solid materials containing the calcium salts 12

1.2.1.2. Determination of calcium in the extracted solutions 16

1.2.2. Thermodynamic models by Hyperquad-simulation and speciation (HYSS) 17

1.2.3. Characterization of sodium-calcium citrate 19

1.3. Conclusions 21

2. *Dry cleaning* methods for conservation treatment of paintings: characterization and application 23

Introduction 23

2.1. Experimental 25

2.1.1. Materials and equipments 25

2.1.1.1. Selection of products and characterization of polymers 25

2.1.1.2. Preparation and characterization of acrylic and oil painted samples 32

2.1.2. Experimental procedures 33

2.1.2.1. Physico-chemical characterization of polymers 33

2.1.2.2. Physico-chemical characterization of acrylic and oil painted samples before and after treatments 34

2.2. Results and discussion 35

2.2.1. Erasers 35

2.2.1.1. Styrene-ethylene-butadiene-styrene copolymer (SEBS) 35

2.2.1.2. Chlorosulphonated polyethylene (CSPE) 40

2.2.1.3. Polyvinyl chloride (PVC) 44

2.2.1.4. Vulcanized oils (Factice) 49

2.2.2. Sponges 53

2.2.2.1. Styrene-butadiene rubber (SBR) 53

2.2.2.2. Natural rubber (NR) 57

2.2.2.3. Styrene-butadiene rubber (SBR)/Natural rubber (NR) 61

2.2.2.4. Nitrile-butadiene rubber (NBR) 68

2.2.2.5. Acrylonitrile-butadiene-styrene rubber (ABS) 72

2.2.2.6. Polyurethane (PU) 75

2.2.2.7. Polyvinyl acetate (PVA) 78

2.2.3. Cloths 82
2.2.3.1. Polyester (PEs)/Polyamide (PA) 82
2.2.3.2. Polyurethane (PU)/Polyamide (PA) 87
2.2.4. Acrylic and oil painted samples 90
2.2.4.1. Physico-chemical characterization 90
2.2.4.2. Evaluation of cleaning tests 94
2.2.4.2.1. Stereomicroscopy 101
2.2.4.2.2. Environmental Scanning Electron Microscopy 132
2.2.4.2.3. Colorimetric and gloss tests 134

2.3. Examples of application of *Dry Cleaning* methods on real works of art 139

2.4. Conclusions 145

3. Conclusions 149

References 152

Acknowledgments 163

Appendices: 164
Appendix I 164
Appendix II 168

Introduction

The conservative project of a work of art is complex and it is the result of a multidisciplinary approach.
Each class of artistic objects, i.e. paintings, wooden sculptures, painted wooden boards, wall paintings, architectural elements, archaeological evidences and so on, has its way to act. Conservation ethics and correct behaviour are general rules among professionals, but there is no univocal better way to act.
Each artistic products preserved and handed down unreproducible values, which are expressed through aesthetic and material instances.
The correct conservation of constitutive materials guarantees longer preservation of these values.
Conservation means scientific knowledge, not only due to practical experience, that appears to be equally important. Each scientific sector (chemistry, physics, geology, engineering, etc.) gives its contribution on specific fields.
Multidisciplinary approach regards all conservation fields at multiple level, from surveying and cataloguing, applicative procedures, to musealization and divulgation.
Among specialized stages of project, i.e. fixing, cleaning, consolidation, lacuna reintegration, pictorial retouching and final protection, this thesis focuses attention on one of these, cleaning treatment.
Cleaning operation is the one of most tricky one, because all dirty and materials removal cannot be replaced. For this reason, it is of paramount importance to operate only on removable layer and not on constituent substrate.
During the last ten years, a novel scientific approach gives a great improvement on so-called *surface cleaning*, suggesting materials and methods less invasive.
Traditional systems are not to be considered unsuitable, but a systematic evaluation of properties and interaction with support, have to be performed[1].
This project presents two studies about, the first one a traditional cleaning treatment on inorganic supports and wall paintings and the latter a new application of dry methods as *surface cleaning* treatment.
In particular, the first one concerns the application of chelating agents solutions on inorganic substrates, in order to remove calcium patinas present as decay products due to interaction between artistic support with environment.

[1] E. Beltrami, M. Berzioli, M. Cagna, A. Casoli, P. Cremonesi, N. Cuaz, V.E. Selva Bonino, "La pulitura dei dipinti murali: studio comparativo di materiali e metodi", Progetto Restauro n.58, Primavera 2011, pp. 1 – 15.

Study about ability of two solutions of chelating agents, in particular ethylenediaminetetraacetic acid trisodium salt dihydrate and tribasic sodium citrate dihydrate, to solubilize calcium salts, i.e. calcium carbonate, calcium sulfate and calcium oxalate, are presented.

The importance of knowing properties of these systems permits to make conscious choices on conservative treatments point of view. In fact, because of lack of knowledge of these materials, restorers employ them only for results obtained (often, "too clean") or do not use them at all, thus excluding a useful and extremely effective method.

Knowing properties and mode of action, it is possible to operate with a less strong chelating agents solutions, or regulate pH, or choosing correct chemical species, i.e. EDTA bisodic, EDTA trisodic or EDTA tetrasodic, for example, or reducing the time of contact, or, finally, controlling deep penetration of solutions with supporting material, as thickeners and gels[2].

In addition, in the case of tribasic sodium citrate dihydrate, the formation of a novel sodium calcium double citrate salt has been detected and salt characterized. This fact can be very important from practical point of view, in particular in the choice of better treating method of substrates in presence of calcium sulfate.

Dry cleaning methods can be considered, on the contrary, a proper *surface cleaning* treatment.

In fact, the absence of solvent or aqueous solutions, guarantees no penetration of themselves into deep constituent layers, but mechanical action due to superficial rubbing can caused unwanted alterations.

Therefore, also innovative techniques have to be tested in order to evaluate their applicability.

The second project presented, concerns verifications of inner physico-chemical characteristics of these materials, in particular important aspects as polymers identification, evaluation of residues, i.e. chemical or crumbs and mechanical interactions with surfaces.

Products selected are not state precisely for conservation treatments, on the contrary, they are borrowed by different commercial and industrial fields. This is the reason why systematics characterization is required. Not all useful materials can be suitable for restoration practice.

[2] E. Beltrami, M. Berzioli, M. Cagna, A. Casoli, V.E. Selva Bonino, *"La pulitura dei dipinti murali: uno studio di applicabilità di sistemi tradizionali e sistemi addensati con gel acquosi di poliacrilato"*, QUADERNO N.10/CESMAR7, il Prato ed., Padova 2012.

The presence of additives, which can be left on surfaces after applications, may be dangerous for matters conservation, because of their chemical reactivity.
In addition to application on painted samples created ad hoc for testing, is important to apply method on real works of art and on different types of support.
Testing samples were modern acrylic and oil paints, while examples of application presented were on ancient XV century wooden shelves, graphite drawing wall painting and external acrylic paint.
Considerations about effectiveness of erasers, sponges and cloths, must be mediated with the type of dirt and soiling, level of cleaning wanted, object decay and comparison with results of traditional solvent or aqueous systems.
In restoration practice, there is no procedure completely safety or without risks for material conservation; any actions cause irreversible changes in composition, so compromise choice is necessary.
What is more important is to ensure the possibility of re-operate in time, without further damaging artistic support.

Aim of the research

The aim of research is the study of two cleaning treatments: the first one belonging to so-called "traditional" systems and the second one to "innovative" ones.
Fundamental criterion for either researches is physico-chemical evaluation of materials, analytical characterization and the test of methods to determine their applicability.
For this reason, thesis is divided into different parts: a general introduction of works, which provides a framework for issues treated, followed by two main chapters, in which researches are presented and ends with general conclusion about projects.
Each chapters is divided into a detailed introduction, an experimental section and conclusions.

In particular, in Chapter 1 study about "*Model study of solubility of the constituents of wall painting degradation patinas treated with chelating agents"* is presented.
An introduction contextualizes study into conservation survey, giving basis for experimental procedure.
Selection of calcium compounds and chelating agents and reaction conditions are explained in experimental sections, in which main results are presented too.
Solubility differences among chelating agents and three calcium salts, i.e. calcium carbonate, calcium sulfate dihydrate and calcium oxalate monohydrate, are highlighted; an important section is dedicated to analytical characterization of a unexpected novel sodium calcium double citrate salt, formed from reaction between calcium sulfate dihydrate and trisodium citrate dihydrate.
Complete and specific conclusions are reported, in which general summary of the results obtained is presented.

The biggest part of work, the main PhD project, is presented in Chapter 2 and concerns "*Dry cleaning methods for conservation treatment of paintings: characterization and application*".
Once again, after an exhaustive introduction, experimental section is presented divided into two principal parts: the first one concerns analytical characterization of dry methods, i.e. erasers, sponges and cloths, by several physico-chemical techniques. In this section, products were classified according to polymer composition.

The second part, instead, gives examples of application of treatments on two different substrates, i.e. acrylic and oil painted samples created ad hoc.
Effectiveness and interactions with supports are discussed and compared with each other.
In addition, examples of application of some dry methods on real works of art are presented, followed by results discussion. This section is particularly important to underline that testing materials on real contests help researchers to evaluate applicability parameters and focus problems or aspects, which have to be better analysed.
Conclusions provide a summary of considerations about this method and give insights on the choice of a material over another. Moreover, five and six points diagrams were carried out to easily visualize characteristics, described by selected parameters.

Considering all aspects described briefly in this section, the general aim of both works is to verify if methodologies are less invasive and more respectful with the intrinsic characteristics and behaviour of supports, when subjected to these type of cleaning treatments.
Such results may help restorers to identify better methods or materials in relation to specifics and constitutive matter condition.

1. Model study of solubility of the constituents of wall painting degradation patinas treated with chelating agents

Introduction

The important aspect in the approach of conservative treatment is, as well as effectiveness, the respect of materials that constitute work of art. In fact, conservators and restorers have to choose the better way to act, often making compromises between aesthetic and conservative aspect.
During the last years, the scientific research on materials, in term of elucidating their chemical-physical properties, gave a new and more complete knowledge to restorers for making conscious choices.
Among the most useful techniques for the conservation of cultural heritage the use of chelating agents is of paramount importance, particularly in the cleaning protocols of wall paintings and inorganic materials [1,2], but often with no adequate cognizance by restorers, of the chemical aspects of the interaction with the support. Actually, chelating agents are able to form stable complexes with metal ions and in particular with Ca^{2+}, which is present in plasters (mainly containing calcium carbonate) [3], and in many degradation products [4] arising from superficial carbonation, sulfation [5,6] and formation of oxalate patinas [7,8,9]. For the latter, nowadays, superintendents, conservators and art historians choose to leave it [10] for its historical value and because any treatment could be resulted too much invasive for the integrity of inorganic carbonate support. Also, in literature is reported efficiency and resistance of oxalate as protection treatment on marble against chemical weathering also as artificial conservative protection treatment [11,12].
For these reasons, it is extremely important to study the interactions of chelating agents with wall brackets in order to carry out selective extractions of the materials to be removed with no deterioration of the substrate constituting the work of art [13]. In this regard, we focused our attention on ethylenediaminetetraacetic acid (H_4EDTA) and on citric acid (H_3Citr) as chelating agents, in the form of their salts, respectively $Na_3HEDTA \cdot 2H_2O$ (trisodium salt dihydrate) and $Na_3Citr \cdot 2H_2O$ (tribasic sodium citrate dihydrate), which are two of the most commonly used in the conservative practice. Here we present our investigation on the reactivity of

these chelating anions with the three main compounds present in the plaster, i.e. calcium carbonate, calcium sulfate dihydrate and calcium oxalate monohydrate. Different analytical techniques, Fourier-transform infrared spectrometry in attenuated total reflectance mode (FTIR-ATR), powder X-ray diffraction (XRD) and inductively coupled plasma atomic emission spectroscopy (ICP-AES) were used to clarify the different capacity of the two chelating agents to affect the solubility of the three calcium compounds, and the products which are formed by reacting the latter with the solution of the salts containing the chelators. The experimental observations have been compared with those expected on the basis of the speciation models calculated using of the formation constants of calcium(II) complexes and the solubility products of the related salts available in the literature. Finally, we also report the physical-chemical characterization of a novel sodium-calcium double citrate, obtained as an unexpected by-product originated by the exposure of calcium sulfate to the citrate solution.

1.1. Experimental

1.1.1. Materials and equipments

Powders of the following compounds (>99% purity) were used: $CaCO_3$ (calcite, Janssen Chimica), $CaSO_4 \cdot 2H_2O$ (gypsum, Carlo Erba) and $CaC_2O_4 \cdot H_2O$ (wewhellite, Carlo Erba). The salts of the chelating ligands were: ethylenediaminetetraacetic acid trisodium salt dihydrate, ($Na_3HEDTA \cdot 2H_2O$, Fluka, purity >98%) and tribasic sodium citrate dihydrate ($Na_3Hcitr \cdot 2H_2O$, Sigma Aldrich, purity 99%).

High purity silica gel powder was purchased from Silicagel Merck, concentrated hydrochloric acid (37%) from Riedl-de Haen, and HNO_3 65% from Pan Reac Quimica s.a.u.

The aqueous solutions of the salts used for the studies were prepared by dissolving the proper amount of the salts in high purity distilled water to obtain a 0.1M aqueous solution of $Na_3HEDTA \cdot 2H_2O$ and a 0.5M aqueous solution of $Na_3Hcitr \cdot 2H_2O$. The resulting final pH values were 8.35 and 8.60 for the two solutions respectively.

The morphology of the samples was studied using an SZN-2 Optika optical microscopy. The IR spectra were collected using a Nicolet - Nexus 5PC Fourier Transform IR Attenuated Total Reflectance Spectrophotometry (FTIR-ATR), equipped with Smart Orbit Diamond Crystal (measuring range 400-4000 cm^{-1}).

Powder X-ray Diffraction (XRD) were collected using a Thermo Electron–WinXRD diffractometer (range 2θ: 5 – 70°). Elemental Microanalysis (CHN) were performed with a Carlo Erba Model EA 1108 analyzer using acetanilide as CHN standard. Thermogravimetric Analysis (TGA) were performed using a Perkin-Elmer Delta Series TGA 7 apparatus from 25 °C to 300 °C (10 °C/min) under nitrogen. Scanning Electron Microscopic analysis were collected using a Jeol 6400 Scanning Electron Microscope coupled with Microprobe (SEM-EDS) and with an energy dispersive spectrometer for the detection of X-rays (equipped with an Oxford microanalysis 15KV, 0.28 nA). A mechanical mixture of calcium sulfate and sodium citrate (Na:Ca 1/1 molar ratio) was used as standard for chemical analysis.
The calcium(II) content in the solutions was determined using a Leeman/Philips ICP PU 7450 ICP Spectrometer and a Jobin-Yvon ULTIMA 2 ICP-AES spectrometer (Power generator 1000 Watt, Plasma Gas Flow rate 12 l/min, Nebulizer Flow rate 0.85 l/min, λ_{Na}: 588.995 nm, λ_{Ca}: 315.887 nm, 0.5 – 8 mg/L). The pH of solutions were collected with a Crison Instruments Basic 20 pH - meter, provided with an Hamilton glass electrode calibrated daily using standard buffers. The melting point was determined by means of a Gallenkamp -OPTO-LAB s.n.c. melting point apparatus.

1.1.2. Experimental procedures

1.1.2.1. Treatments of calcium salts with chelating agents solutions

Samples of 1.000 g of powder of each of the calcium salts were added to 1.000 g of silica to obtain six samples of 2.000 g total (two for each calcium salt). The six mixtures of calcium carbonate/silica, calcium sulfate/silica and calcium oxalate/silica were mixed thoroughly by means of a ceramic mortar and photographed using an optical microscope before and after mixing.
The obtained mixtures were subsequently heated to 80°C for 1h in an oven to remove moisture, and then let them cool in a desiccator for 30 min, before their FTIR-ATR and XRD spectra were collected.
Three out of the six mixtures (one for each calcium salt) were treated with the trisodium EDTA solution, while the other three mixtures with the sodium citrate solution. The treatment with the chelators was carried out as follows: the powdered samples were suspended under stirring in 50 ml of solution of the chelating agents, and the mixture allowed reacting for 24 h (Fig. 1) The pH of the solutions were monitored before and after treatment.

The suspensions were filtered (Fig. 2), the solid materials washed with 30 ml of distilled water, and the filtrate solutions transferred into 100 ml volumetric flasks (Fig. 3).

Figure 1. Reaction flask with calcium salt powder and chelating solution.

Figure 2. Filtration system consisted of a Büchner filter, a flask and a water pump for the vacuum.

Figure 3. Filtered solution in volumetric flask, separated from the calcium salt powder.

The solutions were added with 3 drops of concentrated hydrochloric acid to eliminate any insoluble residue and diluted to 100 ml. The obtained solutions were diluted 1:2000 and analyzed by ICP to quantify the concentration of Ca^{2+} ions obtained by solubilization of the calcium salts during the reaction.
The solid recovered from the filtration of the reacting mixtures was heated in an oven at 80°C for 1h and allowed to cool in a desiccator for 30 min. The solid samples were then weighed and their FTIR-ATR and XRD spectra collected.
The same experimental procedure was followed for solid samples treated with the solutions of the chelators for 7 and 30 days.

1.1.2.2. Calculations of the speciation models in solution

The speciation for the Ca^{2+}/EDTA or Ca^{2+}/citrate systems in the presence of either oxalate, carbonate or sulfate ions was determined by calculations using the software HySS (Hyperquad Simulation and Speciation, Protonic Software, UK). The software was used to take into account the presence of the multiple formation equilibria of the Ca^{2+} e Na^{+} complexes and taking into account the protonation of the ligands.

The stability constants of the complexes used in the calculations are those reported in the NIST-Critically Selected Stability-Constants databases [14].
The solubility product reported in the same database for calcium oxalate, calcium sulfate and calcium carbonate (calcite) were also taken into account in the calculations. The ionic strength of a 0.1 M Na_3HEDTA or Na_3Citr solution results 0.6 M and therefore the stability constants at this ionic strength and in the presence of Na^+ as the background cation were used, where available. Where not available, the stability constants determined under the closest ionic strength conditions were used. The full list of stability constants of the complexes, the protonation constants of the ligands and the solubility products used in the calculations is reported in Appendix I.

1.1.2.3. Characterization of $NaCaC_6H_5O_7$ (NaCaCitr)

The NaCaCitr salt was isolated using two different procedures. In the first procedure, 5 ml of a 1 M sodium citrate solution in water was added to 5 ml of a 1 M calcium acetate aqueous solution. A solid appeared and the suspension was left to stir at room temperature for 24 h. The solid was recovered by filtration, washed with distilled water and dried under reduced pressure for 2 h at 80 °C. In the second procedure, 5 ml of a 1 M sodium citrate solution in water was added to 5 ml of a 1 M calcium acetate aqueous solution. A solid appeared and the suspension was left to stir at 40 °C for 3 h. The solid was recovered by filtration, washed with distilled water and dried under reduced pressure for 2 h at 80 °C.
The dried powder were characterized by FTIR-ATR. Hemihydrate salt 1 (cm^{-1}): 1603s, 1576ms, 1540vs, 1467msh, 1428s, 1388s, 1272m, 1084mw, 846w, 657mw, 598m and 538m. Bihydrate salt 2 (cm^{-1}): 1616ms, 1563s, 1540vs, 1467msh, 1428s, 1388s, 1266m, 1077mw, 839w 671w, 601m e 535m. XRD characterization of hemihydrate salt 1 (deg): 11.4(100), 17.38(25), 19.8(50), 22.76(60), 28.84(30), 34.44(60), 38.28(30), 44.60(30), 46.04(40), 52.04(20). XRD characterization of bihydrate salt 2 (deg): 5.98(100), 11.56(45), 17.32(45), 22.76(35), 29.08(30), 30.21(20), 34.84(30), 37.64(20), 44.52(25), 46.66(20). CHN elemental analysis of hemihydrate salt 1: calc. C% 27.5, H% 2.3; found C% 27.0, H% 2.4. Bihydrate salt 2: calc. C% 24.9, H% 3.1; found C% 25.3, H% 3.1. TGA, hemihydrate salt 1: experimental weight loss % 4.9, theoretical hemihydrates (PM 262) weight loss % 3.4 (Fig. 4), bihydrate salt 2: experimental weight loss % 12.5, theoretical bihydrate (PM 289) weight loss % 12.5 (Fig. 5) and SEM-EDS.

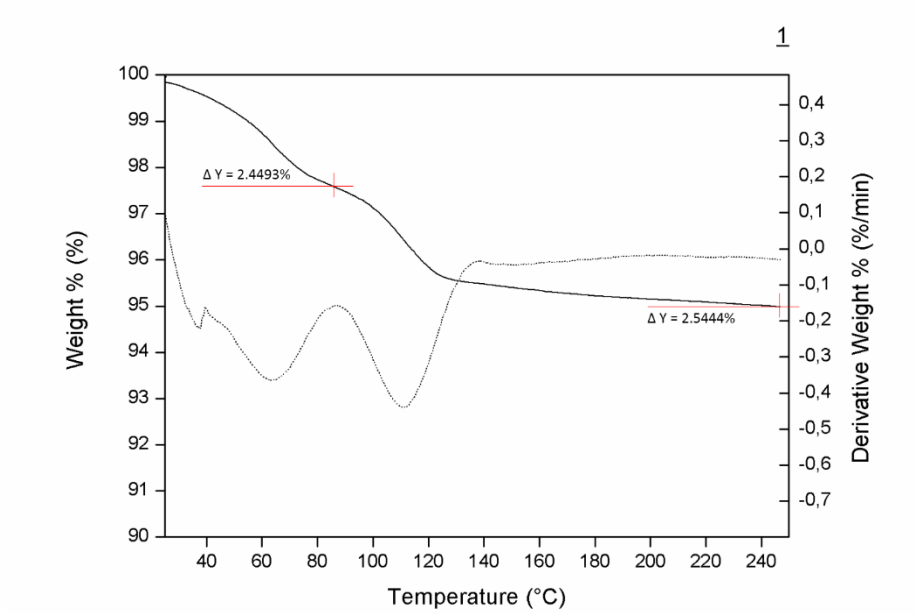

Figure 4. TGA Thermogram of sample 1 hemihydrate salt: total weight loss 4.9% (theoretical: 3.4%).

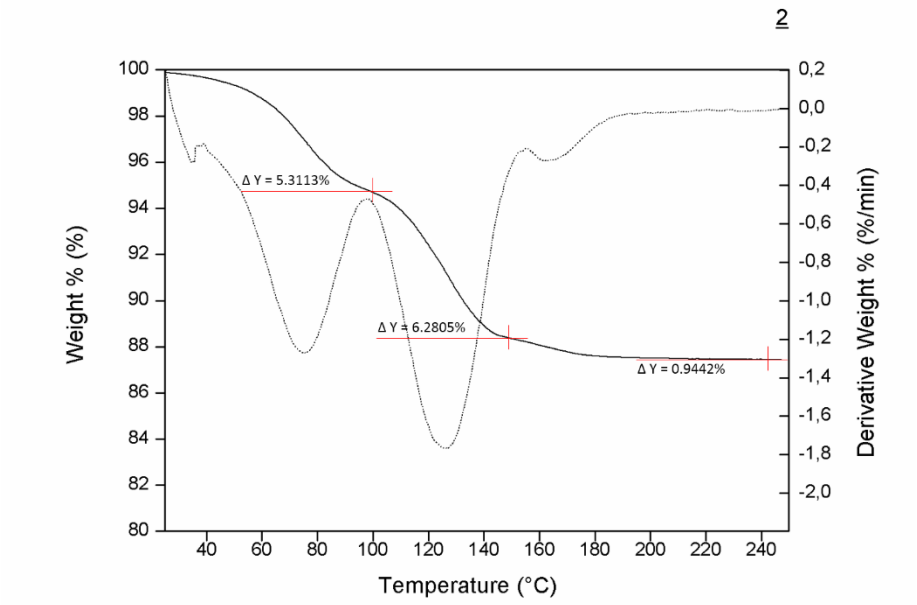

Figure 5. TGA Thermogram of sample 2 dihydrate salt: total weight loss 12.5% (theoretical: 12.5%).

The Na/Ca ratio in the NaCaCitr salt was determined as follows: 0.02 g of compound were placed in a 100 ml volumetric flask and added with six drops of concentrated nitric acid. The mixture was heated to 83 °C (boiling point). The sample was diluted to 100 ml with distilled water to yield a clear solution. A 10 ml portion was transferred into a 100 ml volumetric flask, diluted to 100 ml and analyzed by ICP-AES to determine the Ca^{2+} and Na^{+} concentrations.
The solubility of the salt was determined by stirring 0.2 g of salt in 10 ml of distilled water in a reacting flask for 7 days. An aliquot of the supernatant was transferred into a volumetric flask diluted 1:1000. The resulting solution was analyzed by ICP-AES to determine the Ca^{2+} concentration.

1.2. Results and discussion

1.2.1. Treatments with chelating ligands

1.2.1.1. Characterization of solid materials containing the calcium salts

The three solid materials containing respectively calcium oxalate, calcium sulfate and calcium carbonate, mixed with silica (acting as internal standard), were placed in contact with sodium EDTA or sodium citrate.
The dry residues of the three samples treated with sodium EDTA, at pH 8.35 for 24 h, were characterized by IR spectroscopy and X-ray powder diffraction and compared with the corresponding materials before the treatment. Figure 6 displays the IR spectra of the $CaCO_3/SiO_2$ mixture before and after treatment.

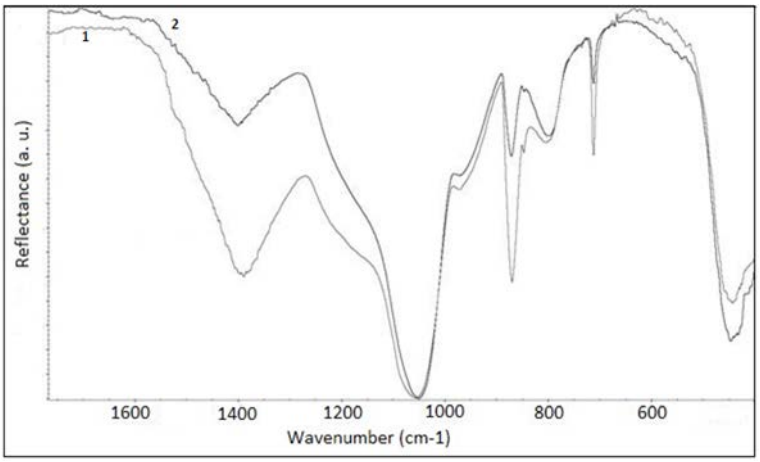

Figure 6. FTIR-ATR spectra of the calcium carbonate/silica sample before (1) and after (2) the treatment with EDTA.

Comparison of the two spectra shows that the intensities of the peaks attributable to the carbonate anion (1398, 869 and 711 cm^{-1}) undergo significant lowering after the treatment, while that of SiO_2 at 1050 cm^{-1} remained the same. Similarly, in the case of the $CaSO_4/SiO_2$ and CaC_2O_4/SiO_2 samples, the IR spectra show a significant decrease of the intensities of the peaks attributable to the calcium salts at 1682, 1619, 666 and 594 cm^{-1} for $CaSO_4$ and at 1600 and 780 cm^{-1} for CaC_2O_4.

IR data clearly indicate significant extraction amounts of calcium salts by the EDTA solution. Comparative XRD analyses have been carried out on the same salt/silica mixtures in order to confirm this evidence. In all the three cases, a significant decrease of the diffraction peaks of the calcium salts was observed, while the background profile due to amorphous silica remained unchanged. This evidence is reported in Fig. 7, which shows the diffraction profiles relevant to $CaSO_4/SiO_2$ before (1) and after (2) contact with EDTA.

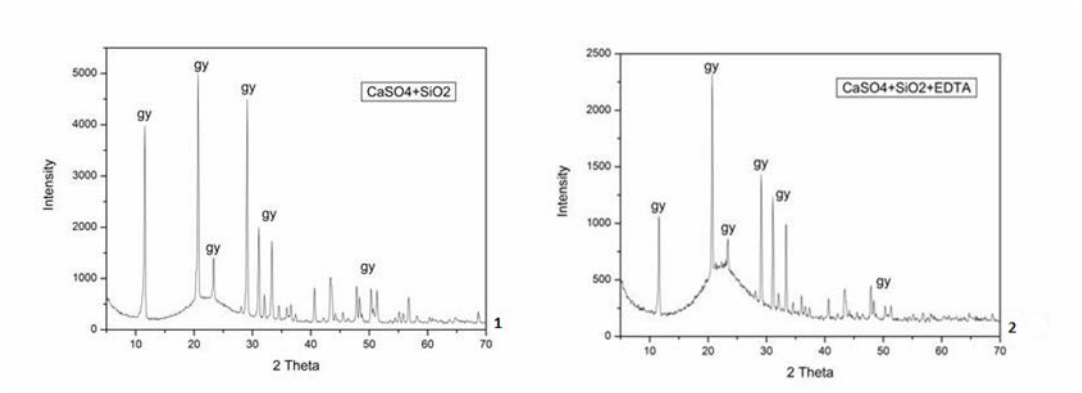

Figure 7. Powder X ray diffraction spectra of the calcium sulfate/silica sample before (1) and after (2) the treatment with EDTA (gy= gypsum).

The three samples treated with citrate at pH 8.64 for 24 h were analyzed by IR and XRD, in a similar way to that described for the treatment with EDTA. As for the previous chelator, the two $CaCO_3/SiO_2$ and CaC_2O_4/SiO_2 samples exhibit significant decrease of both of the IR bands and the XRD peaks relevant to the calcium salts. Figure 8 shows the IR spectra of the $CaCO_3/SiO_2$ sample before and after treatment.

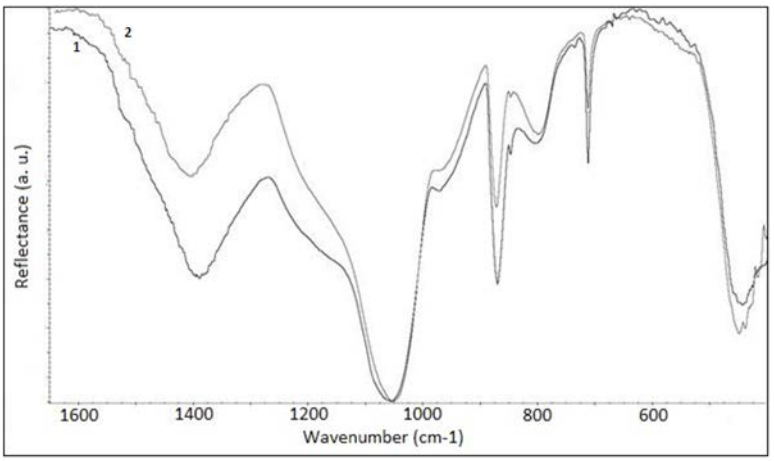

Figure 8. FTIR-ATR spectra of the calcium carbonate/silica sample before (1) and after (2) the treatment with sodium citrate.

However, in the case of the system $CaSO_4/SiO_2$, both the IR spectra and the XRD patterns (before and after) indicate the unexpected appearance of a chemical species different from calcium sulfate. The IR spectrum after the treatment with citrate appears deeply changed with respect to that of the original material, exhibiting novel bands attributable to the citrate anion as shown in Fig. 9. This suggests that a novel insoluble calcium or calcium/sodium citrate compound could be formed

from the reaction of calcium sulfate with sodium citrate (1618mw, 1560s, 1542ms, 1466w, 1420m, 1390mw, 666m, 593m e 526m cm^{-1}).

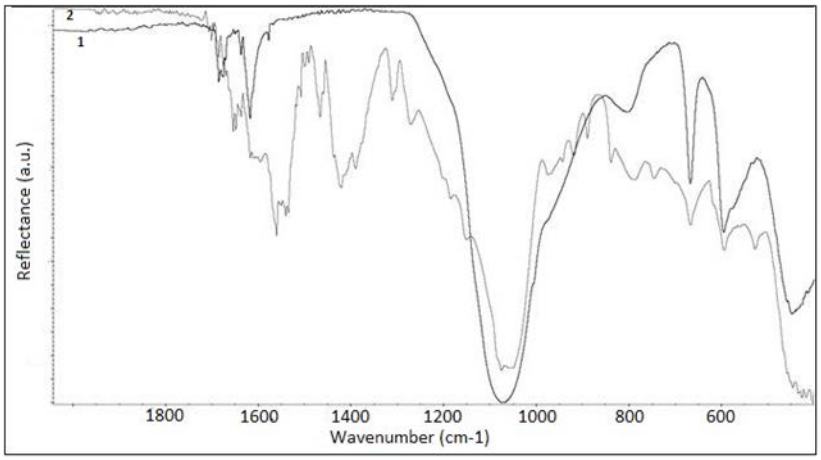

Figure 9. FTIR-ATR spectra of the calcium sulfate/silica sample before (1) and after (2) the treatment with sodium citrate.

A deep change occurs also in the diffraction pattern, on which the treatment produces the appearance of novel diffraction peaks. At the same time, those due to $CaSO_4$ (gypsum) resulted undetectable after treatment (Fig. 10).

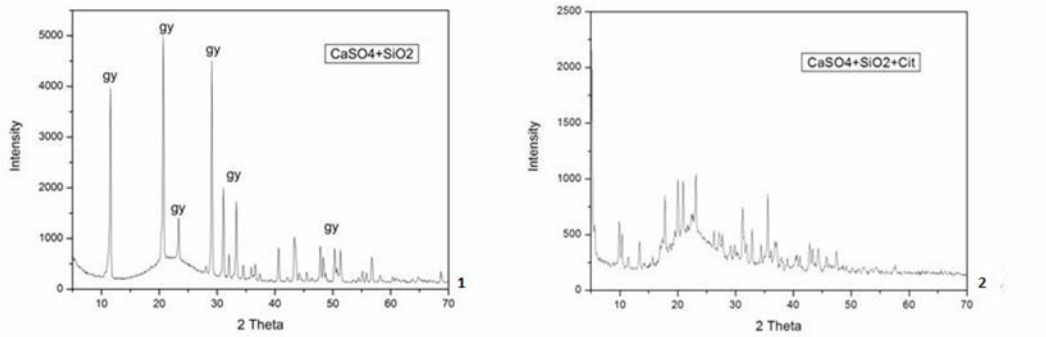

Figure 10. Powder X ray diffraction spectra of the calcium sulfate/silica sample before (1) and after (2) treatment with sodium citrate (gy= gypsum).

IR spectroscopy and XR diffraction data suggest that both EDTA and citrate exhibit significant solubility power towards $CaSO_4$, $CaCO_3$ and CaC_2O_4, under the conditions examined. In addition, it appears that by treating calcium sulfate with sodium citrate a novel insoluble citrate salt is formed.

1.2.1.2. Determination of calcium in the extracted solutions

ICP-AES analyses have been carried out on solutions obtained by treating the salts with the ligands in order to investigate the solubilization capacity the two chelating agents on the three calcium salts.
The well-known sensitivity of lime to acidic substances has necessarily led to the use of solutions at high pH. The results (calcium concentration and percentage of solubilization) are reported in Table 1 for the treatment with EDTA and Table 2 for the treatment with citrate.

Table 1 Ca^{2+} concentration in solution obtained by treating samples of the calcium salts with 50 ml of a 0.1 M solution of $Na_3HEDTA{\cdot}2H_2O$, pH 8.35, for 24 h, 7 d and 30 d respectively. Data obtained by ICP-AES on samples diluted 1:2000 prior to analysis.

	24 h		**7 d**		**30 d**				
	Ca (mg/L)	**[Ca] (mol/L)**	**Ca (mg/L)**	**[Ca] (mol/L)**	**Ca (mg/L)**	**[Ca] (mol/L)**	**calcd. [Ca] (mol/L)***	**final pH**	**% salt dissolved**
$CaSO_4{\bullet}2H_2O$	1.54±0.02	0.08	1.48±0.06	0.07	1.60±0.06	0.08	0.12	4.17	62
$CaCO_3$	1.91±0.04	0.09	1.84±0.07	0.09	1.57±0.08	0.08	0.10	9.37	40
$CaC_2O_4{\bullet}H_2O$	0.59±0.01	0.03	0.53±0.04	0.03	0.82±0.04	0.04	0.08	5.85	29

*** calculated by HYSS**

Table 2 Ca^{2+} concentration in solution obtained by treating samples of the calcium salts with 50 ml of a 0.5 M solution of $Na_3Citr{\cdot}2H_2O$, pH 8.64, for 24 h, 7d and 30 d respectively. Data obtained by ICP-AES on samples diluted 1:2000 prior to analysis.

	24 h		**7 d**		**30 d**				
	Ca (mg/L)	**[Ca] (mol/L)**	**Ca (mg/L)**	**[Ca] (mol/L)**	**Ca (mg/L)**	**[Ca] (mol/L)**	**calcd. [Ca] (mol/L)***	**final pH**	**% salt dissolved**
$CaSO_4{\bullet}2H_2O$	1.25±0.02	0.06	0.82±0.06	0.04	0.83±0.08	0.04	0.11	8.21	31
$CaCO_3$	0.63±0.06	0.03	0.10±0.01	0.005	0.11±0.01	0.006	0.005	10.80	3
$CaC_2O_4{\bullet}H_2O$	0.21±0.01	0.01	0.020±0.002	0.001	0.09±0.01	0.005	0.001	8.34	4

*** calculated by HYSS**

The values reported in both Tables 1 and 2 are in substantial agreement with the solubility products of the three salts ($9.55{\bullet}10^{-4}$ for calcium sulfate, $9.33{\bullet}10^{-8}$ for calcium carbonate and $1.38{\bullet}10^{-8}$ for calcium oxalate) [14].
Calcium sulfate exhibits the highest solubility in the presence of both EDTA and citrate, followed by carbonate and oxalate, the last one being the least prone to the

attack of both chelating ligands. Citrate appears less effective than EDTA and in particular towards carbonate and oxalate, (the calcium concentration is one order of magnitude lower). Moreover, EDTA is able to solubilize the three salts to a higher extent although in a less selective way than citrate.

Table 1 shows that, under the adopted conditions, the equilibrium concentration for EDTA is reached after 24 h for the three samples, whereas in the case of citrate it appears that prolonged exposures to the chelating agent cause poorer extraction efficacy, mainly for carbonate and oxalate. This anomalous behavior can be explained for $CaSO_4$ taking into account the lowering of calcium concentration in solution after the first 24 h due to the subsequent formation of a novel, insoluble calcium-sodium double citrate (vide infra). Kinetic phenomena could be responsible for the lower solubility of $CaCO_3$ and CaC_2O_4 after longer treatment time, as no novel insoluble compounds have been detected anywhere. It is possible that the observed concentration decrease after the first 24 h of exposure is due to the aggregation of fine colloidal particles formed at the beginning of the treatment or just present in the solid samples.

1.2.2. Thermodynamic models by Hyperquad-simulation and speciation (HYSS)

In the attempt to rationalize the observed solubilities of the salts and the concentration of Ca^{2+} reported in Tables 1 and 2, we calculated the species distribution at the equilibrium for the suspensions of the calcium salts in the chelators solutions under the same conditions (concentration of the chelating ligands, amount of calcium salts and pH). The logarithms of the protonation and complex-formation constants of the ligands and the anions present in the systems and of the solubility products of the calcium salts are those of the NIST Critically Selected Stability Constants database. These values are reported as supporting information in Table S1 (Appendix I).

The calculated total Ca^{2+} concentrations ([Ca^{2+}], soluble calcium) are reported in Table 1 and 2 and correspond to the sum of the concentration of all soluble calcium species obtained in the calculations. The distribution of calcium in the different soluble complex species and insoluble salts is reported in the Appendix I (Figure S1).

The predominant species in the EDTA solution at pH 8.35 is $HEDTA^{3-}$. For the calcium salts treated with this solution, the calculated total [Ca^{2+}] are slightly higher than that observed experimentally. However, they correspond to the same order of

magnitude and underline how calcium oxalate is more insoluble when treated with the chelator than the other two salts as expected based on the K_{sp}. The trend of the calculated total $[Ca^{2+}]$ values is particularly interesting if we consider the solubility products: calcium oxalate has a K_{sp} less than one order of magnitude lower than that of calcium carbonate, while in turn the K_{sp} of the carbonate salt is more than three order of magnitude lower than that of calcium sulfate. On the basis of these K_{sp} values one expects that the $[Ca^{2+}]$ concentrations follow the same trend sulfate >> carbonate > oxalate. Instead, both the experimental evidence and the calculated total $[Ca^{2+}]$ show that the trend is rather sulfate ≥ carbonate > oxalate, apparently irrespective of the K_{sp} values. An interpretation of this behavior is given here below.
By treating the sample of calcium sulfate and calcium oxalate with EDTA the pH decreased significantly from 8.35 to 4.17 and 5.85, respectively. This is a quite expected behavior, as the reaction of calcium with $HEDTA^{3-}$ releases one proton per metal bound ($Ca^{2+} + HEDTA^{3-} = [Ca(EDTA)]^{2-} + H^{+}$). This proton is not buffered neither by sulfate nor by oxalate, resulting in a moderate acidic solution. In this respect, the higher calcium concentration observed in the sample of calcium sulfate simply reflects directly the values of the solubility products: by treating of the most soluble salt, the highest calcium concentration is obtained. On the contrary, the treatment of calcium carbonate produces the complexation of the metal ion with release of protons from $HEDTA^{3-}$, but more importantly also produces a release of an equimolar amount of carbonate anions. These anions act as a strong base, which buffer the protons released from $HEDTA^{3-}$ upon complexation and also produce a final alkaline solution (pH = 9.37). Therefore, the deprotonation of $HEDTA^{3-}$ into $EDTA^{4-}$ produces a species more prone to bind calcium and the presence of these simultaneous complexation-protonation equilibria results in the observed sulfate ≥ carbonate > oxalate solubility. Finally, the species distribution reveal that for oxalate and carbonate the Ca^{2+} ion is distributed between only two species: the $[Ca(EDTA)]^{2-}$ complex, and the solid salt. For these systems the contribution to the total $[Ca^{2+}]$ comes solely from the soluble $[Ca(EDTA)]^{2-}$ species. On the contrary, calcium sulfate is significantly more soluble that the other two salts, and a significant contribution to the total $[Ca^{2+}]$ comes from the inherent soluble fraction of $CaSO_4(aq)$, and from the $[Ca(HEDTA)]^{-}$ species present at pH ca 4.
For the salts treated with citrate, the calculated total $[Ca^{2+}]$ matches quite well with the experimental ones (only slightly lower) with the exception of the sulfate system where the calculated total $[Ca^{2+}]$ is remarkably higher than the experimental one. This observation is quite well rationalized taking into account the formation and precipitation of the mixed calcium sodium citrate, which is more significant in the

case of sodium sulfate (see below) by virtue of the higher Ca^{2+} concentration present in solution for the most soluble salt. Because the K_{sp} of this mixed salt is still undetermined and it was not taken into account in the calculation, the calculated total [Ca^{2+}] for this system resulted higher than experimental one. For the salts treated with citrate, therefore, the trend for the total [Ca^{2+}] is sulfate >> carbonate > oxalate which quite well reflects the trend in the K_{sp} values and the formation of the mixed citrate salt, as described. For these systems, the lower complexing capacity of citrate for calcium compared to that of EDTA (log βCaL = 3.48 and 10.47 for L = citrate and EDTA, respectively) results in the limited capacity of this chelator to dissolve the calcium salts. Moreover, because citrate contains only carboxylato groups, the calcium binding equilibria does not displace protons and the pH of the suspensions resulted therefore higher than 8 for the systems containing sulfate and oxalate. The higher pH value of the carbonate system on the other hand is due to carbonate ions released in solution upon dissolution of the salt, as observed for the treatment with EDTA. The species distribution for these systems (see supporting information) reveal how they are dominated by the presence of the insoluble salts for the more insoluble carbonate and oxalate calcium salts. On the other hand, the species distribution of the sulfate system is dominated by the Ca-citrate complex present as the insoluble mixed Na-Ca citrate salt was not taken into account into calculations.

From these results, we conclude that the lowest solubility of calcium oxalate in the presence of the chelating agents reflects the lowest K_{sp} value for this salt. Calcium sulfate is very soluble in the presence EDTA, both by virtue of the high stability of the $[Ca(EDTA)]^{2-}$ complex and of the inherent solubility of calcium sulfate. On the other hand, this behavior was not observed experimentally in the presence of citrate, as the mixed Na-Ca salt precipitates out. As concerns calcium carbonate, its solubility is significantly higher in the presence of EDTA than expected from a simple comparison of the K_{sp} values. This behavior originates from the basicity of the released carbonate ions which influence the $[Ca(EDTA)]^{2-}$ formation equilibrium. Finally citrate, which forms a less stable complex with calcium compared to $[Ca(EDTA)]^{2-}$, produces a remarkable lower solubilization of calcium carbonate compared to that obtained using EDTA.

1.2.3. Characterization of sodium-calcium double citrate

As reported above, it has been found that the reaction between sodium citrate and calcium sulfate leads to the formation of a novel, sparingly soluble citrate salt

containing calcium and sodium. In medical literature [15,16,17] the existence of a calcium sodium double citrate of formula $C_6H_5O_7CaNa$ [18] is summarily reported. We report here the preparation and characterization of the mixed citrate salt. The reaction between sodium citrate and calcium acetate led to the precipitation of a calcium sodium (1:1) double salt both in the hemihydrate and in the dihydrate form, respectively of formula $C_6H_5O_7CaNa \cdot 1/2H_2O$ and $C_6H_5O_7CaNa \cdot 2H_2O$. Both compounds decompose at ca 300 °C without melting. Their IR spectra, reported in Fig. 11, are similar and not significantly different from those of the species formed from calcium sulfate/silica treated with the citrate solution (as shown in Fig. 9).

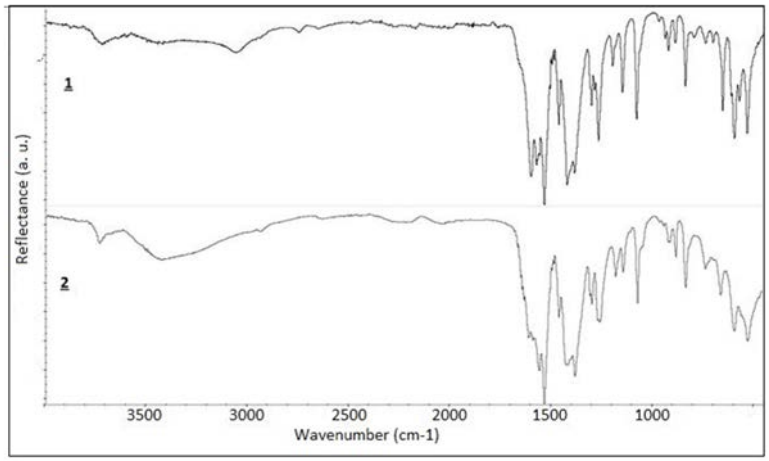

Figure 11. FTIR-ATR spectra of the mixed calcium/sodium citrate salt. Spectra of the hemihydrate species 1, and dihydrate species 2.

The SEM image in Fig. 12 a shows the micrometric sized of precipitated crystallites. EDS microanalysis (Fig. 12 b) carried out on the hemihydrate salt confirmed the Ca/Na atomic ratio of ca. 1:1 (0.96:1).

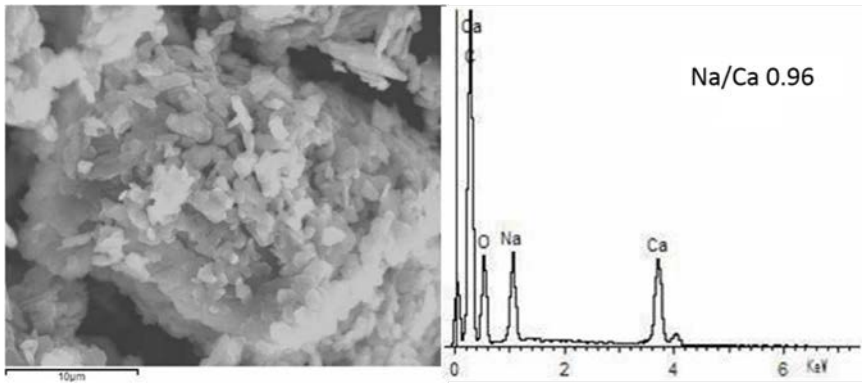

Figure 12. SEM-SE image (3700X) and EDS spectra of the mixed calcium/sodium citrate salt (hemihydrate species 1).

The hemihydrate salt 1 has been subjected to solubility investigations in water and aqueous HNO_3 and the obtained data are reported in Table 3.

Table 3. Ca^{2+} and Na^{+} concentration in solution for the calcium/sodium citrate salt treated with water or HNO_3(aq). Data obtained by ICP-AES on samples diluted 1:1000 prior to analysis.

	Sample amount (g)	Ca (ppm)	Na (ppm)	Mole fraction Ca/Na	Ca dissolved (mg)	Na dissolved (mg)
1(water)	0.2	0.38±0.03	0.66±0.05	0.33	3.8	6.6
1(HNO₃aq)	0.02	3.31±0.05	1.78±0.03	1.08	3.3	1.8

In aqueous nitric acid, the compound is completely soluble. ICP data confirmed that the solution contains Ca and Na in 1:1 molar ratio, as expected.
When suspended in water, the obtained solution contains Ca and Na in 0.33:1 molar ratio, suggesting that the double salt undergoes decomposition forming insoluble calcium citrates. This in turn results in the presence in solution of a larger amount of sodium compared to calcium. However, considering that only 37.6 % of total sodium present in the solid sample is solubilized, a significant amount of the original double salt remains intact as a mixed citrate.

1.3. Conclusions

The research presented here focused the attention on a well-known method in wall painting conservative practice: the use of chelating agents for the treatment of deterioration calcium patinas.
The results presented in this work compared two chelating agents: EDTA trisodium dihydrate and tribasic sodium citrate dihydrate, and their capacity to react with calcium carbonate, sulfate and oxalate.
The ability of EDTA to chelate Ca^{2+} is higher than that of citrate, as expected on the basis of the stability constants of the obtained complexes. Actually, the solution of EDTA trisodium dihydrate at pH 8.35 was able to dissolve the calcium salts more effectively than the solution of sodium citrate tribasic dihydrate at pH 8.60. The final concentration of Ca^{2+} in solution for the different salts treated with the two chelators have been quite well explained on the basis of the stability of the complex species and the solubility products of the salts.
This study confirms what restorers usually observe in their practical work: the use of chelating agents solutions in variable percentage to remove sulfatation or

carbonatation patinas does not guarantee that the action is only superficial and not dangerous for the integrity of the support. Especially in the case of the use of the strongest EDTA chelator, the control of these drawbacks has to be attained by reducing time of application.

In the case of calcium oxalate patinas, the application of these chelators results less dangerous by virtue of the lower solubility product of this salt. For this salts, moreover, a reduced time of application should result not effective.

Finally, our results show an unexpected though important result originated by the use solutions of sodium citrate to treat materials containing calcium sulfate. The reaction between the solution of sodium citrate and calcium sulfate caused the formation of an unexpected sparingly soluble sodium calcium double citrate ($NaCaC_6H_5O_7$), which has been characterized by physical-chemical analyses.

This result has important impact in conservation practice: the treatment of plaster surfaces with sodium citrate in the presence of calcium sulfate (either derived from degradation of plaster via sulfatation or as constituent material) can lead to the formation of this sparingly soluble salt resulting in a permanent compositional and morphological modification of the substrate[3].

[3] V.E. Selva Bonino, M. Tegoni, C. Mucchino, G. Predieri, A. Casoli, "*Model study of the costituents of wall painting degradation patinas: The effect of the treatment with chelating agents on the solubility of the calcium salts*", (2015), Microchemical Journal 118, pp.62-68.

2. *Dry cleaning* methods for conservation treatment on paintings: characterization and application

Introduction

The cleaning of unvarnished paintings (such as oil and acrylic [19,20] films) can be made by swab rolling surfaces with different type of solutions, aqueous or solvents, but only if films are not sensitive to these [21,22,23]. In fact, these treatments can cause leaching, swelling, superficial skin of medium, loss of adhesion, discoloration and so on [24,25,26,27,28].

This behaviour is not only due to incorrect conservative treatments or due to inner characteristic of the film, but also to the poor quality of additives and synthetic medium of commercial colours [29,30].

In such instances, *Dry cleaning* methods may provide an alternative [31,32,33]. Surface cleaning, synonymously referred to as *dry cleaning,* is a mechanical cleaning technique used to reduce superficial soil, dust, grime, insect droppings, accretions or other surface deposits. *Dry cleaning,* as the term is used in paper conservation [34,35,36], does not employ the use of organic solvents. Surface cleaning may be used as an independent cleaning technique, as one-step (usually the first) in a more comprehensive treatment, or as a prelude to further treatments.

The purpose of surface cleaning is to reduce the potential for damage by removing foreign material, which can be abrasive, acidic, hygroscopic or degradative. The decision to remove surface dirt is also for aesthetic reasons when it interferes with the visibility of the imagery. A decision must be made balancing the probable care of each object, against the possible problems related to surface cleaning.

In fact, cleaning approach using these materials, consist on mechanical action obtained using natural and synthetic polymers, such as rubber, various type of sponges and clothes. Because of their industrial production, not intended for art and conservation practice, is of paramount importance to have an exact and complete physico-chemical characterization to better understand their properties and to evaluate particulate or chemical residues.

More generally, there are several factors to consider: chemical compositions and physical natures of surface cleaning materials; materials of known composition are preferable; manufacturer's formulations may change and provided product

information may not be adequate for conservation purposes, so reliable sources of products should be selected.

Some components, or the amount of a given component in dry methods, may adversely affect the quality of materials and the treatment results. Factors that may adversely affect supports are: abrasives, sulphur, calcium carbonate (pH), hydrochloric acid, plasticizers, drying oils, antioxidants, etc.

Physical properties, such as stiffness, tackiness and abrasiveness affect the efficiency of surface dirt removal and the possibility for damage to the artwork. *Dry cleaning* materials should be selected that will not damage or physically alter surfaces and media. Variation in size and fineness of particles, for example, contributes to the effectiveness of cleaning and minimizes the possibility of disturbing surfaces.

For instance, a smoother surface may require the use of very fine eraser crumbs, while a rough surface may benefit from application of something coarser and therefore less likely to become trapped in the irregularities of the surface texture. The fineness or coarseness of eraser crumbs can vary due to manufacture.

The ease of polymers residues removal and the amount and aging characteristics of residues remaining in an artefact, may influence selection of a product or method of application.

Potential alteration or damage to object have to be carefully consider; in fact surface cleaning may alter the support and media in objects selected for treatment.

Potential damages from dry cleaning may include: planar distortion, abrasion, roughing, compression, tears, detachment or loss in areas of previous support insecurities, change of surface gloss or texture, chemical reactions with the support, colour changes, loss or disruption of friable material.

Media may be adversely affected by direct application of surface cleaning materials. Many types of media cannot withstand surface cleaning.

By the light of results obtained in a previous project carried out at the *Cultural Heritage Agency of the Netherland (RCE)* in collaboration with painting conservators in the Netherlands and the *Courtauld Institute of Art* [37], this study is focused on a selection of materials available in Italian large-scale retail trade. The aim of the project is to determine composition and properties of unconventional products for conservation treatments, all the same increasingly used by restorers.

Analytical characterization of selected materials was performed by Pyrolysis gas-chromatography mass-spectrometry (Py GC-MS), Fourier-transform infrared spectrometry in attenuated total reflectance mode (FTIR-ATR), Scanning Electron Microscopy coupled with microanalysis (SEM-EDS) and Thermogravimetric analysis (TGA).

General evaluation of each materials was performed, in particular based on: chemical composition, presence of antioxidants, plasticizers, stabilizers and fillers, which can be left on the surfaces after treatment.

2.1. Experimental

2.1.1. *Materials and equipments*

2.1.1.1. Selection of products and characterization of polymers

The cleaning materials selected for this study were, in principal, based on information retrieved from the knowledge and experience of the application of *Dry cleaning* materials in paper conservation and from preliminary results obtained by Maude Daudin et al. studies. Along the research, the range of materials was expanded with other types of erasers and sponges available both in Italian large-scale retail trade, both in specialty retailers of materials for restoration.
The tested materials were divided in three distinct groups, namely: erasers (Table 1), sponges (Table 2) and cloths (Table 3).
The complete list of cleaning materials used in this study, their supplier and manufacturer, as well as features and properties of importance in use and chemical composition, are listed in tables into Appendix II.

Table 1 Samples of erasers analysed and tested, listed specifying cleaning product type, year of purchase, manufacturer, supplier, name of sample and a photo of the product.

Cleaning product (year of purchase) Manufacturer Supplier	**Name of sample**	**Photo**
Vulcanized gum (Smoke Sponge) (2013) - CTS	**G_SS_0001**	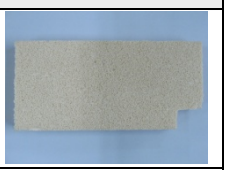
Vulcanized gum (Smoke Sponge) (2013) - CTS	**G_SS_0003**	

Wishab (white) (2013) Akapad Antares	**G_Wb_2**	
Akawipe (white powder) (2013) Akachemie Antares	**G_Awb**	
Gum file dust (2013) Made in USA by Lineco CTS	**G_Lli_1**	
Gum file dust (2013) Made in USA by Alvin & Company, INC. CTS	**G_Lal_2**	
PVC free gum 2 (2013) Made in Malaysia Faber Castell	**G_FC_1**	
PVC free sleeve mini eraser (2013) Made in Malaysia Faber Castell	**G_FC_2**	
PVC free gum (2013) Made in Malaysia Faber Castell	**G_FC_3**	
Factis OV12 (2013) Made in Spain -	**G_FOV12**	
Factis extra soft ES20 (2013) Made in Spain -	**G_FES20**	

Epure (2013) - Maped	**G_Ep**	
Dick Blick Gum Erasers (2013) **-** **-**	**G_DB**	
Design Artgum eraser (2013) - Prismacolor	**G_Art**	
Magic Rub (2013) Made in USA Prismacolor	**G_Mrub**	
Milan 403 Gigante (2014) Made in Spain -	**Mi_403**	

Table 2 Samples of sponges analysed and tested, listed specifying cleaning product type, year of purchase, manufacturer, supplier, name of sample and a photo of the product.

Cleaning product (year of purchase) Manufacturer Supplier	**Name of sample**	**Photo**
Oval Make-up sponge (2013) Made in China Pro Professional style & care (C.G.A. Caldara s.r.l)	**S_PP_ov**	
Triangle Make-up sponge (2013) Made in China Pro Professional style & care (C.G.A. Caldara s.r.l)	**S_PP_tr**	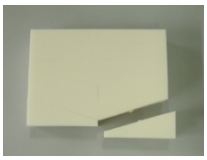

Round Make-up sponge pcs.2 (2013) Made in China Pro Professional style & care (C.G.A. Caldara s.r.l)	**S_PP_ro**	
Triangle Make-up sponge (2013) Made in China Royal Beauty (Golden Group s.r.l.)	**S_RB_tr**	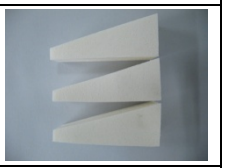
Egg make-up sponge (2013) Made in China Royal Beauty (Golden Group s.r.l.)	**S_RB_uo**	
Pink make-up sponge (2013) Made in China Royal Beauty (Golden Group s.r.l.)	**S_RB_py**	
Round make-up sponge (2013) Made in China Royal Beauty (Golden Group s.r.l.)	**S_RB_ro**	
Triangle make-up sponge (2013) Made in UK Kiko make-up	**S_KK_tr**	
Round make-up sponge (2013) Made in Japan Kiko make up	**S_KK_ro**	
Egg make-up sponge (2013) Made in China H&M	**S_HM_uo**	
Triangle make-up sponge (2013) Made in China H&M	**S_HM_tr**	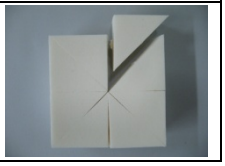

Wedges make-up sponge (2013) Made in Korea Sephora	**S_Sph_sp**	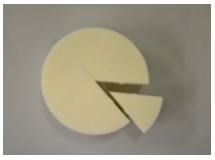
Egg make-up sponge (2013) Made in Korea Sephora	**S_Sph_uo**	
Half-moon make-up sponge (2013) Made in Malaysia Sephora	**S_Sph_ml**	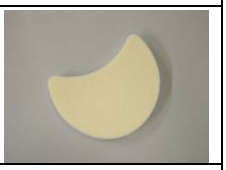
Round make-up sponge (2013) Made in Malaysia Sephora	**S_Sph_ro**	
ART SPONGE		
Sofft art knives e covers (2014) Made in China Colorfin LLC	**AS_kc_1**	
Sofft art sponge - sponge bars (2014) Made in China Colorfin LLC	**AS_sft_2**	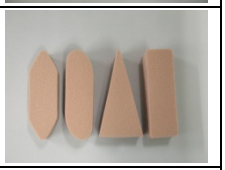
Sofft art sponge slice (2014) Made in China Colorfin LLC	**AS_sft_3**	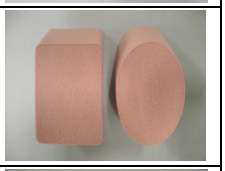
Sofft art applicators mini (2014) Made in China Colorfin LLC	**AS_sft_4**	
Sofft art sponge - big oval (2014) Made in China Colorfin LLC	**AS_sft_5**	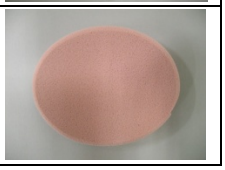

Sofft art applicators heads (2014) Made in China Colorfin LLC	**AS_sft_6**	
Suction block (2013) Made in Germany Saugwunder	**S_SB**	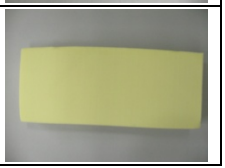

Table 3 Samples of cloths analysed and tested, listed specifying cleaning product type, year of purchase, manufacturer, supplier, name of sample and a photo of the product.

Cleaning product (year of purchase) Manufacturer Supplier	**Name of sample**	**Photo**
Yellow "effect deer" microfibre cloth (2013) Made in Corea Mapa Spontex	**P_Sp_1**	
Light blue microfibre cloth plus (2013) Made in France Freudenberg Vileda	**P_Vi_2**	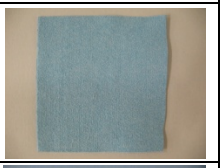
Green Ultrafibra cloth (2013) Dianex	**P_Di_3**	

The morphology of the samples was studied using an SZN-2 Optika stereomicroscopy. The IR spectra were collected using a Nicolet - Nexus 5PC Fourier Transform IR Attenuated Total Reflectance Spectrophotometry (FTIR-ATR), equipped with Smart Orbit Diamond Crystal (measuring range 400-4000 cm-1).

Pyrolysis was performed with a CDS Pyroprobe 1500 (Analytical Inc., USA) filament pyrolyzer directly connected to a GC/MS system. Pyrolysis temperature was set at 600 °C.

The GC is a 6890N Network GC System (Agilent Technologies, USA) gas chromatograph with a methyl-phenyl-polysiloxane cross-linked 5% phenyl methyl silicone (30 m, 0,25 mm i.d., 0,25 µm film thickness) capillary column. The temperature program was: 50°C for 2 minutes, then a temperature ramp (heating rate 10°C/min) to 300 °C held for 5 minutes. The temperature of the injector and of the Py-GC interface was kept at 300°C. The carrier gas was helium (1.0 mL/min) and split ratio was 1/20 of the total flow.

The mass spectrometer coupled to the GC apparatus was a 5973 Network MASS Selective Detector (Agilent Technologies, USA). Mass spectra are recorded under electron impact at 70 eV, scan range 40-600 m/z. The interface was kept at 280°C, ion source at 230 °C and quadrupole mass analyzer at 150 °C.

All instruments were controlled by Enhanced Chem Station (ver. 9.00.00.38) software. The mass spectra assignment was done with the NIST2008 libraries and by comparison with literature data.

Thermogravimetric Analysis (TGA) were performed using a Perkin-Elmer Delta Series TGA 7 apparatus from 25 °C to 600 °C (10 °C/min) under nitrogen.

Scanning Electron Microscopic analysis were collected using a Jeol 6400 Scanning Electron Microscope coupled with Microprobe (SEM-EDS) and with an energy dispersive spectrometer for the detection of X-rays (equipped with an Oxford microanalysis 15KV, 0.28 nA).

Non-polarized Raman spectra were recorded at 632.8 nm (nominal 15 mW He-Ne laser excitation) in a nearly backscattered geometry with a Jobin Yvon LabRam micro-spectrometer (300 mm focal length spectrograph) equipped with an integrated Olympus BX40 microscope provided with 10-50-50-100X objectives. The spectral resolution was about 1.5-2 cm^{-1}.

The Rayleigh radiation was blocked by an edge filter and the backscattered Raman light was dispersed by an 1800 grooves/mm holographic grating on a Peltier cooled CCD, consisting of an array of 1024/256 pixels. The entrance slit width was fixed at 100 µm. The laser power was adjusted by means of a series of density filters to avoid any damage to the samples or uncontrolled thermal effects. The power on the sample was always less than 2-3 mW.

Spectra were collected using both 100X or long working distance and 50X microscope objectives. Typical exposures was 10 s repeated 10-20 times.

The system was regularly calibrated using the 520.6 cm^{-1} Raman band of silicon or by means of reference emission lines of Ar or Cd light sources. The data analysis was performed by LabSpec built-in software.

2.1.1.2 Preparation and characterization of acrylic and oil painted samples

Drafting samples were prepared using priming linin paperboard "Per belle arti-Italy" with standard primer (25X30 cm) and Maimeri Puro oil series 00 Titanium White and Ultramarine light blue colours, diluted in linseed oil Maimeri and Maimeri Brera acrylic series 08 Titanium White and Ultramarine blue colours, diluted in water.

The morphology of the surfaces of pictorial samples was studied using an SZN-2 Optika steromicroscopy and images were collected with a digital camera Canon PowerShot A630.

Pyrolysis was performed with a CDS Pyroprobe 1500 (Analytical Inc., USA) filament pyrolyzer directly connected to a GC/MS system. Pyrolysis temperature was set at 600 °C.

The GC is a 6890N Network GC System (Agilent Technologies, USA) gas chromatograph with a methyl-phenyl-polysiloxane cross-linked 5% phenyl methyl silicone (30 m, 0,25 mm i.d., 0,25 μm film thickness) capillary column. The temperature program was: 50°C for 2 minutes, then a temperature ramp (heating rate 10°C/min) to 300 °C held for 5 minutes. The temperature of the injector and of the Py-GC interface was kept at 300°C. The carrier gas was helium (1.0 mL/min) and split ratio was 1/20 of the total flow.

The mass spectrometer coupled to the GC apparatus was a 5973 Network MASS Selective Detector (Agilent Technologies, USA). Mass spectra are recorded under electron impact at 70 eV, scan range 40-600 m/z. The interface was kept at 280°C, ion source at 230 °C and quadrupole mass analyzer at 150 °C.

All instruments were controlled by Enhanced Chem Station (ver. 9.00.00.38) software. The mass spectra assignment was done with the NIST2008 libraries and by comparison with literature data.

Environmental Scanning Electron Microscopic (ESEM) analysis were collected using a EVO60 Zeiss electron microscope equipped with EDX microprobe Oxford PentaFET for the semi-quantitative analysis.

Gloss test was performed with a Novo-Gloss™ (Glossmeters) Rhodopoint Instrumentation LTD with triple angles 20°/60°/75°, while Colorimetric test, with a Spectro-Densitometer Spectro Dens B110040 Premium Techkon GmBH, on CIE L*a*b* mode (Polfilter off, white reference absolute, illuminant D50 and 2° observer). Data were compared using ΔUG% (unit gloss %), considering variations between cleaned and not treated surfaces. This evaluation is useful to determine if

treatments cause alteration on brightness and gloss characteristics, due to mechanical rubbing of dry methods on surfaces.
Determination of colour variations before and after treatment is useful to quantify the effectiveness of cleaning procedures. This is evaluable using ΔE^*_{ab} parameter, calculated following CIE76 formula:

$$\Delta E^*_{ab} = \sqrt{(L_2^* - L_1^*)^2 + (a_2^* - a_1^*)^2 + (b_2^* - b_1^*)^2}$$

where (L_1^*, a_1^*, b_1^*) and (L_2^*, a_2^*, b_2^*) are two colours to be compared and L* meaning lightness (darkest black at L* = 0 and the brightest white at L* = 100), a* red/green opponent colours (with cyan at negative a* values and magenta at positive a* values) and finally, b* the yellow/blue opponent colours (with blue at negative b* values and yellow at positive b* values).
The difference or distance between two colours is a metric of interest in colour science. It allows quantified examination of a notion that formerly could only be described with adjectives.
The International Commission on Illumination (CIE) [38] calls their distance metric ΔE^*_{ab} (also called ΔE^*, dE*, dE, or "Delta E") where **E** stands for *Empfindung*, German for "sensation".
Several studies have proposed different ΔE values that have a JND (just noticeable difference). Unempirically, a value of 1.0 is often mentioned, but a recent study [39], assessed a JND of 2.3 ΔE.

2.1.2 Experimental procedures

2.1.2.1 Physico-chemical characterization of polymers

Stereomicroscopy observation was carried out with 7X, 30X and 45X magnification, using VIS light.
For Py GC-MS, the solid sample was loaded in a quartz tube closed with two small pieces of quartz wool. When required 5 µL of TMAH in aqueous solution was added to the sample using a micro-syringe [40,41].
For FTIR-ATR and µRaman analysis, samples were not prepared and spectra were collected directly on bulk [42], while in the case of SEM-EDS, samples were covered with graphite metallization. Also for TGA analysis, samples were not pre-treated.

2.1.2.2 Physico-chemical characterization of acrylic and oil painted samples before and after treatments

For Py GC-MS characterization of commercial colours (oil and acrylic), the solid sample was loaded in a quartz tube closed with two small pieces of quartz wool. Then, 5 µL of TMAH in aqueous solution was added to the sample using a micro-syringe.
The painting of the background of drafting samples were made both with smooth and brushed surfaces, left drying naturally at environmental temperature and relativity humidity (RU%) for 8 months (Fig. 1 and 2).
Consequently, all the areas were soiled with artificial soiling [43] dividing each surfaces into three parts: one not treated, one soiled and one soiled-then-cleaned and left drying (Fig. 3).

Figure 12. White acrylic drafting sample, with not treated and soiled areas.

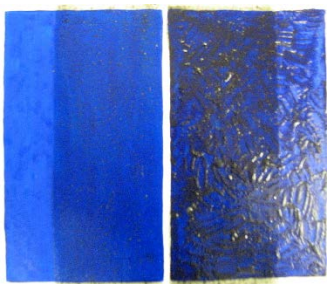

Figure 13. Blue oil drafting sample, with not treated and soiled areas.

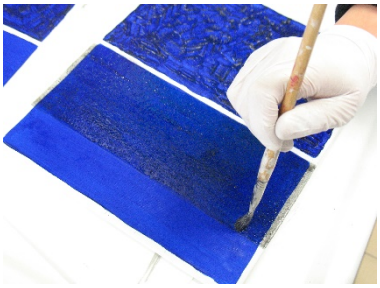

Figure 14. Example of sample soiled using a brush.

Cleaning tests were made rubbing soiled surfaces for 30 sec, using each *dry methods* and then, macroscopic residues were gently removed with a soft brush.
After cleaning treatments, all the areas were observed and characterized, in order to identify any changes due to mechanical or chemical actions.
Stereomicroscopy observation was carried out with 7X, 30X and 45X magnification, using VIS light; in the case of drafting samples analysed by ESEM, they were not pre-treated in any way (metallization with gold or graphite) and were analysed using instrumental variable pressure method (VP). Only blue colour was analysed, both oil and acrylic, of most representatives cleaning products (Fig. 83 and 91, Par. 2.2.4.2).
Previous sponges characterization (Par. 2.2.2), shown the presence of TiO_2 (both Rutile and Anatase), used as filler. As discussed below, the presence of these

nanoparticles on artistic surfaces after treatment could be dangerous for conservation of organic dyes [44,45,46,47].
For this reason, ESEM analysis were not performed on white paints, because of its composition: in fact, both oil and acrylic industrial colours contain Titanium dioxide as pigment.
Ultramarine blue oil and acrylic not present TiO_2 but, unfortunately, standard primer of priming linin paperboard used, contains Titanium dioxide as pigment. For this reason, it was not possible to characterize TiO_2 residues by ESEM microanalysis.
Nevertheless, this analysis was useful to better rate morphology characteristic of paint film and to study in detail changes that took place following cleaning procedure.
Gloss test was performed using two windows areas with different dimensions (1.3X3.5 cm and 1.3X4 cm) to restrict analysis surface and measurements were made three times for each samples.
Colorimetric data were collected with five acquisitions for each areas, not treated, soiled and cleaned and for statistical evaluation, a media of these values were considered.

2.2 Results and discussion

2.2.1 Erasers

2.2.1.1 Styrene-ethylene-butadiene-styrene copolymer (SEBS)

SEBS is the abbreviation for styrene-ethylene-butadiene-styrene block copolymer, a thermoplastic elastomer (TPE).

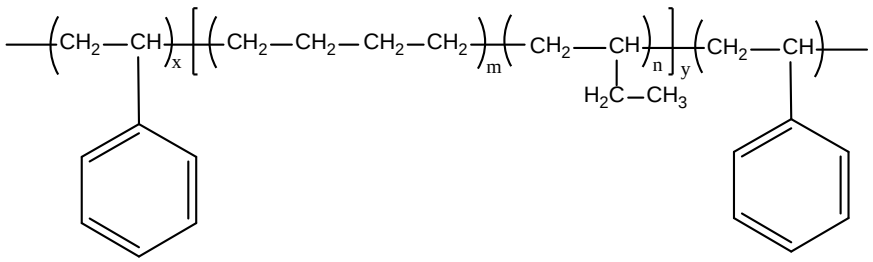

Figure 15. SEBS polymer structural formula.

In this type of styrenic TPE the polybutadiene mid-block used in the SBS types is replaced with ethylene-butylene which is saturated. SBS is based on two-phase block copolymers with hard and soft segments. The styrene end blocks provide the thermoplastic properties and the Butadiene mid-blocks provide the elastomeric properties.
SBS, when hydrogenated, becomes SEBS, as the elimination of the C=C bonds in the butadiene component generated ethylene and butylene mid-block. SEBS is characterised by improved heat resistance, mechanical properties and chemical resistance. Compounds based on SEBS exhibit excellent weathering, UV and ozone resistance making them ideal choice for outdoor and long service life applications.

Samples that give this composition are G_FC_3 and G_Wb_2, both erasers. Analytical results are reported below.
Observation of samples at stereomicroscopy reveals different characteristics of surfaces. Despite of the same composition, sample G_FC_3 appears more compacting and hard compared with G_Wb_2, which seems softer (Fig. 5). Macroscopic observation of materials confirms this appearance.
SEM-EDS analysis cannot be performed because of the difficulty to metallize surfaces with graphite.

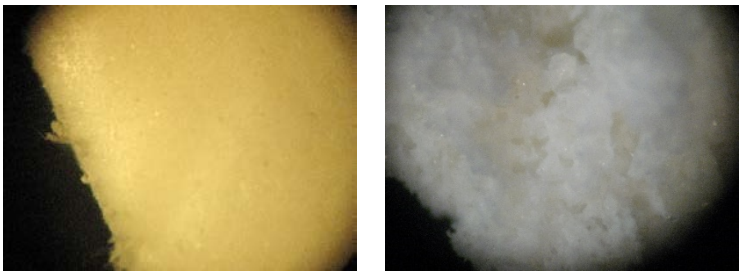

Figure 16. Stereomicroscopy images of samples: G_FC_3 (left) and G_Wb_2 (right) (30X).

µRaman spectrum acquired on sample G_Wb_2 reveals the presence of TiO_2 as nanoparticles of Rutile (see Fig. 30, Par. 2.2.2.1).
Characterization by FTIR-ATR spectroscopy gives spectra presented below.
Both samples G_FC_3 and G_Wb_2, gives signals of styrene-butadiene rubber (SBR) (Fig. 29): 3081w, 3058w, 3025w, 3005w, 2919vs, 2849s, 1809w, 1739w, 1642w, 1600w, 1450s, 1377ms, 1024w, 991w, 968ms, 909mw, 876ms, 756w, 729w and 700ms cm^{-1}.

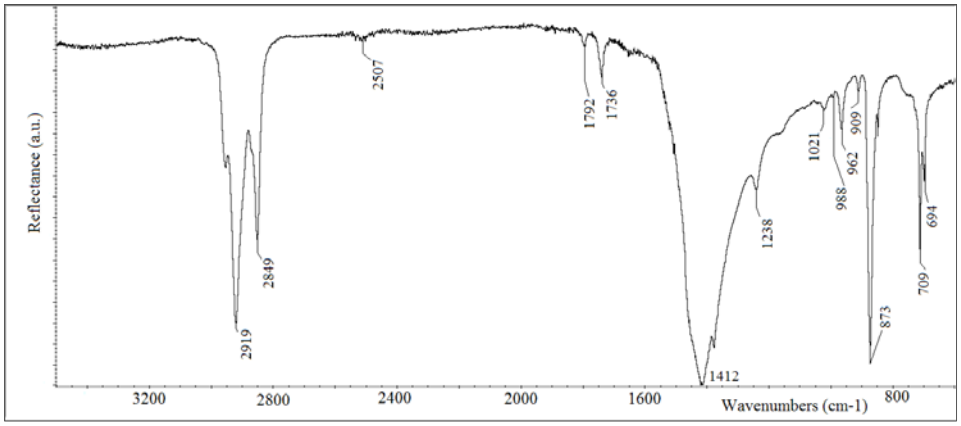

Figure 17. FTIR-ATR spectrum of sample G_FC_3.

In particular, G_FC_3 spectrum (Fig. 6) gives signals of SBR rubber (2919vs, 2849s, 1736mw, 1238mw, 1021w, 988vw, 909w and 694 cm^{-1}) and calcite ($CaCO_3$) too (2510w, 1789w, 1412vs, 873vs and 712ms cm^{-1}) added to polymer as inert filler to improve mechanical properties of material [48,49,50].

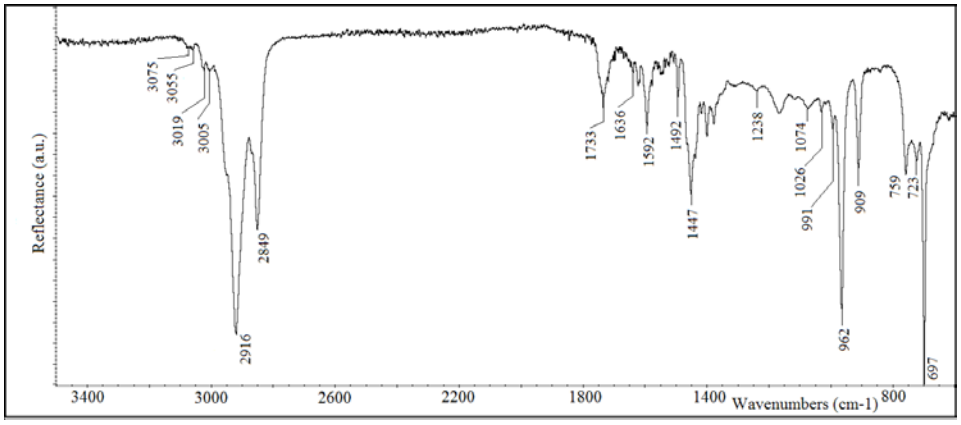

Figure 18. FTIR-ATR spectrum of sample G_Wb_2.

On the contrary, G_Wb_2 spectrum (Fig. 7), shows only peaks of SBR rubber (3075w, 3055w, 3019w, 3005w, 2916vs, 2849s, 1733w, 1636w, 1592w, 1492s, 1447ms, 1238w, 1074w, 1026w, 991w, 962ms, 909mw, 759w, 723w, 697ms cm^{-1}).

Py GC-MS chromatogram is shown in Fig. 8, while pyrolysis products are reported in Table 4. This characterization confirms polymer composition, as styrene-ethylene-butadiene-styrene block copolymer (SEBS).

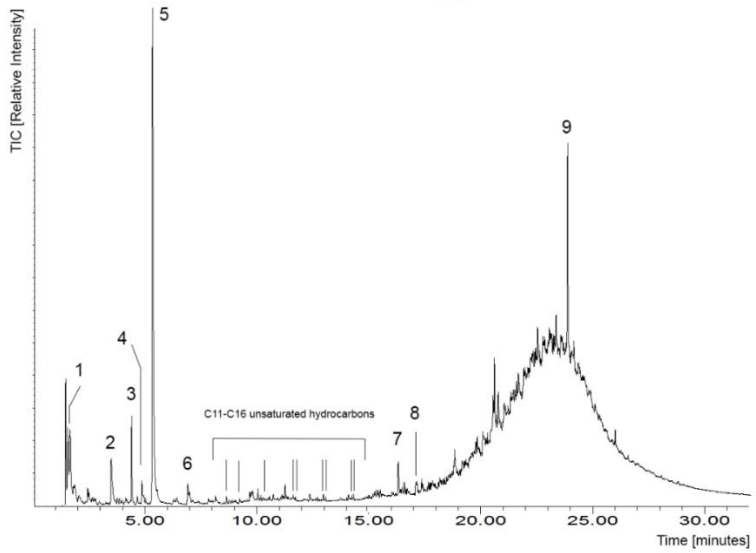

Figure 19. Py GC-MS chromatogram of sample G_FC_3, identified as SEBS.

Table 4. Styrene-ethylene-butadiene-styrene block copolymer (SEBS) pyrolysis products.

Peak n°	Retention Time [min]	Assignment	Principal ions [m/z]	MW
1	1,54	1,3-butadiene	39,54,53,50,51	54
2	3,38	toluene	91, 92, 65, 63, 51	92
3	4,29	4-vinylcyclohexene	54,79,80,66,67	108
4	4,76	ethylbenzene	91,106,51,92,65	106
5	5,23	styrene	104,103,78,51,77	104
6	6,8	alpha-methylstyrene	118,117,103,78,77	118
-	8,50-14,30	C11-C16 unsaturated hydrocarbons	-	-
7	16,21	1,3-diphenyl-propane	92,91,105,196,77	196
8	16,99	but-3-ene-1,3-diyldibenzene (S dimer)	91,104,130,208,65	208
9	23,77	5-hexene-1,3,5-triyltribenzene (S trimer)	91,117,194,207,312	312

Py GC-MS chromatogram reported below (Fig. 9), of sample G_Wb_2, show typical SEBS pyrolysis products (see Table 4), but it is possible to find pyrolysis products referable to the presence of two antioxidants [51], Hydrossytoluene butylate (BHT) (Fig. 10) and BKF (2,2'-methylenebis(4-methyl-6-tert-butylphenol)) (Fig. 11) too, at peaks at 14.57 min (7*) and 23.61 min (8*) respectively.

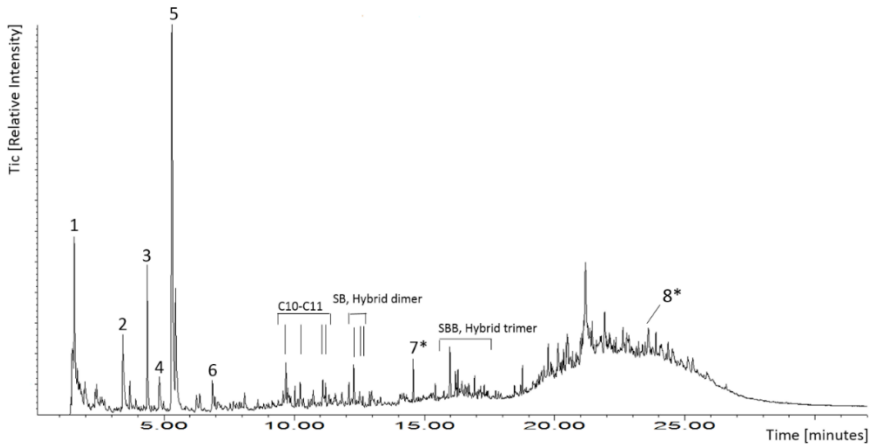

Figure 20. Py GC-MS chromatogram of sample G_Wb_2, identified as SEBS, with addition of an antioxidants (7, 8*).*

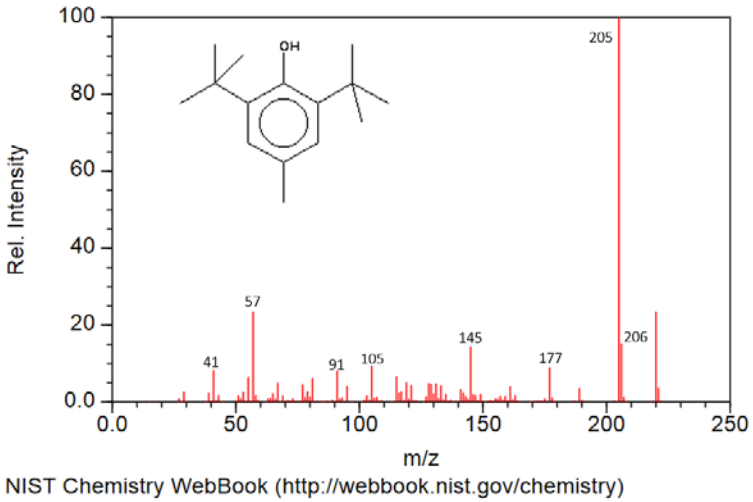

Figure 21. Mass spectrum of antioxidant BHT with structural formula.

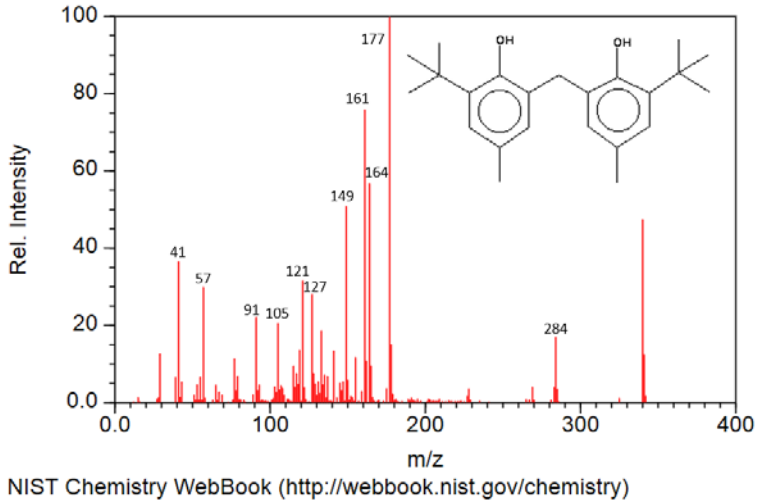

Figure 22. Mass spectrum of antioxidant BKF with structural formula.

2.2.1.1 Chlorosulphonated polyethylene (CSPE)

A product of the chemical modification of polyethylene by chlorine and sulphur dioxide, chlorosulphonated polyethylene has a chlorine content of 27–45 % and a sulphur content of 0.8–2.2 %.

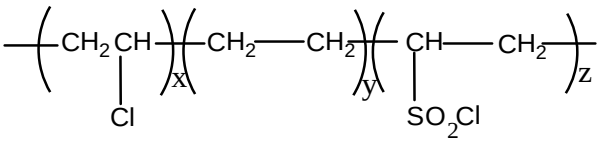

Figure 23. CSPE polymer structural formula.

Owing to the presence of chlorine, it is resistant to fire, oil and the action of microorganisms. It is insoluble in aliphatic hydrocarbons and alcohols, slightly soluble in ketones and esters and readily soluble in aromatic hydrocarbons, such as toluene and xylene and in chlorinated hydrocarbons.

Chlorosulphonated polyethylene is superior to other rubbers in its resistance to the effects of ozone and inorganic acids, such as chromic, nitric, sulphuric and phosphoric acids, as well as to the effects of concentrated alkalis, chlorine dioxide and hydrogen peroxide. It is resistant to light, is impermeable to gas and has good dielectric properties. Chlorosulphonated polyethylene made from high-density polyethylene may also be used in unvulcanised form.

Chlorosulphonated polyethylene is used in the production of industrial and household goods and of anticorrosion coatings to be applied by the rubberizing method. It is also used as a film-forming agent in varnishes and paints for the preservation of wood, metal and reinforced concrete and as a base for adhesives and hermetic sealants.

Dry methods materials made of this polymer are: G_Art, G_DB, G_Lal_2, G_Lli_1, G_Mi403 and G_Awb.
Images of samples observed at stereomicroscopy are reported below (Fig. 13).

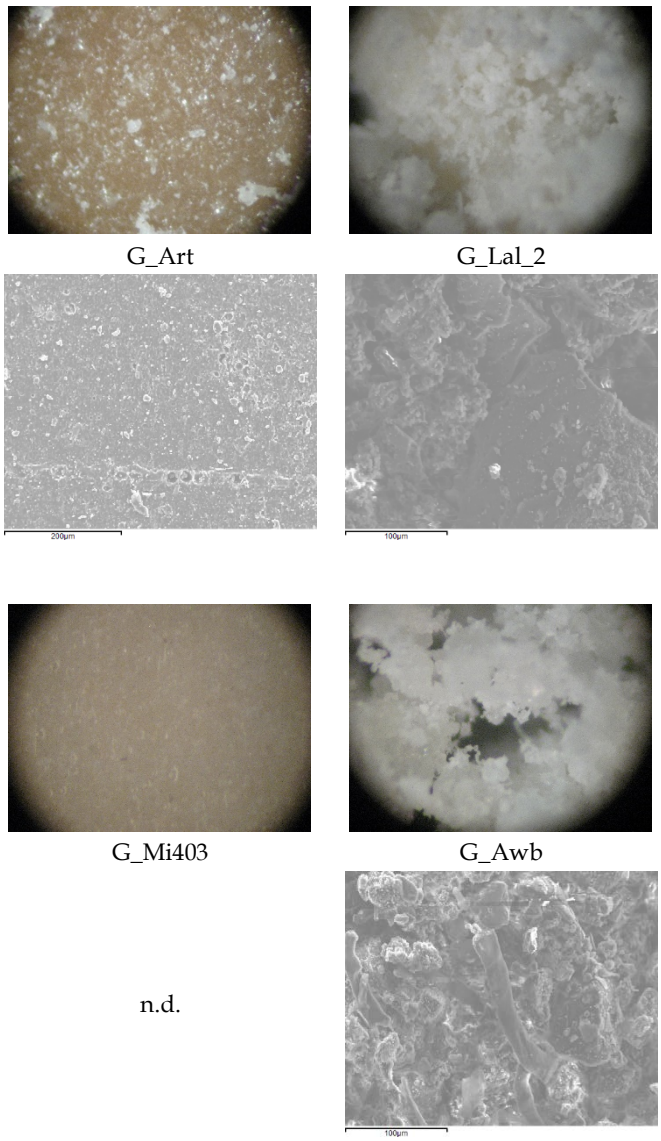

Figure 24. Stereomicroscopy (45X) and SEM-SEI (230X, 400X and 400x respectively) images of CSPE samples.

The sample G_Art is very different from G_Lal_2 and G_Lli_1 ones, that are quite similar. In fact, they are both gum file dust. The same observation can be made for sample G_DB that is very similar to G_Art one.

SEM_SEI images are very different, also between gum file dust and compact erasers. Into sample G_Lal_2, EDS microanalysis find out presence of Ti element; µRaman analysis confirms the addition of TiO_2 nanoparticles, in Rutile polymorph.

FTIR-ATR spectrum of sample G_DB is presented in Fig. 14 and shows both Chlorosulphonated polyethylene [52] signals (2959, 1259, 1089, 1023, 864 and 800cm-

[1]) and Factice ones (2921, 2851, 1739, 1459, 1376 and 1153 cm^{-1}) (see Fig. 24 b, Par. 2.2.1.4).

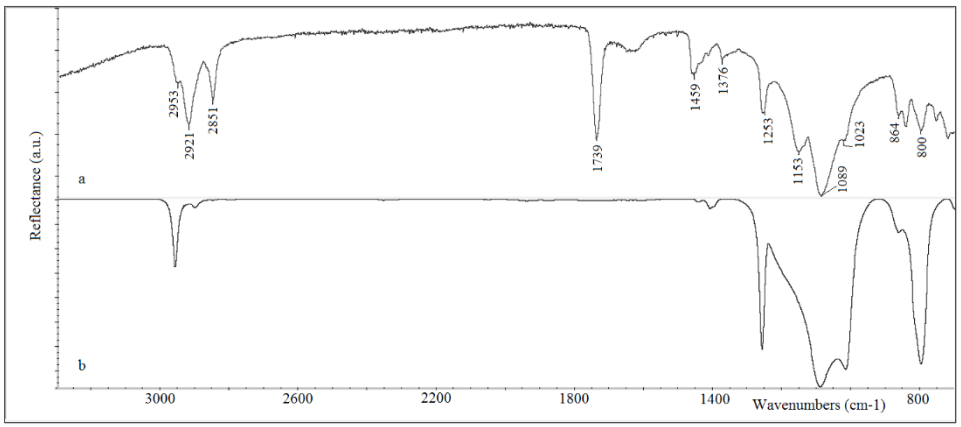

Figure 25. FTIR-ATR spectra of samples G_DB (a) and CSPE reference (b).

Fig. 15 reports Py GC_MS chromatogram of sample G_Art, classified as Chlorosulphonated polyethylene (CSPE) and pyrolysis products in Table 5.

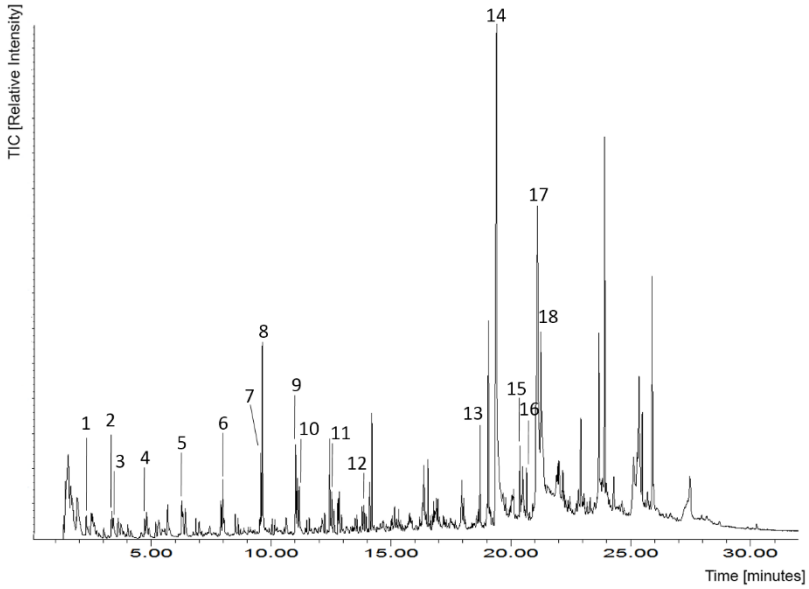

Figure 26. Py GC-MS chromatogram of sample G_Art, identified as CSPE.

Table 5. Chlorosulphonated Polyethylene (CSPE) pyrolysis products.

Peak n°	Retention Time [min]	Assignment	Principal ions [m/z]	MW
1	2.28	Benzene	78,77,52,39,74	78
2	3.34	Toluene	91,65,51,89	92
3	3.41	2-methyl thiophene	97,45,53,58,69,98	98
4	4.73	Ethylbenzene	91,106,51,65,77	106
5	6.27	Propylbenzene	91,120,65,78	120
6	7.97	Butylbenzene	91,134,65,105,78,51	134
7	9.57	Pentylbenzene	91,148,65,41,105,77,51	148
8	9.63	2-pentyl-thiophene	97,154,45,53	154
9	11.02	2-(trimethylacetyl)thiophene	111,57,41,168,83	168
10	11.09	Hexylbenzene	91,162,105,43,65	162
11	12.52	Heptylbenzene	92,176,43,65,105	176
12	13.87	Octylbenzene	92,190,57,43,105	190
13	18.71	2-heptadecanone	43,58,71,254	254
14	19.40	n-hexadecanoic acid (Palmitic Ac.)	60,73,43,129,83,97,115,256	256
15	20.38	Octadecanoic acid, 2-propenyl ester	43,57,100,113,71,83,267,324	324
16	20.66	2-nonadecanone	58,43,71,85,282	282
17	21.10	Cis-13-octadecenoic acid	55,69,41,83,97,111	282
18	21.25	Octadecanoic acid (Stearic Ac.)	43,73,60,129,69,284,185	284

Among this class of materials, some samples give also pyrolysis products different from CSPE polymer. This is the case of G_Awb, in which we find also PVC pyrolysis products, G_Lal_1, G_Lal_2 and G_Art, in which Factice pyrolysis products are present, maybe present also in samples G_DB and G_Mi403, but not easily detectable into Py GC-MS chromatograms.

2.2.1.2 Polyvinyl chloride (PVC)

Poly(vinyl chloride), commonly abbreviated PVC, is the third-most widely produced polymer, after polyethylene and polypropylene.
PVC comes in two basic forms: rigid (sometimes abbreviated as RPVC) and flexible. The rigid form of PVC is used in construction for pipe and in profile applications such as doors and windows. It is also used for bottles, other non-food packaging, and cards (such as bank or membership cards). It can be made softer and more

flexible by the addition of plasticizers, the most widely used being phthalates. In this form, it is also used in plumbing, electrical cable insulation, imitation leather, signage, inflatable products and many applications where it replaces rubber.
Pure Poly(vinyl chloride) is a white, brittle solid. It is insoluble in alcohol but slightly soluble in tetrahydrofuran.

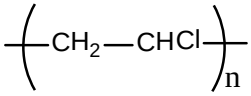

Figure 27. PVC structural formula.

Polyvinyl chloride is produced by polymerization of the monomer vinyl chloride (VCM).
About 80% of production involves suspension polymerization. Emulsion polymerization accounts for about 12% and bulk polymerization accounts for 8%. Suspension polymerizations affords particles with average diameters of 100–180μm, whereas emulsion polymerization gives much smaller particles of average size around 0.2μm.
The polymers are linear and are strong. The monomers are mainly arranged head-to-tail, meaning that there are chlorides on alternating carbon centres. PVC has mainly an atactic stereochemistry, which means that the relative stereochemistry of the chloride centres are random. About 57% of the mass of PVC is chlorine. The presence of chloride groups gives the polymer very different properties from the structurally related material polyethylene.
The product of the polymerization process is unmodified PVC. Before PVC can be made into finished products, it always requires conversion into a compound by the incorporation of additives such as heat stabilizers, UV stabilizers, plasticizers, processing aids, impact modifiers, thermal modifiers, fillers, flame retardants, biocides, blowing agents and smoke suppressors, and, optionally pigments.
Most vinyl products contain plasticizers, which dramatically improve their performance characteristic [53,54]. The most common plasticizers are derivatives of phthalic acid. These materials are usually oily colourless substances that mix well with the PVC particles.
Bis(2-ethylhexyl) phthalate was a common plasticizer for PVC but is being replaced by higher molecular weight phthalates.
Phthalates can be divided into three groups based on their molecular weight. Low molecular weight phthalates have six or seven carbon atoms in their alcohol chain. Medium molecular weight phthalates have eight or nine carbons in their alcohol

chain. High molecular weight phthalates have from ten to thirteen carbons in their alcohol chain. Low molecular weight phthalates are no longer used because of high volatility at PVC processing temperatures. The most common medium molecular weight phthalates are DOP (dioctyl phthalate, also known as DEHP, di-2-ethylhexyl phthalate) and DINP (diisononyl phthalate) [55]. High molecular weight phthalates have a limit of twelve carbons (if linear) or thirteen carbons (if branched) in the alcohol chain because phthalates with longer alcohol chains are incompatible with PVC resin.

Only one product selected among dry methods gives PVC composition: G_MRub.

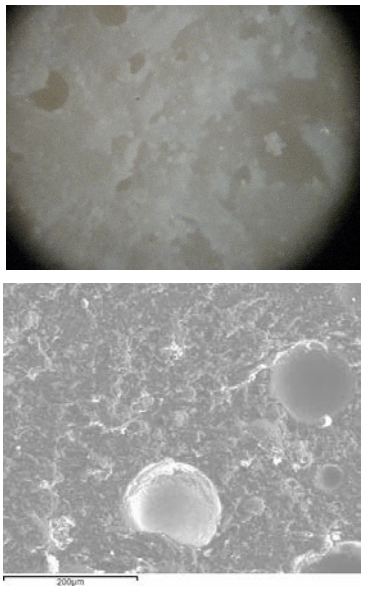

Figure 28. Sample G_MRub: (a) stereomicroscopy (45X) and (b) SEM-SEI (230X) images.

Surface is characterized by the presence of holes and unevenness (Fig. 17 a), but material seems to be hard. Handling this eraser, it is flexible and compact. SEM-EDS image confirms rubber superficial morphology (Fig. 17 b).
Comparison between FTIR-ATR G_MRub spectrum with database, highlights the presence of phthalates in the composition of rubber.
In spite of high signals of additives, it is possible to recognize PVC signals (Fig.18 a): 2960mw, 2927mw, 2852mw, 1410ms, 952w, 703s, 632w and 612w cm^{-1}. Spectrum also presents peaks of Polyester terephthalic acid used as plasticizer in rubber (Fig.18 b) (1726vs, 1511w, 1478mw, 1412ms, 1377ms, 1273vs, 1174w, 1123s, 1105ms, 1019ms, 976mw, 875w and 733s cm^{-1}).

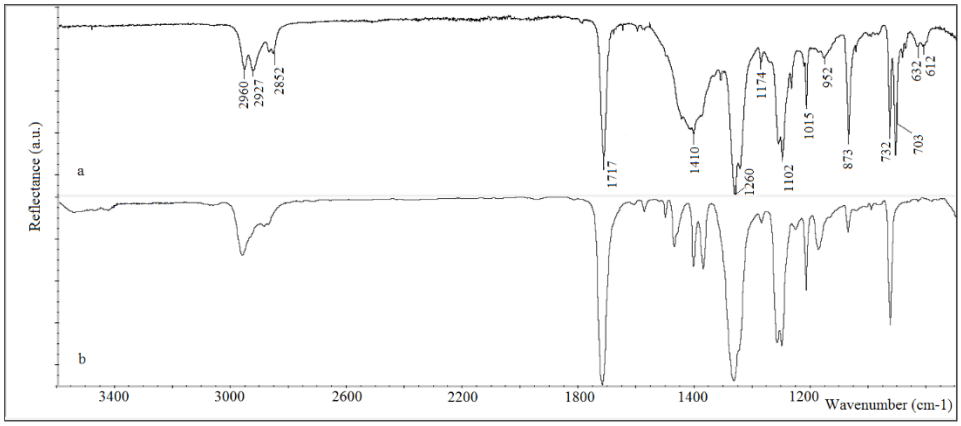

Figure 29. FTIR-ATR spectra of sample G_MRub (a) and Polyester terephthalic acid (b) as reference.

Py GC-MS spectrum is shown in Fig. 19. Besides PVC pyrolysis products (Table 6), other signals are present. They are attributable to plasticizers, in particular phthalates (Table 7). Mass spectra of Benzoic acid, 2-ethylhexyl ester, Terephthalic acid, di(4-octyl) ester and Diethylene-glycol dibenzoate are reported in Fig. 20, 21 and 22.

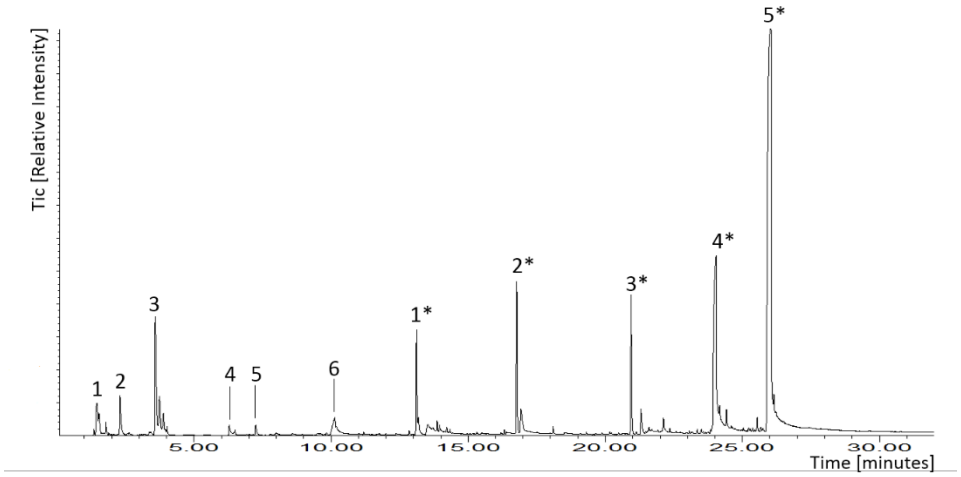

Figure 30. Py GC-MS chromatogram of sample G_Mrub, identified as PVC.

Table 6. Poly-vinyl-chloride rubber (PVC) pyrolysis products.

Peak n°	Retention Time [min]	Assignment	Principal ions [m/z]	MW
1	1.47	CO_2	44,28,16,12,22	44
2	2.30	Benzene	78,52,39,74	78
3	3.62	3-methylene heptane	70,55,41,42,27,29	112
4	6.31	Styrene	104,103,78,51,39,63	104
5	7,24	3-chloromethyl heptane	57,41,43,55,29,27,99	148

Table 7. PVC plasticizers pyrolysis products.

Peak n°	Retention Time [min]	Assignment	Principal ions [m/z]	MW
6	10.14	Benzoic acid	105,77,51,50,74,106	122
1*	13.11	Benzoic acid, 2-chloroethyl ester	105,122,77,51,23	184
2*	16.77	Benzoic acid, 2-ethylhexyl ester	105,70,77,123,83,55	234
3*	20.94	Methyl 2-ethylhexyl phthalate	-	292
4*	24.05	Diethylene glycol dibenzoato	105,147,77,51	314
5*	26.05	Therephthalic acid, di (4-octyl) ester	261,167,149,112,279,70	390

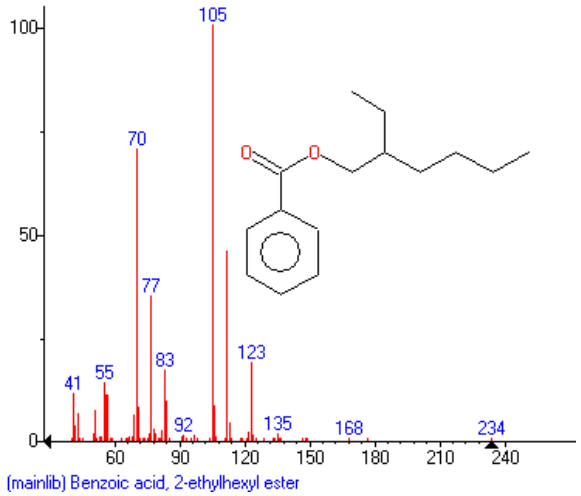

Figure 31. Benzoic acid, 2-ethylhexyl ester plasticizer.

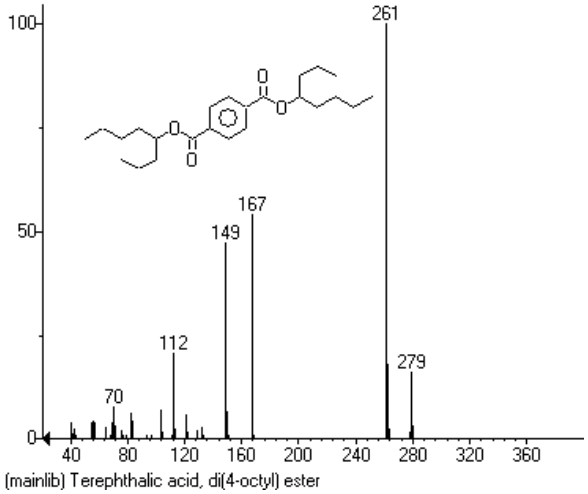

Figure 32. Terephthalic acid, di(4-octyl) ester plasticizer.

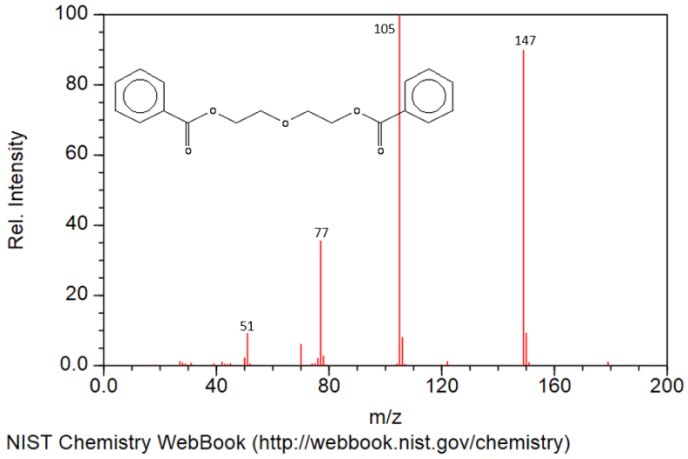

Figure 33. Diethylene-glycol dibenzoate plasticizer.

2.2.1.3 Vulcanized oils (Factice)

Factice is a vulcanized oil used as a compounding ingredient with the main functions of a processing aid or extender.

The oils from which factices are manufactured are unsaturated vegetable and animal oils, which react with sulphur [56]. Fatty oils with iodine number[4] greater than 80 are generally used, i.e., oils with three or more double bonds per triglyceride

[4] Iodine number is defined as the number of grams of iodine absorbed by 100 g of fat/oil.

molecule. Rapeseed oil is the most common oil used for general purpose grades and castor oil is used for oil resistant factice.
Factice has a number of uses in rubber compounds where it can stabilise dimensions of products such as hoses and tubing during the early stages of heating of the vulcanisation cycle. It imparts stability to extruded products, a silkiness to calendared products, gives good dimensional stability and overcomes many of the problems of "crow's feet" and blistering.
The addition level for the different applications varies from 5-10 phr for moulded articles to 15-30 phr for extrusions. Special products such as erasers use factice, usually white factice, at levels between 200-400 phr.
In general terms, factice gives benefits to rubber processing without causing any undue effects on physical properties [57].
There are different types of factice: dark and golden one, made by crosslinking unsaturated oils with sulphur (and an amine catalyst, usually triethanolamine) at 140-160 °C. These products will give dark coloured vulcanized that have poor contact stain properties when in contact with painted surfaces.
White factice, instead, is obtained by clear unsaturated oils, vulcanised at room temperature with sulphur monochloride to give a white, friable solid that is nonstaining and suitable for use in coloured compounds. Crosslinking using sulphur monochloride produces a white factice, but care had to be taken in its use, for if not used when fresh it develops a high level of acidity that affects compound cures severely. Modern white factices contain a small addition of alkali to counteract any developed acidity.
In appearance, factices are friable, slightly elastic materials, the colour ranging from white to dark brown depending on the method of manufacture. Factice has been popular for many years as a low-gravity resilient filler, finding particular application in spread sheeting compounds vulcanised by the cold cure method, and in erasers where the factice content may be as high as 300 phr. In recent years, work has been done on the use of factice in quite small amounts, since it has been found to have accelerating powers. Factices are available for use with most synthetic rubbers: SBR, polychloroprene, butyl-nitrile and chlorosulphonated polyethylene.

Samples that give this composition are: G_Fes_20, G_Fov12 and G_Ep.
Figure 23 shows stereomicroscopy and SEM_SEI images, which are quite similar from macroscopic point of view.

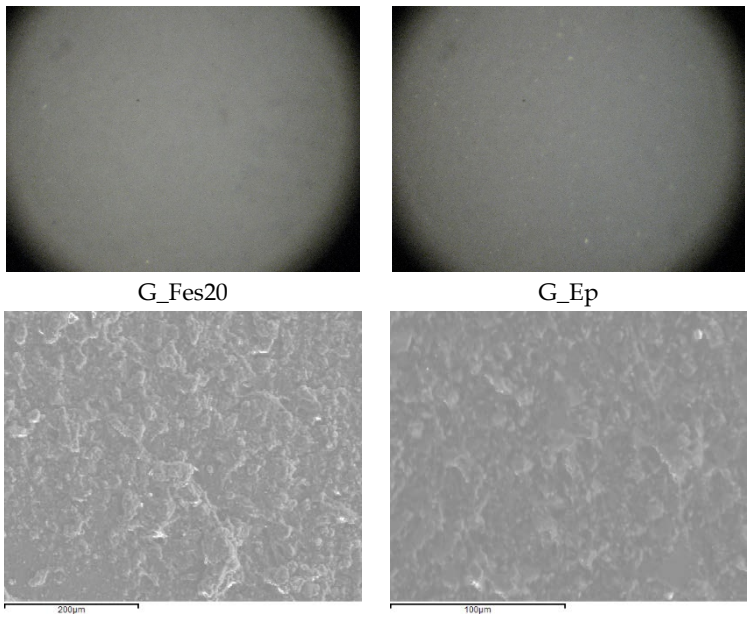

Figure 34. Stereomicroscopy (45X) and SEM-SEI (230X and 600x respectively) images of Factice samples.

In particular, sample G_Ep EDS microanalysis reveals abundance of Ti and Ca elements. µRaman spectrum confirms the presence of Ti as nanoparticles of TiO_2 as Rutile, while FTIR-ATR spectrum, the presence of $CaCO_3$. In addition, FTIR-ATR spectrum of G_Fes20 shows peaks attributable to $CaCO_3$ (2516, 1790, 1415, 870 and 711 cm^{-1}), besides peaks of oil (a: 3002, 2918, 2848, 1742, 1162, 1143, 962 and 905 cm^{-1}) according to reference spectrum (b: 3010, 2918, 2854, 1742, 1464, 1377, 1170, 1099 and 975 cm^{-1}) (Fig. 24).

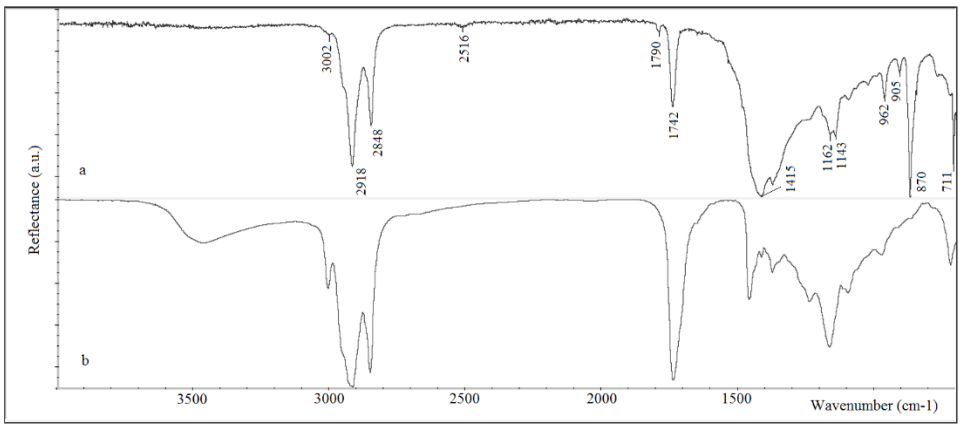

Figure 35. FTIR-ATR spectra of samples G_Fes20 (a) and Linseed oil reference (b).

To represent this type of polymer, Py GC-MS chromatogram of sample G_Fes20 is reported in Fig. 25 while pyrolysis products in Table 8.

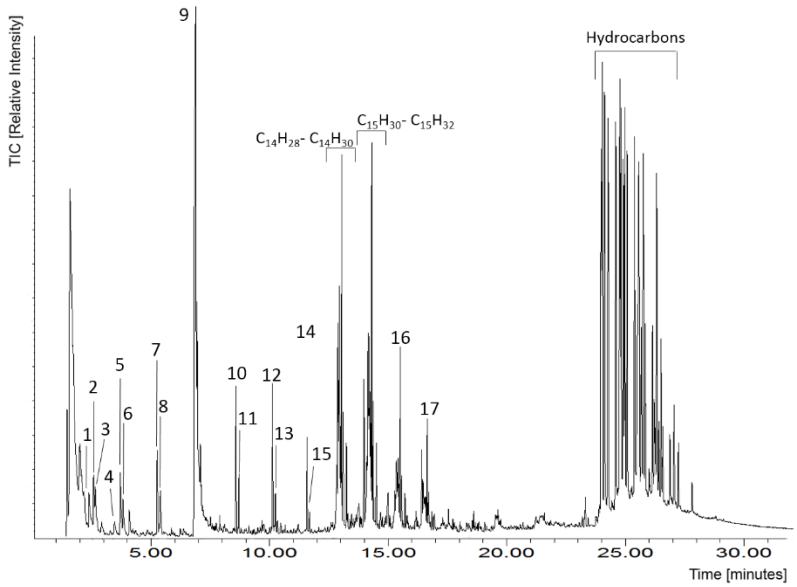

Figure 36. Py GC-MS chromatogram of sample G_Fes20, identified as Factice.

Table 8. Factice rubber pyrolysis products.

Peak n°	Retention Time [min]	Assignment	Principal ions [m/z]	MW
1	2.28	Benzene	78,52,39,74	78
2	2.47	1-Heptene	41,56,70,98	98
3	2.54	Heptane	43,41,57,71,100	100
4	3.53	Toluene	91,65,51,89	92
5	3.60	1-Octene	43,55,70,41,83,112	112
6	3.71	Octane	43,57,85,41,71,114	114
7	5.15	1-Nonene	43,55,69,83,97,126	126
8	5.29	Nonane	43,57,85,71,128	128
9	6.76	α-Methylstyrene	118,103,78,91,51	118
10	8.47	1-Undecene	41,55,70,83,97,111,154	154
11	8.60	Undecane	57,43,71,85,156	156
12	10.02	1-Dodecene	55,41,83,69,97,111,168	168
13	10.14	Dodecane	57,43,71,85,170	170
14	11.47	1-Tridecene	55,41,83,69,97,111,182	182
15	11.58	Tridecane	57,43,71,85,99,184	184
16	15.40	Hexadacane	57,43,71,85,99,226	226
17	16.54	Heptadecane	57,43,71,85,99,240	240

2.2.2 Sponges

2.2.2.1 Styrene-butadiene rubber (SBR)

During the Second World War, in order to supply natural rubber, many countries sought to produce a synthetic alternative; SBR was the result and at one stage it was the most commonly used synthetic rubber.
It can be produced by both emulsion and solution polymerization techniques, with the emulsion grades being the most widely used.
Emulsion polymerization yields a random copolymer, but the temperature of the polymerization reaction also controls the resultant properties obtained. "Cold" polymerization yields polymers with superior properties to the "hot" polymerized types.
Solution polymerization can yield random, di-block, tri-block or multi-block copolymers. It is important to note that the tri-block, or multi-block copolymers, belong to that class of material termed *thermoplastic elastomers.*
Both random emulsion and solution polymerized SBR contain about 23% styrene.

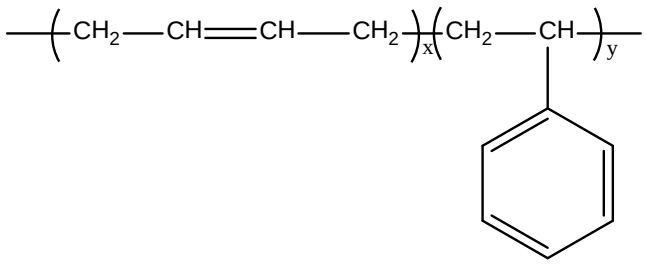

Figure 37. SBR polymer structural formula.

SBR continues to be used in many of the applications where it earlier replaced natural rubber, even though it requires greater reinforcement to achieve acceptable tensile and tear strengths and durability.
The oil resistance of SBR is poor, and the polymer is not resistant to aromatic, aliphatic or halogenated solvents. Due to the unsaturation in the main chain, protection is required against oxygen, ozone and UV light.
The major use of SBR is in tyres, predominantly car and light truck; in the latter use it is frequently blended with NR and BR. SBR also finds use in conveyor belts, moulded rubber goods, shoe soles, hose and roll coverings. SBR is also available as a latex which is used in carpet backing and other applications.

Among *dry cleaning* materials, only one product belong to this class of polymer. It is a make-up sponge and in particular is sample S_HM_uo. Most of make-up sponges, show a double composition, as reported below (Par. 2.2.2.3).
Observation of surface by stereomicroscopy of sample S_HM_uo, reveals holes matter with open porosity (Fig. 27 a), confirmed by SEM-EDS image (Fig. 27 b) where big and open porosity is visible.
From EDS microanalysis spectrum (Fig. 27 c) is visible the presence of a quite intense signal of Ti element, besides other elements, as S, used, probably as cross linker [58,59,60].

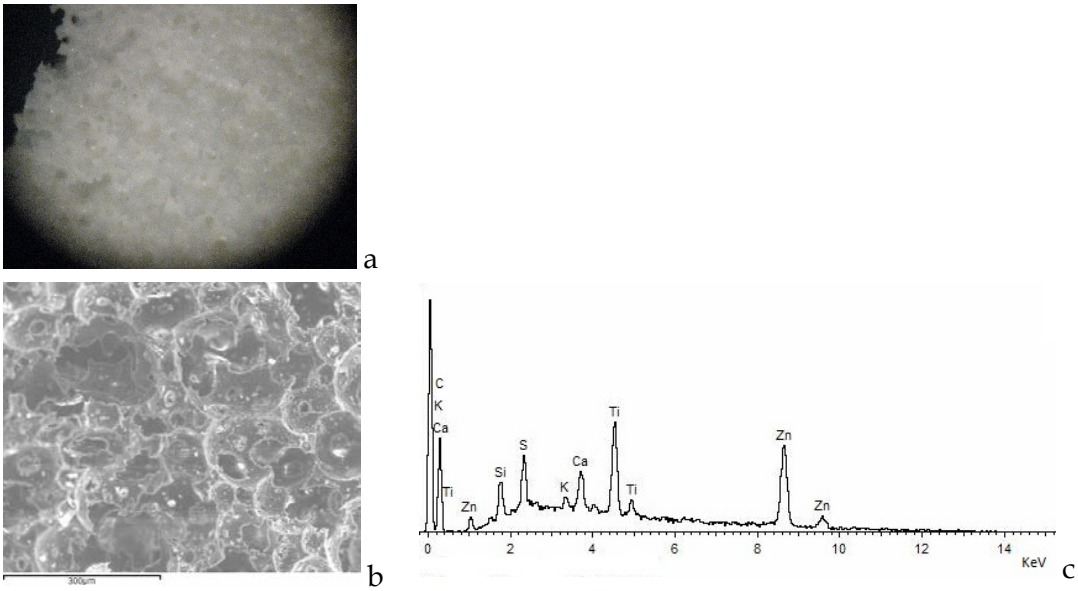

Figure 38. Sample S_HM_uo: (a) stereomicroscopy (30X), (b) SEM-SEI (180X) images and (c) EDS spectrum.

Spectrum shown in Fig. 28 related to sample S_HM_uo, reports FTIR-ATR peaks of SBR rubber: 3058w, 3022w, 2916ms, 2843mw, 1633w, 1598w, 1492w, 1450mw, 1433w, 1347w, 1306w, 1233w, 1068w, 1029w, 991w, 959vs, 96mw, 756mw and 697s cm^{-1}. Reference spectrum of database SBR rubber is reported in Fig. 29.

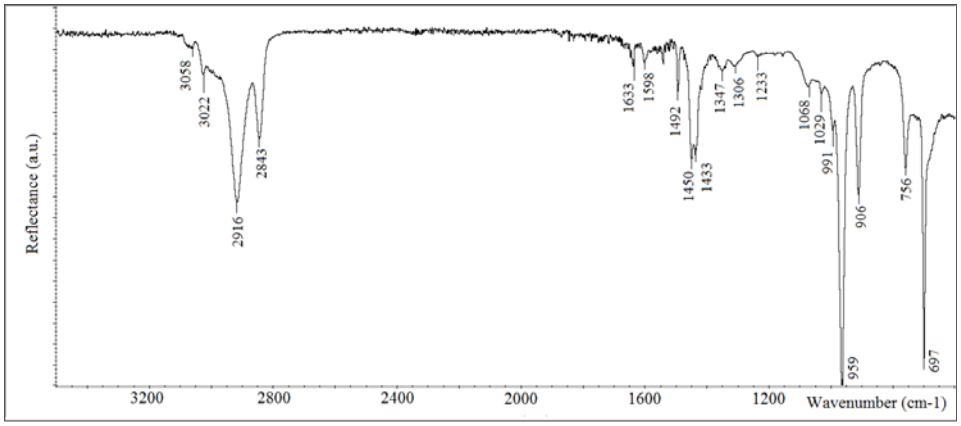

Figure 39. FTIR-ATR spectrum of sample S_HM_uo.

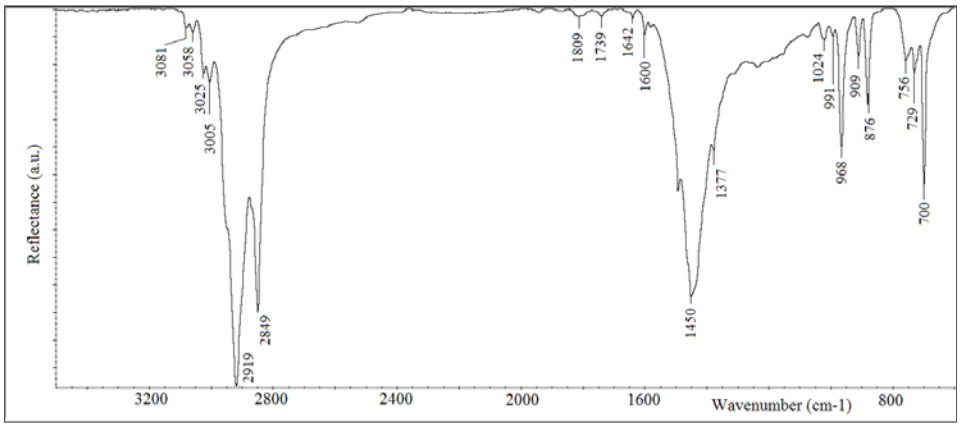

Figure 40. FTIR-ATR spectrum of SBR rubber reference.

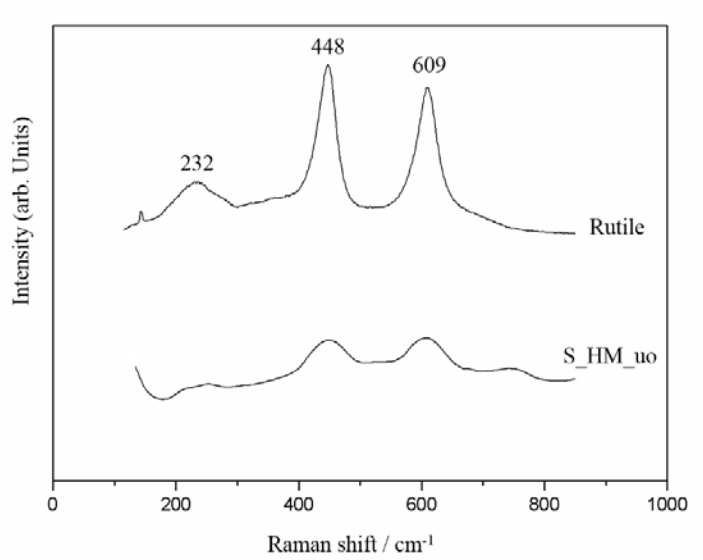

Figure 41. µRaman spectrum of sample S_HM_uo compared with TiO_2 Rutile reference one.

Considering EDS microanalysis results, also µRaman analysis was performed on S_HM_uo sample.

Spectrum shown in Fig. 30 reveals the presence of TiO_2 nanoparticles, due to addition on polymeric dough, of Rutile (232, 448 and 609 cm^{-1}) as filler, used both as whitening and as mechanical resistance improver [61,62,63].

Py GC-MS chromatogram confirms FTIR-ATR previous attribution; in Fig. 31 spectrum is reported and Styrene-butadiene pyrolysis products are listed in Table 9.

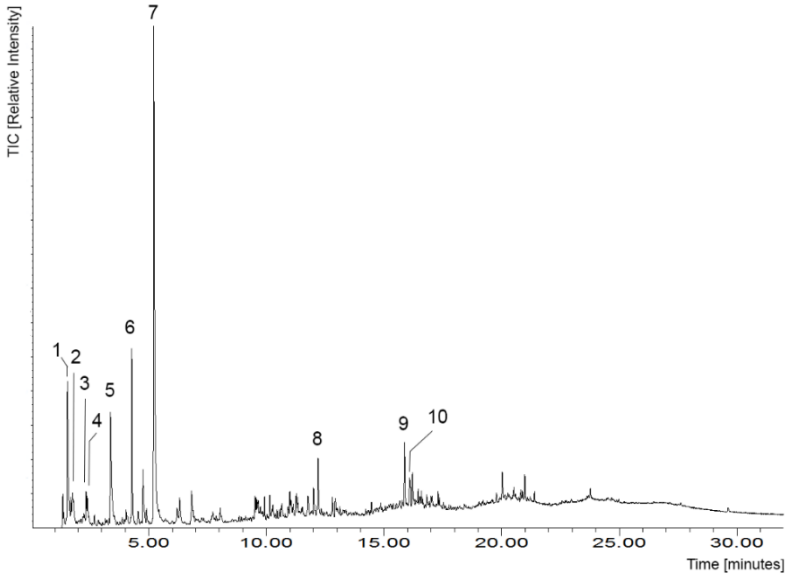

Figure 42. Py GC-MS chromatogram of sample S_HM_uo, identified as SBR.

Table 9. Styrene-butadiene rubber (SBR) pyrolysis products.

Peak n°	Retention Time [min]	Assignment	Principal ions [m/z]	MW
1	1,54	1,3 - butadiene	39,54,53,50,51	54
2	1,76	cyclopentadiene	66,65,40,63,67	68
3	2,33	benzene	78,77,51,50,52	78
4	2,38	cyclohexadiene	79,78,77,80,51	80
5	3,37	toluene	91,92,65,63,51	92
6	4,28	4-vinylcyclohexene (butadiene dimer)	54,79,66,93,41	108
7	5,21	styrene	104,103,78,51,63	104
8	12,2	styrene-butadiene hybrid dimer	104,158,81,128,78	158
9	15,87	styrene-butadiene-butadiene hybrid trimer	104,91,129,143,108	204
10	16,09	styrene-butadiene-butadiene hybrid trimer	104,91,117,79,129	204

2.2.2.2 Natural rubber (NR)

NR can be isolated from more than 200 different species of plant; only one tree source, *Hevea Brasiliensis*, is commercially significant.

Latex is an aqueous colloid of NR and is obtained from the tree by "tapping" into the inner bark and collecting the latex in cups. The latex typically contains 30-40% dry rubber by weight and 10-20% of the collected latex is concentrated by creaming, or centrifuging and used in its latex form. The remaining latex is processed into dry rubber as sheets, crepes and bales.
NR is cis-1,4-polyisoprene, of molecular weight 200.000-500.000, but it also contains a small level of highly important non-rubber constituents. Of these, the most important are the proteins, sugars and fatty acids which are antioxidants and activators of cure. Trace elements present include K, Mn, P, Cu and Fe which can act as catalysts for oxidation.

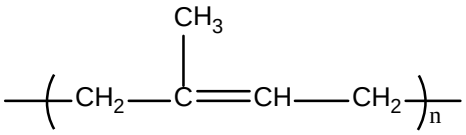

Figure 43. NR polymer structural formula.

Since the main chain of NR contains unsaturation (residual double bonds) it, along with other unsaturated rubbers, is susceptible to attack by oxygen, ozone and light and compounds therefore require protection against these agencies.
NR is not oil resistant and is swollen by aromatic, aliphatic and halogenated hydrocarbons. It is resistant to many inorganic chemicals, but not to oxidising acids and had limited resistance to mineral acids. It is unsuitable for use with organic liquids in general, the major exception being alcohols of low molecular weight.
NR can be crosslinked by the use of sulphur, sulphur donor systems, peroxides, isocyanate cures and radiation, although the use of sulphur is the most common method [64,65].
The sulphur vulcanisation of NR generally requires higher added amounts of sulphur and lower levels of accelerators than the synthetic rubbers.
The uses of NR are myriad and a complete summary is not really possible. Its unique and excellent properties are utilized in tyres, shock mounts, seals, isolators, couplings, bridge bearings, building bearings, footwear, hose, conveyor belts, plant linings and many other moulding applications.
Latices and solutions are used to produce adhesives, carpet backings, upholstery foam, gloves and medical devices such as catheters. NR is also frequently used in blends with other elastomers.

Among *dry methods* considered, three samples give very natural rubber composition: AS_Sft_4, AS_Sft_6 and G_SS_0001.

Figure 44. Stereomicroscopy images of samples: AS_Sft_4 (left), AS_Sft_6 (centre) and G_SS_0001 (right) (30X).

Observation of surfaces with stereomicroscopy reveals differences, especially between Art sponges (Fig. 33 a, b) and Smoke sponge (Fig. 33 c). AS_Sft_4 and AS_Sft_6 have similar porosity, the only difference is colour: pink and white; otherwise, G_SS_0001 shows very bigger and opener porosity. This characteristic is clear also from macroscopic point of view.

In addition, in this case, SEM-EDS analysis cannot be performed because of the difficulty to metallize surfaces of these samples with graphite.

FTIR-ATR spectra of samples AS_Sft_4, AS_Sft_6 and G_SS_0001 do not give clear signals attributable to any polymer. Only for the latter sample, spectra reveals the presence of a great amount of calcite ($CaCO_3$) added as filler (see sample G_FC_3 Par. 2.2.1.1), confirmed also by SEM-EDS microanalysis, μRaman spectroscopy and TGA.

Py GC-MS chromatogram of sample AS_Sft_4 is presented in Fig. 34. It finally clarifies the composition, i.e. natural rubber (NR). Table 10 reports the pyrolysis products.

Unlike SBR material, in NR products a variable amount of antioxindant is added. In fact, at 14.57 min, chromatogram reports a BHT (Hydrossytoluene butylate) pyrolysis product (1*).

Also samples AS_Sft_6 and G_SS_0001 show comparable Py GC-MS chromatograms, consequently the same polymer asseignments.

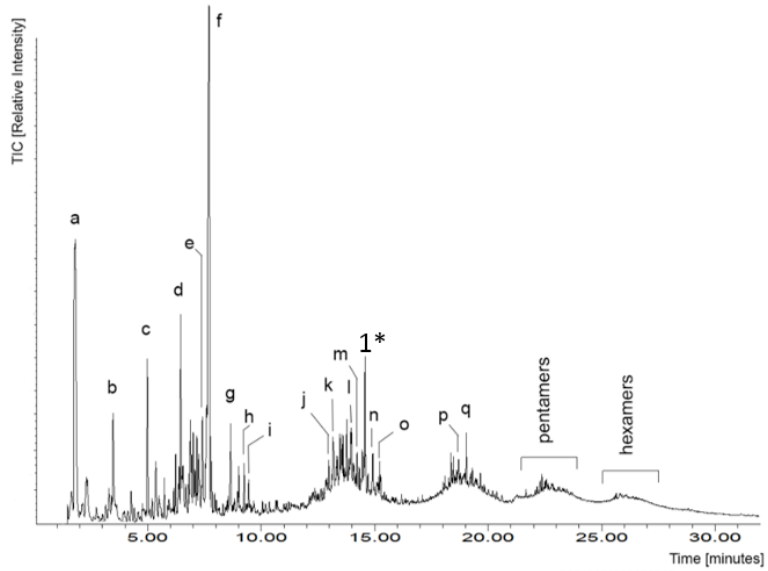

Figure 45. Py GC-MS chromatogram of sample S_Sft_4, identified as NR.

Table 10. Natural rubber (NR) pyrolysis products.

Peak n°	Retention Time [min]	Assignment	Principal ions [m/z]	MW
a	1,65	isoprene	67, 68, 53, 41, 39	68
b	3,42	toluene	91, 92, 65, 63, 51	92
c	4,85	xylene	91, 106, 105, 77, 92	106
d	6,31	limonene	68, 93, 107, 121, 136	136
e	7,37	2,5-dimethyl-3-methylene-1,5-heptadiene	91, 107, 79 ,121 ,41	136
f	7,54	limonene	68, 93, 107, 121, 136	136
g	8,62	1-Methyl-4-isopropenylbenzene	132, 117, 115, 91, 131	132
h	9,21	isoprene dimer	121,136,105,91,79,77	136
i	9,41	isoprene dimer	121,136,105,91,79,77	136
j	12,97	isoprene trimer	119, 93, 105, 120, 107	204
k	13,18	isoprene trimer	107, 93, 91, 105, 79	204
l	13,77	isoprene trimer	93,107,69,134,81	204
m	14,22	isoprene trimer	93,107,119,79,55	205
n	14,91	isoprene trimer	93,119,79,107,189	206
o	15,23	isoprene trimer	109,93,79,204,67	207
p	18,71	isoprene tetramer	93,107,119,81,55	272
q	19,06	isoprene tetramer	121,93,107,134,81	272

2.2.2.3 Styrene-butadiene rubber (SBR)/Natural rubber (NR)

SBR/NR mixture is the most representative class of compounds among materials selected for this research.

In fact, quite all make-up sponges are attributable to this mixture, in particular: AS_Sft_2, S_RB_py, S_HM_tr, S_KK_ro, S_PP_ov, S_PP_ro, S_PP_tr, S_RB_ro, S_RB_tr, S_RB_uo and S_Sph_sp.

Fig. 35 reports stereomicroscopy and SEM-SEI images of these samples; first observation is that porosity of each material is not homogeneous. Comparing products of the same producers (for example Royal Beauty – RB) at the same magnification, morphology of polymer changes from one type to another. This fact is more visible, observing SEM-SEI images (acquired at the same magnification): some sponges have open and inhomogeneous holes, while others closed and more or less homogenous pores size, even though are made of the same polymer.

EDS microanalysis of sponges, gives different results: among samples, some present traces of Ti (as for spectrum of Fig. 27 c, Par. 2.2.2.1), in particular: S_RB_tr, S_KK_ro, S_HM_tr and S_Sph_sp. The latter contains nanoparticles of TiO_2 as Rutile polymorph (see Fig. 30, Par.2.2.2.1), while other samples, Anatase one. µRaman spectra of sample S_RB_tr and Anatase are reported in Fig. 36; in the first one are visible Raman shift signals of Anatase at 144, 397, 518 and 640 cm^{-1}.

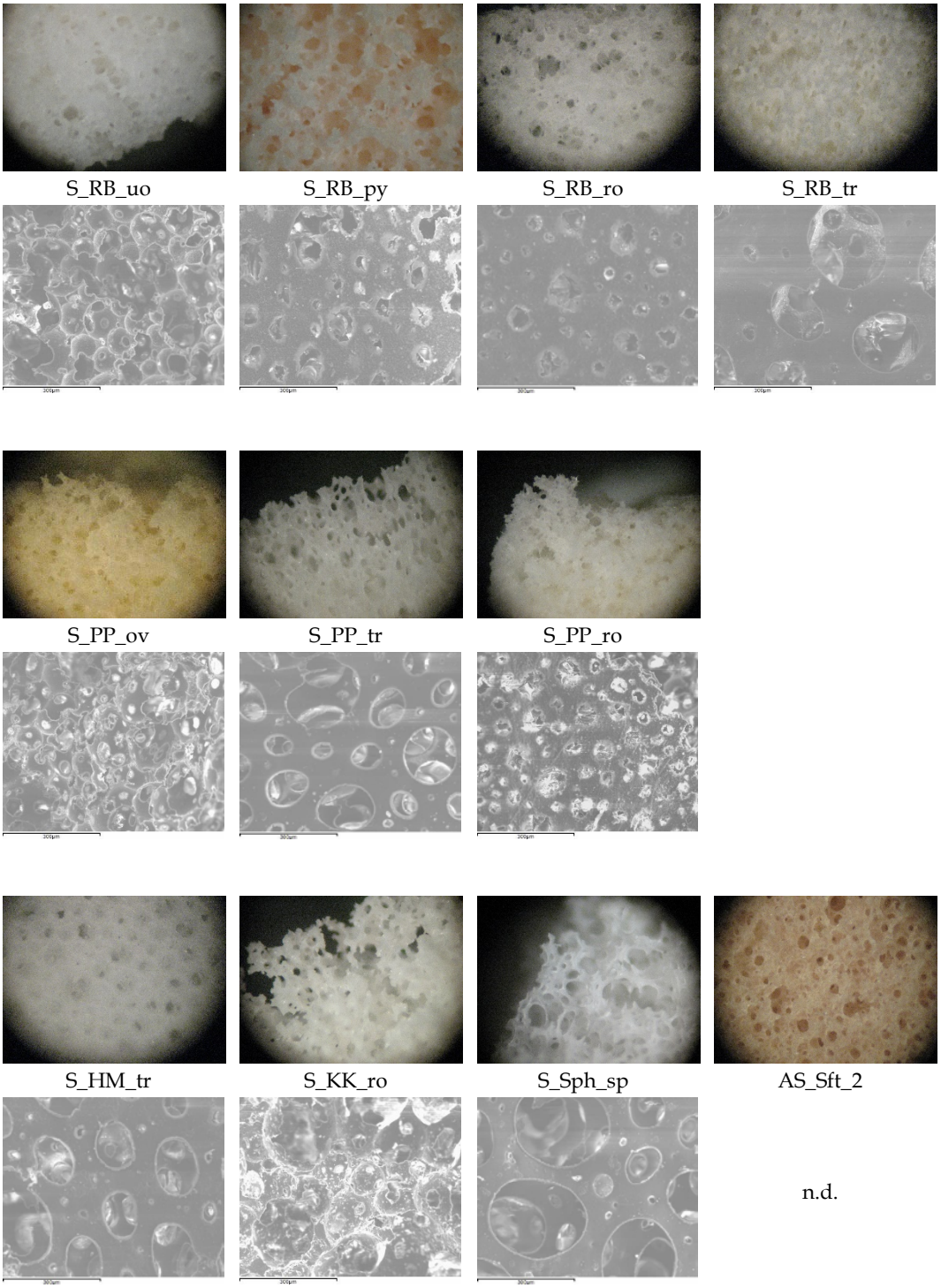

Figure 46. Stereomicroscopy (30X) and SEM-SEI (180X) images of SBR/NR samples.

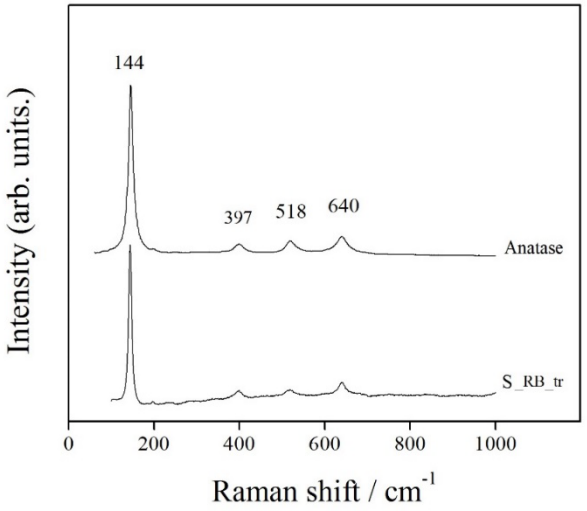

Figure 47. µRaman spectrum of sample S_RB_tr compared with TiO_2 Anatase reference one.

Characterization of samples with FTIR-ATR gives comparable spectra. For this reason, only spectrum of sample S_Sph_sp is reported (Fig. 37).
It is possible to identify SBR peaks (3061vw, 3025w, 2960ms, 2919s, 2843ms, 1636w, 1595w, 1447ms, 1026w, 991mw, 962vs, 912mw, 759mw and 697vs cm^{-1}) and NR peaks too (2960ms, 2919s, 2843ms, 1548mw, 1521mw, 1489w, 1374ms, 1308w, 1271w, 1207w, 1126w, 1078w, 838ms cm^{-1}).

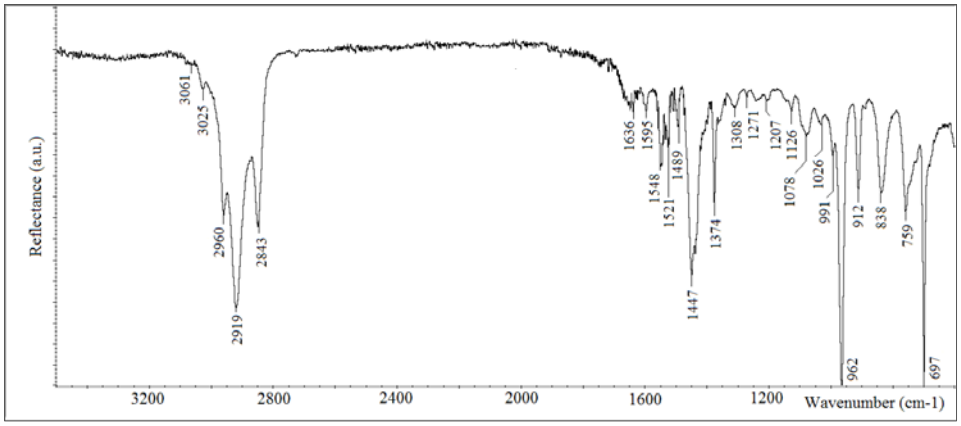

Figure 48. FTIR-ATR spectrum of sample S_Sph_sp.

Py GC_MS chromatograms are comparable, so only sample S_RB_uo is reported (Fig. 38). Pyrolysis products reveal the presence of both polymers, SBR and NR (numbers and letters marks in chromatogram respectively) (see Table 9, Par.2.2.2.1

and Table 10, Par.2.2.2.2, respectively). It shows BHT pyrolysis product too (14.59 min).

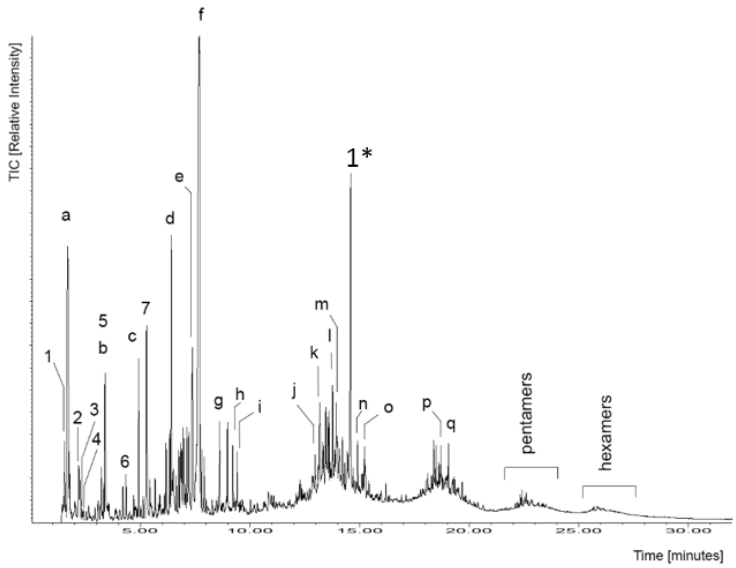

Figure 49. Py GC-MS chromatogram of sample S_RB_uo, identified as SBR/NR.

Quite all SBR/NR make-up sponges samples contain BHT or BKF antioxidants; three samples, plasticizers too (Hexadecanoic acid, bis (2-ethylhekyl) ester- DEHA Fig. 41 and Di-isooctyl isophthalate – DIOIP Fig. 43) (Table 11).

Table 11. SBR/NR Make-up sponges containing antioxidants and plasticizers.

Samples	Antioxidant	Plasticizers
AS_Sft_2	BHT	-
S_KK_ro	-	DEHA
S_HM_tr	BHT	-
S_PP_ro	BKF	-
S_PP_ov	BKF	DIOIP
S_PP_tr	BHT	-
S_RB_py	BHT	-
S_RB_ro	BHT	-
S_RB_tr	BHT	DIOIP
S_RB_uo	BHT	-
S_Sph_sp	BHT	-

Figures 39 and 41 report Py GC-MS chromatograms of samples S_KK_ro and S_PP_ov respectively.
In the first one, peaks referable to DEHA are presents, while in the second one, DIOIP signals are shown, plasticizer commonly used in cosmetics and personal care products.

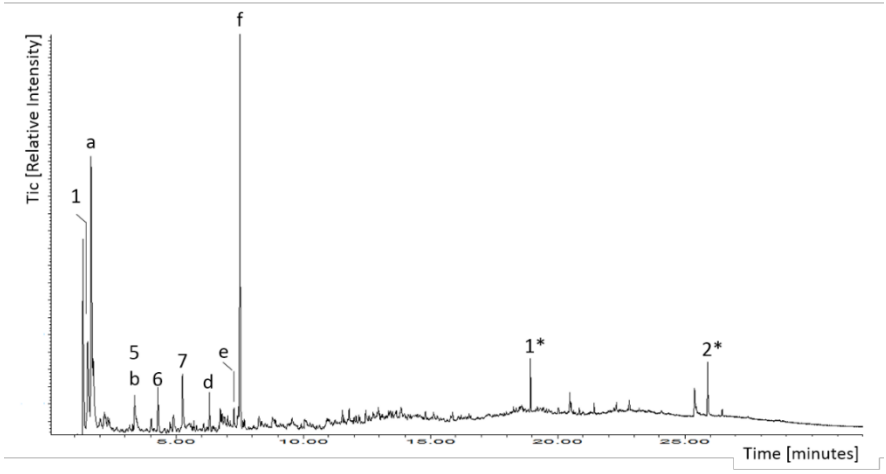

Figure 50. Py GC-MS chromatogram of sample S_KK_ro, identified as SBR/NR with the presence of DEHA (peaks 1 and 2*).*

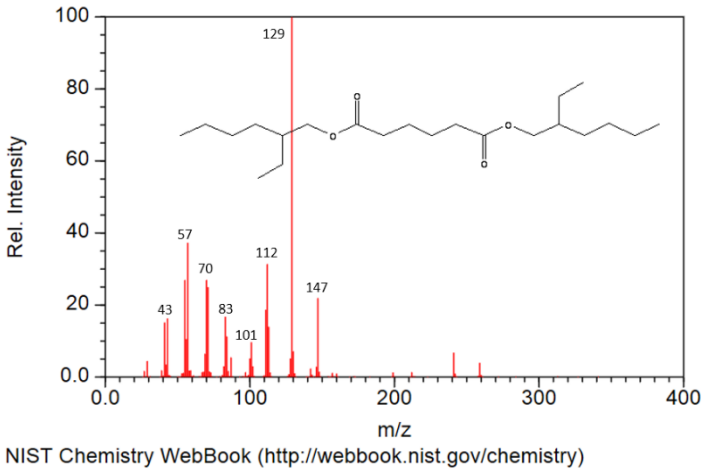

Figure 51. Mass spectrum of DEHA plasticizer.

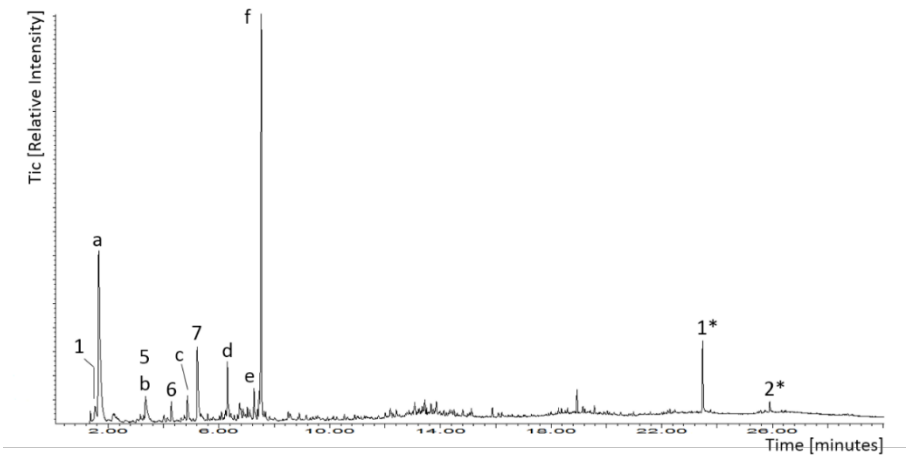

Figure 52. Py GC-MS chromatogram of sample S_PP_ov, identified as SBR/NR with the presence of DIOIP (peaks 1 and 2*).*

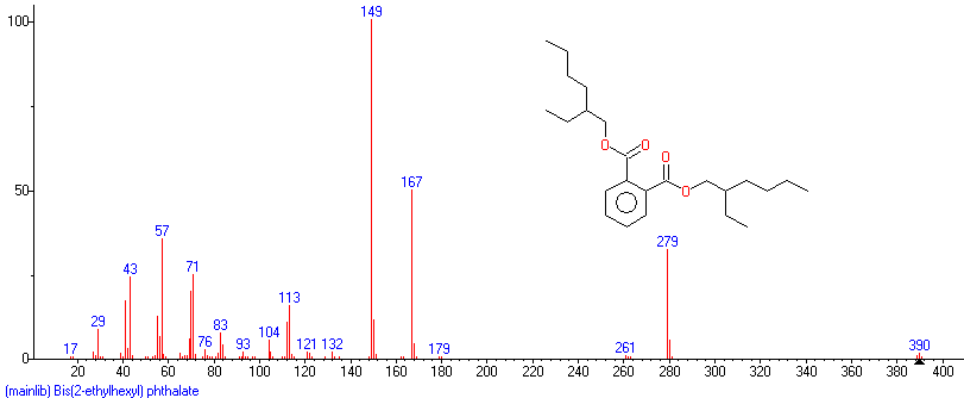

Figure 53. Mass spectrum of DIOIP plasticizer.

Double composition of this class of materials suggested TGA analysis to evaluate the amount of single polymer to the mixture.

Thermogram of sample S_PP_ro is shown in Fig. 43. Weight loss is divided into three steps: the first 2.86% is due to water loss; the second one of 55.17%, is due to natural rubber decomposition and the latter of 35.83% to SBR decomposition. Derivative curve produces two peaks, one at ~380°C, attributable to NR and one at ~440°C attributable to SBR [66].

Observing curves trend it is possible to suppose that the amount of SBR polymer is slightly higher than that of NR.

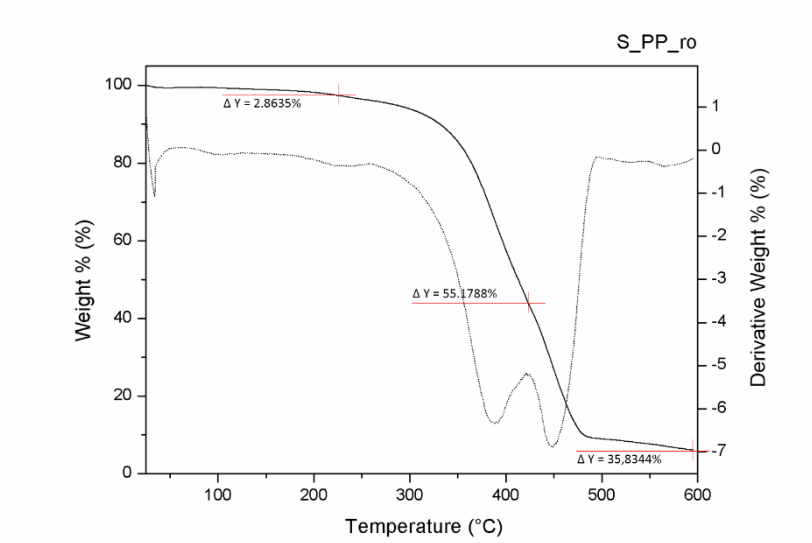

Figure 54. Thermogram sample S_PP_ro with SBR/NR composition.

Comparing previous sample with S_RB_py, we can notice that the trend of the weight loss curve is the same of sample S_PP_ro confirming double composition, while percentages change (1.26%, 75.25% and 20.28%) and, above all, derivative shape is very different, but not from decomposition temperatures point of view (Fig. 44). In fact, it reveals that in this sample there is higher amount of NR than that of SBR.

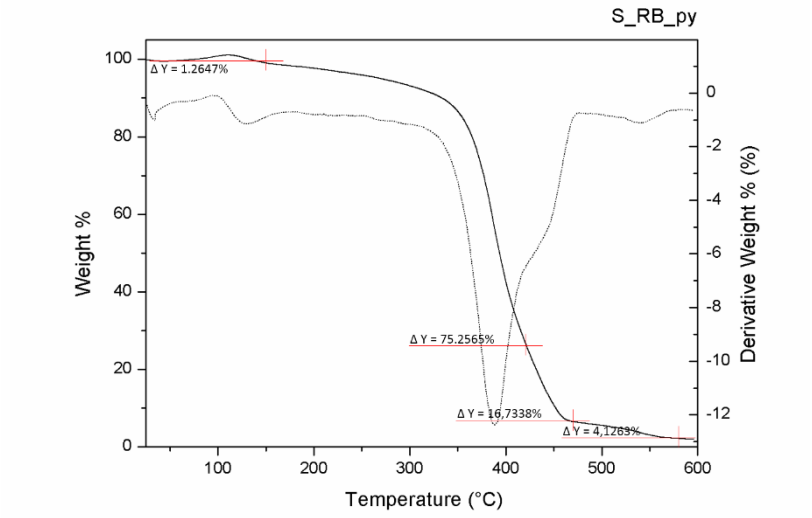

Figure 55. Thermogram sample S_RB_py with SBR/NR composition.

The latter example is about sample S_Sph_sp thermogram (Fig. 45) that confirms the presence of the two polymers, decomposition temperatures, but reveals an equal amount of polymers in mixture (as shown in derivative curve trend and weight loss percentages: 49.36% and 50.64%).

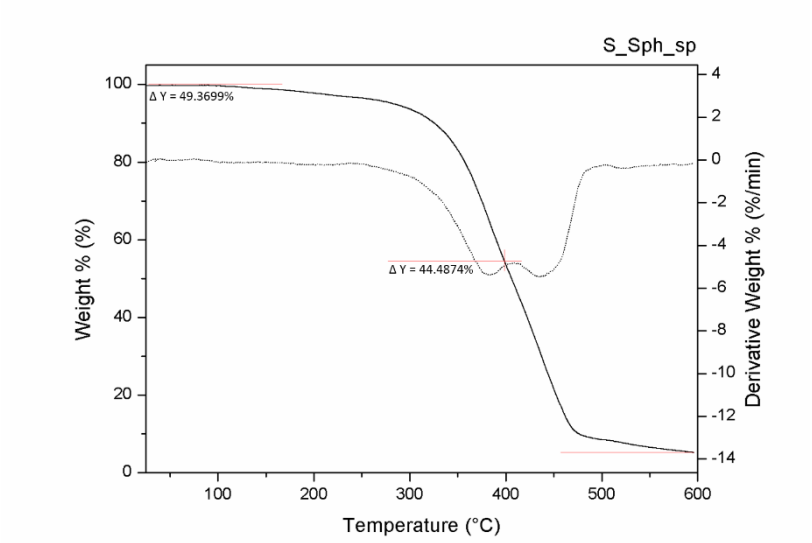

Figure 56. Thermogram sample S_Sph_sp with SBR/NR composition.

Thermogravimetric analysis shows that in spite of the same SBR/NR composition, there are some differences among products in term of percentage of single polymer. This observation can reflect into different behaviour on cleaning treatments and into amount of antioxidants.

2.2.2.4 Nitrile-butadiene rubber (NBR)

Nitrile rubber are copolymers of butadiene and acrylonitrile which are produced by emulsion polymerization; "hot" and "cold" polymerised types are available.
The "hot" polimerized types generally have higher green strenght[5] and are slightly harder to process than "cold" copolymers.

[5] "Green strength" is a term used to describe a molded products ability to withstand handling, molded ejection and machining before it is completely cured or hardened. This physical characteristic is a critical criterion in the productivity levels processes such as injection molding and powder metallurgy. This process must not, of course, damage or alter the finished product so a high green strength rating in any product is a desirable characteristic.

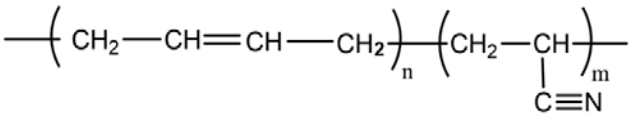

Figure 57. NBR polymer structure formula.

The introduction of acrylonitrile into the polymer backbone imparts oil resistance and affects many other properties. Grades which vary in acrylonitrile content from 18-50% are commercially available, from a low quality (18-24%) to high quality (50%).

Increasing percentage of acrylonitrile, influences many properties: oil resistance, fuel resistance, tensile strength, hardness, abrasion resistance, gas impermeability, heat resistance and plasticizer compatibility improvement, while low temperature flexibility and resilience decrease.

Low molecular weight liquid nitrile grades are available and these can be used as compatible plasticizers in the compounding of nitrile rubber. Such plasticizers can be partially crosslinked to the main chain during cure and hence exhibit extractability.

Nitrile have good resistance to oil, aliphatic and aromatic hydrocarbons and vegetable oils, but are swollen by polar solvents such as ketones. The unsatured main chain means that protection against oxygen and UV light is required.

Nitrile rubber can be cured by sulphur, sulphur donor systems and peroxides; the low temperature properties of nitriles can be improved by the use of suitable plasticizers, e.g. ester plasticizers.

Nitrile rubber, due to its oil resistance, is widely used in sealing applications, hose liners, roll coverings, conveyor belts, shoe soles and plant linings. Nitrile rubber is also available as a latex.

Among materials selected for this study, three samples give NBR compositions: S_Sph_ml, S_Sph_uo and S_Sph_ro.

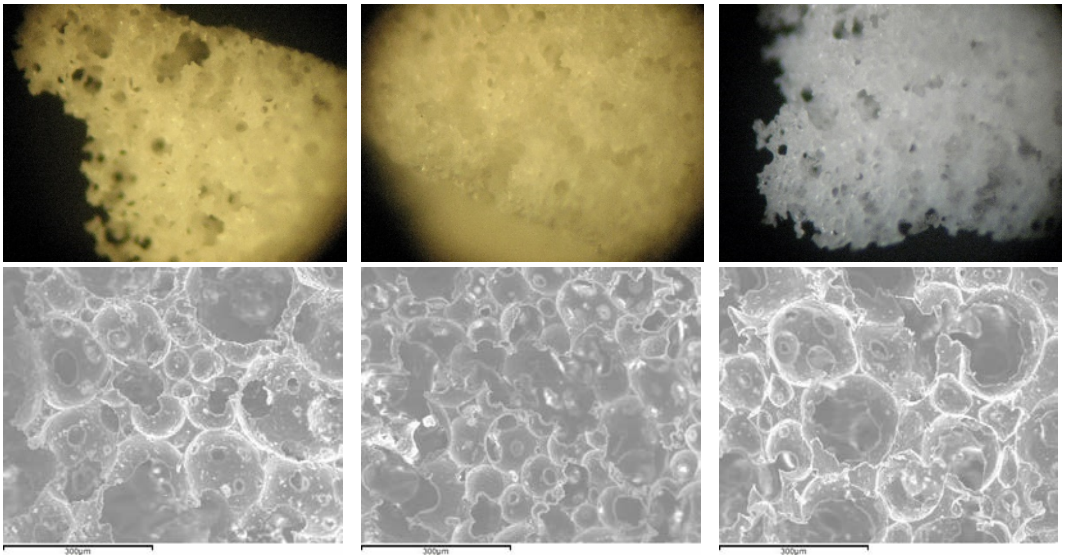

Figure 58. Stereomicroscopy (30X) and SEM-SEI (180X) images of samples: S_Sph_ml (left), S_Sph_uo (centre) and S_Sph_ro (right).

Images reported in Fig. 47 are attributable to NBR composition samples; porosity is opener than that of SBR/NR make-up sponges. Besides, holes are bigger and matter seems to be less compact than previous samples.

SEM-SEI images underline differences among these three products: porosity is open and interconnected, but samples S_Sph_ml and S_Sph_ro have bigger holes compared with sample S_Sph_uo, in spite of the same polymer composition and trademark.

FTIR-ATR spectrum of sample S_Sph_ml (Fig. 48) represents class of Acrylonitrile-butadiene rubber (NBR) [67].

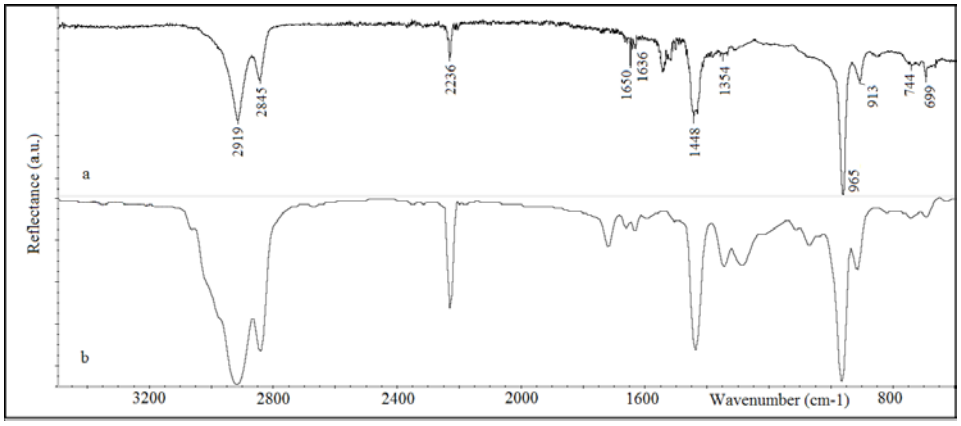

Figure 59. FTIR-ATR spectra of samples S_Sph_ml (a) and NBR rubber reference (b).

Comparing sample and NBR reference spectra, polymer composition is clarify; in fact sample S_Sph_ml presents peaks of NBR rubber. In particular, the first one, 2919ms, 2845mw, 2236mw, 1650w, 1636w, 1448ms, 1354w, 965vs, 913mw, 744w and 699w cm^{-1} and the second one 2928vs, 2847s, 2238ms, 1728mw, 1669w, 1638w, 1446s, 1354mw, 1290mw, 1078w, 974vs, 924mw, 751w and 701w cm^{-1}.

Py GC-MS chromatograms gives comparable signals, so only S_Sph_uo is reported (Fig. 49).

At 14.46 min there is a peak of BHT (A1), at 23.48 min a peak of BKF (A2), at 25.62 min a peak of 2-tert-butyl-4-[1-(5-tert-butyl-4-hydroxy-2-methylphenyl)butyl]-5-methylphenol (SWP) antioxidant (A4) (Fig. 50) and finally, at 25.90 min, a peak of DIOIP (A3).

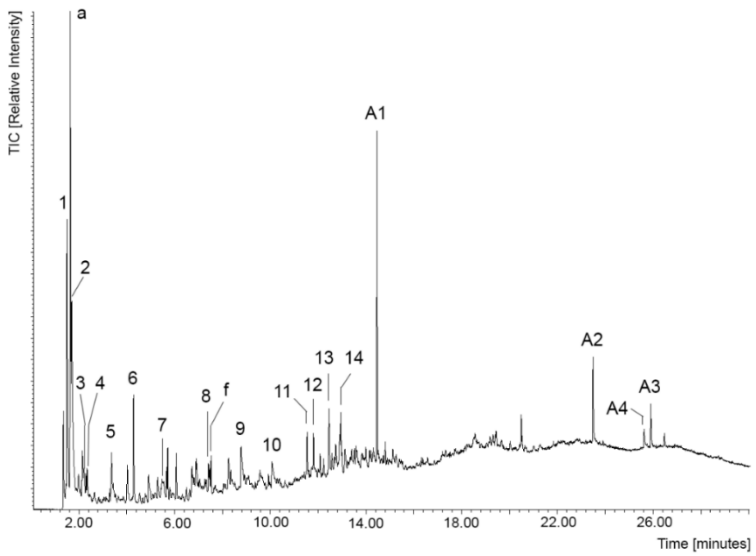

Figure 60. Py GC-MS chromatogram of sample S_Sph_uo, identified as NBR.

Table 12. Acrylonitrile-butadiene rubber (NBR) pyrolysis products.

Peak n°	Retention Time [min]	Assignment	Principal ions [m/z]	MW
1	1,50	1,3-butadiene	39,54,53,50,51	54
2	1,70	acrylonitrile	53,52,51,50,54	53
3	2,29	benzene	78,77,51,50,52	78
4	2,35	cyclohexadiene	79,78,77,80,51	80
5	3,37	toluene	91,92,65,63,51	92
6	4,28	4-vinylcyclohexene	54,79,80,66,67	108
7	5,50	2-methylenepent-4-enenitrile	66,41,93,65,92	93
8	7,42	cyanocyclohexene (AB dimer)	54,41,79,80,107	107
9	8,78	6-methyl-3-cyclehexen-1-nitrile	68,54,121,67,79	121
10	10,07	tetrahydroquinoline	132,133,118,117,130	133
11	11,53	C10H12N2 (hybrid trimer)	67,79,93,133,118	160
12	11,80	C10H12N2 (hybrid trimer)	67,79,93,133,118	160
13	12,45	C10H12N2 (hybrid trimer)	67,79,93,133,118	160
14	12,95	C10H12N2 (hybrid trimer)	67,79,93,133,118	160

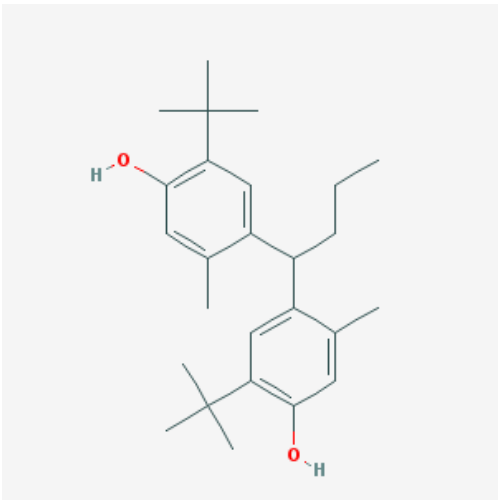

Figure 61. Structure formula of 2-tert-butyl-4-[1-(5-tert-butyl-4-hydroxy-2-methylphenyl)butyl]-5-methylphenol (SWP) antioxidant.

2.2.2.5 Acrylonitrile-butadiene-styrene rubber (ABS)

Acrylonitrile butadiene styrene (ABS) is a common thermoplastic polymer. ABS is amorphous and therefore has no true melting point [68,69].

ABS is a terpolymer made by polymerizing styrene and acrylonitrile in the presence of polybutadiene:

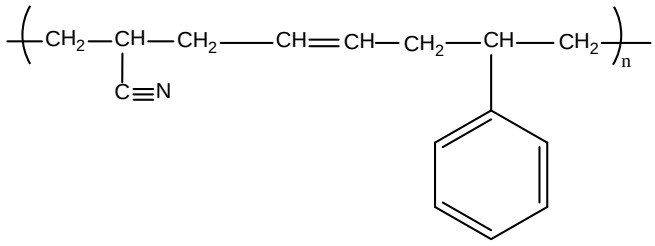

Figure 62. ABS polymer structural formula.

The proportions can vary from 15 to 35% acrylonitrile, 5 to 30% butadiene and 40 to 60% styrene. The result is a long chain of polybutadiene criss-crossed with shorter chains of poly(styrene-co-acrylonitrile). The nitrile groups from neighbouring chains, being polar, attract each other and bind the chains together, making ABS stronger than pure polystyrene. The styrene gives the plastic a shiny, impervious surface. The polybutadiene, a rubbery substance, provides resilience even at low temperatures. For the majority of applications, ABS can be used between −20 and 80 °C as its mechanical properties vary with temperature. The properties are created by rubber toughening, where fine particles of elastomer are distributed throughout the rigid matrix.
The aging characteristics of the polymers are largely influenced by the polybutadiene content and it is normal to include antioxidants in the composition. Other factors include exposure to ultraviolet radiation, for which additives are also available to protect against.

Dry methods samples that give this composition are AS_KC_1, AS_Sft_3 and AS_Sft_5.

Figure 63. Stereomicroscopy (30X) and SEM-SEI (180X) images of samples: AS_Kc_1 (left), AS_Sft_3 (centre) and AS_Sft_5 (right).

Stereomicroscopy observation of morphology of ABS rubber (Fig. 52) reveals porosity and holes size, not so difference respect to SBR, NR, NBR polymers and so on. Nevertheless, manipulation of these sponges reveals different hardness and compactness compared to previous materials.

SEM-EDS analysis cannot be performed because of the difficulty to metallize surfaces of these samples with graphite.

Fig. 53 (a) shows spectrum of sample AS_Kc_1, compared with NBR spectrum (b) and SBR one (c). In fact, sample AS_Kc_1, as for AS_Sft_3 and AS_Sft_5, is made of Acrylonitrile-butadiene-styrene rubber (ABS): 3021w, 2921s, 2845ms, 2236mw, 1665w, 1638w, 1603vw, 1491w, 1449s, 1377w, 1356mw, 1307w, 1074w, 966vs, 912mw, 840mw, 757mw, 698s and 568w cm^{-1}.

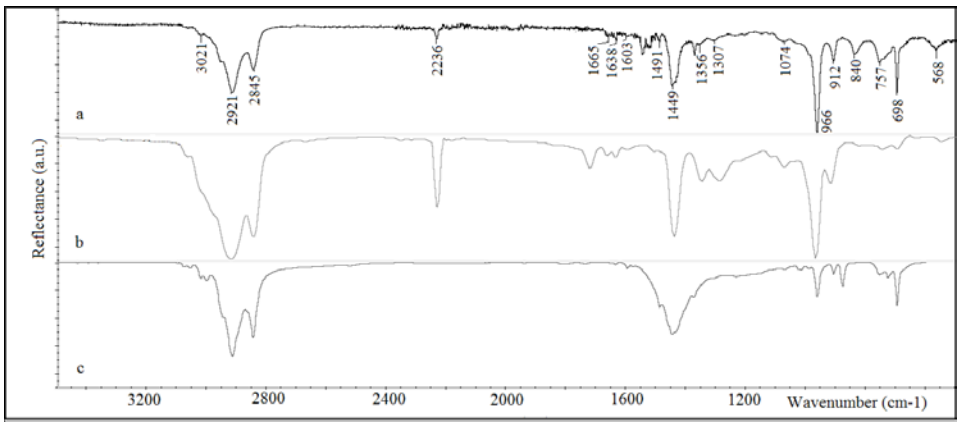

Figure 64. FTIR-ATR spectra of samples AS_Kc_1 (a) NBR rubber reference (b) and SBR rubber reference (c).

Py GC-MS chromatogram of sample AS_KC_1 is reported in Fig. 54. It confirms Acrylonitrile-butadiene-styrene composition (see Table 13), also the presence of natural rubber (see Table 10, Par.2.2.2.2) and BHT [70] (1*).

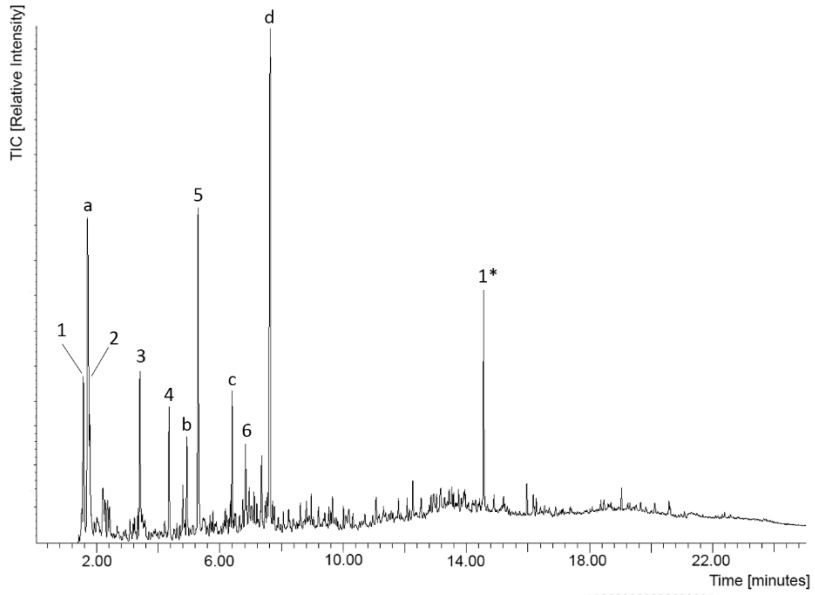

Figure 65. Py GC-MS chromatogram of sample AS_KC_1, identified as ABS.

Table 13. Acrylonitrile-butadiene-styrene (ABS) pyrolysis products.

Peak n°	Retention Time [min]	Assignment	Principal ions [m/z]	MW
1	1.57	1,3-butadiene	39,54,53,50,51	54
2	1.75	Acrylonitrile	53,38,68	53
3	3.40	Toluene	91,92,65,63,51	92
4	4.35	4-vinylcyclohexene	54,79,80,66,39,93	108
5	5.29	Styrene	104,103,78,51,63,39	104
6	6.83	α-methylstyrene	103,78,91,51,39	118

2.2.2.6 Polyurethane (PU)

Polyurethane (PUR and PU) is a polymer composed of a chain of organic units joined by carbamate (urethane) links.

Figure 66. PU polymer structural formula.

While most polyurethanes are thermosetting polymers that do not melt when heated, thermoplastic polyurethanes are also available.

Polyurethane polymers are traditionally and most commonly formed by reacting a di- or polyisocyanate ($R\text{-}(N{=}C{=}O)_{n\geq 2}$) with a polyol ($R'\text{-}(OH)_{n\geq 2}$). Both the isocyanates and polyols used to make polyurethanes contain on average two or more functional groups per molecule.
Because of the isocyanates raise severe toxicity issues, non-isocyanate based polyurethanes (NIPUs) have recently been developed as a new class of polyurethane polymers to mitigate health and environmental concerns [71].
Polyurethane products often are simply called "urethanes", but should not be confused with ethyl carbamate, which is also called urethane. Polyurethanes neither contain nor are produced from ethyl carbamate.
Polyurethanes are used in the manufacture of nonflexible, high-resilience foam seating; rigid foam insulation panels; microcellular foam seals and gaskets; durable elastomeric wheels and tires (such as roller coaster, escalator and skateboard wheels); automotive suspension bushings; electrical potting compounds; high performance adhesives; surface coatings and surface sealants; synthetic fibers (e.g., Spandex); carpet underlay; hard-plastic parts (e.g., for electronic instruments); and hoses.

Among *dry cleaning* materials, presented here, only one sample gives PU pyrolysis products. It is a make-up sponge, in particular S_KK_tr.

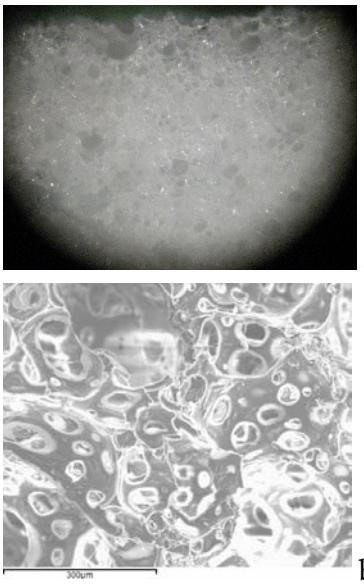

Figure 67. Stereomicroscopy (a) (30X) and SEM-SEI (b) (180X) images of sample S_KK_tr.

Stereomicroscopy observation of PU sample (Fig. 56 a) reveals that porosity and holes size are comparable to previous samples described above. To these magnifications, it seems that different polymer composition does not influence final morphology and porosity.

SEM-SEI image, instead, gives an appearance of different matter: there is a bigger porosity, interconnected and a smaller one with comparable holes size, not connected (Fig. 56 b).

FTIR-ATR spectrum of sample S_KK_tr (3315w, 2915mw, 2873ms, 1721ms, 1601mw, 1536s, 1455mw, 1413w, 1347w, 1324w, 1222s, 1078vs, 945w, 816w, 766w, 680w, 641w and 562w cm^{-1}) (Fig. 57 a) shows peaks quite well attributable to Polyurethane polymer (PU) (3320s, 3199mw, 3122mw, 3046w, 2940vs, 2857vs, 2799ms, 2369w, 1730vs, 1706s, 1600ms, 1536vs, 1412ms, 1365mw, 1312ms, 1227vs, 1079vs, 823mw, 773mw, 667wand 517w cm^{-1}) (Fig. 57 b).

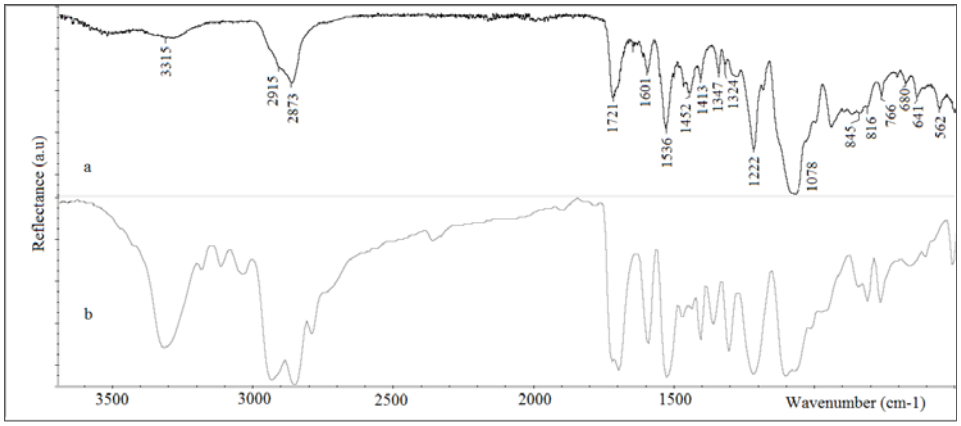

Figure 68. FTIR-ATR spectra of samples S_KK_tr (a) and PU rubber reference (b).

Py GC-MS is reported in Fig. 58, while Polyether Polyurethane (PU) pyrolysis products in Table 14.

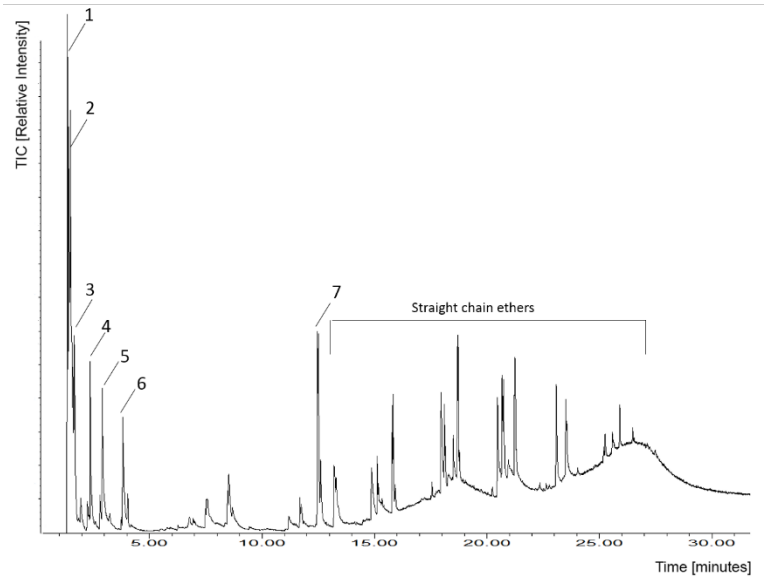

Figure 69. Py GC-MS chromatogram of sample S_KK_tr, identified as PU.

Table 14. Polyether Polyurethane (PU) pyrolysis products.

Peak n°	Retention Time [min]	Assignment	Principal ions [m/z]	MW
1	1.35	CO_2	44,28,16,12,22	44
2	1.41	Propane	29,28,27,43,39	44
3	1.48	n-butane	43,29,27,28,41,39	58
4	2.36	Butylaldehyde	44,29,72,57	72
5	2.90	Tetrahydrofuran (THF)	42,72,29,53	72
6	3.79	2,3-dihydrofurane	-	70
7	12.46	2,4-tolylene diisocyanate	174,145,146,173,91,51	174

2.2.2.7 Polyvinyl acetate (PVA)

Polyvinyl alcohol (PVA), a colourless, water-soluble synthetic resin employed principally in the treating of textiles and paper.

PVA is unique among polymers in that it is not built up in polymerization reactions from single-unit precursor molecules. Instead, PVA is made by dissolving another polymer, polyvinyl acetate (PVAc), in an alcohol such as methanol and treating it with an alkaline catalyst such as sodium hydroxide. The resulting alcoholysis reaction removes the acetate groups from the PVAc molecules without disrupting their long-chain structure. The chemical structure of the resulting vinyl alcohol repeating units is:

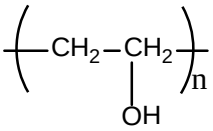

Figure 70. PVA structural formula.

When the reaction is allowed to proceed to completion, the product is highly soluble in water and insoluble in practically all organic solvents. Incomplete removal of the acetate groups yields resins less soluble in water and more soluble in certain organic liquids.
PVA is used in sizing agents that give greater strength to textile yarns and make paper more resistant to oils and greases. It is also employed as a component of adhesives and emulsifiers, as a water-soluble protective film and as a starting material for the preparation of other resins.

Only one sample gives this chemical composition, S_SB.
Fig. 60 reports a stereomicroscopy image of PVA sample. Handling this product, it is less soft than make-up sponges, despite of its porosity and appearance are similar to them.

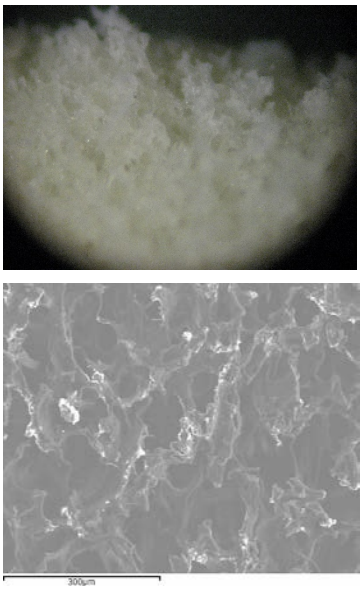

Figure 71. Stereomicroscopy (a) (45X) and SEM-SEI (b) (180X) images of sample S_SB.

Observing stereomicroscopy image (Fig. 60 a) morphology and matter appearance seem to be comparable to products presented above, but SEM-SEI image (Fig. 60 b)

reveals a different distribution of holes compared to make-up sponges. In fact, they present roundish holes, while PVA rubber, very open porosity with no identifiable shape.

Comparing sample S_SB spectrum (Fig. 61 a) with Polyvinyl acetate (PVA) reference one (Fig. 61 b), rubber composition is clarify: S_SB, 3392ms, 2944mw, 2915mw, 2856mw, 2780w, 1644mw, 1431mw, 1404mw, 1361mw, 1239w, 1172ms, 1066s, 1007vs and 783ms cm^{-1} and PVA reference, 3411vs, 2943s, 2916s, 2857ms, 2781mw, 1633mw, 1439s, 1333ms, 1241ms, 1180ms, 1144s, 1097s, 1021vs, 850ms, 797mw, 691mw and 617ms cm^{-1}.

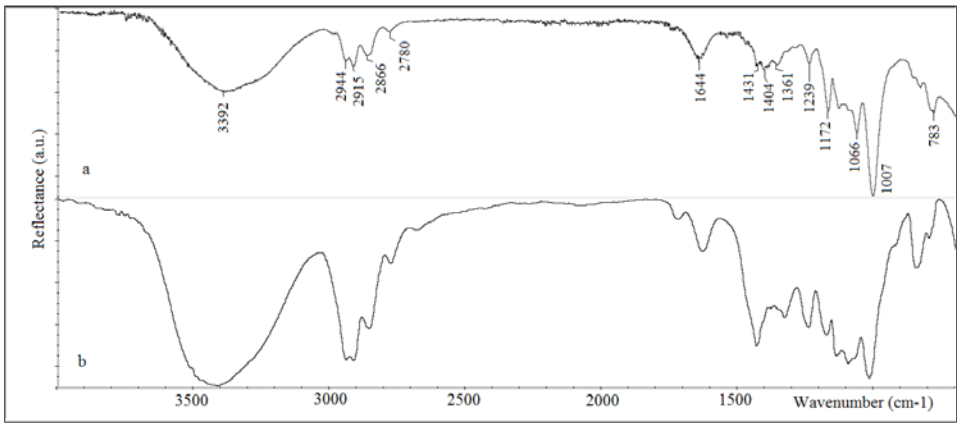

Figure 72. FTIR-ATR spectra of samples S_SB (a) and PVA rubber reference (b).

Py GC-MS chromatogram shows pyrolysis products of PVA (Fig. 62). Signals of two plasticizers, diisobuthyl phthalate (DIBP) at 18.52 min (1*) (Fig. 63) and dibuthyl phthalate (DBP) at 19.47 min (2*) (Fig. 64), are recognizable [72,73]. Table 15 shows PVA pyrolysis products.

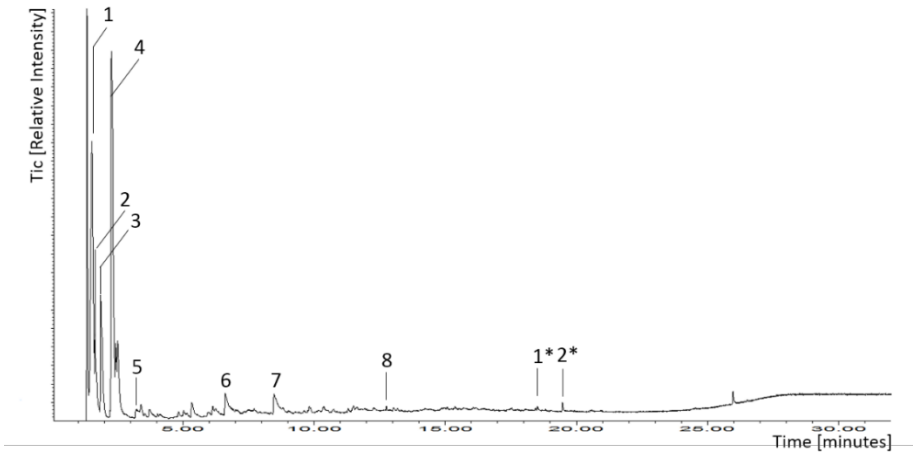

Figure 73. Py GC-MS chromatogram of sample S_SB, identified as PVA.

Table 15. Poly vinyl alcohol (PVA) pyrolysis products.

Peak n°	Retention Time [min]	Assignment	Principal ions [m/z]	MW
1	1.53	Acetaldehyde	29,44	44
2	1.65	Acetone	43,58,29,70	58
3	1.87	2,5-dihydrofuran	41,70,29,50	70
4	2.28	Crotonaldehyde	70,41,29,50	70
5	3.22	Ethylidene acetone	69,41,84,50,29	70
6	6.61	Benzaldehyde	106,77,51,74,39,29	106
7	8.47	Methylbenzaldehyde	91,120,65,77,39,105,51	120
8	12.75	Methyl hexadiene	81,96,39,53,67,29	96

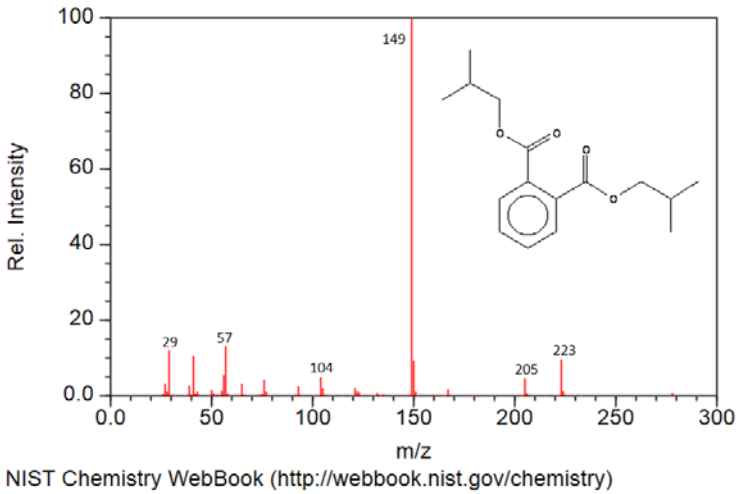

Figure 74. Mass spectrum of DIBP plasticizer.

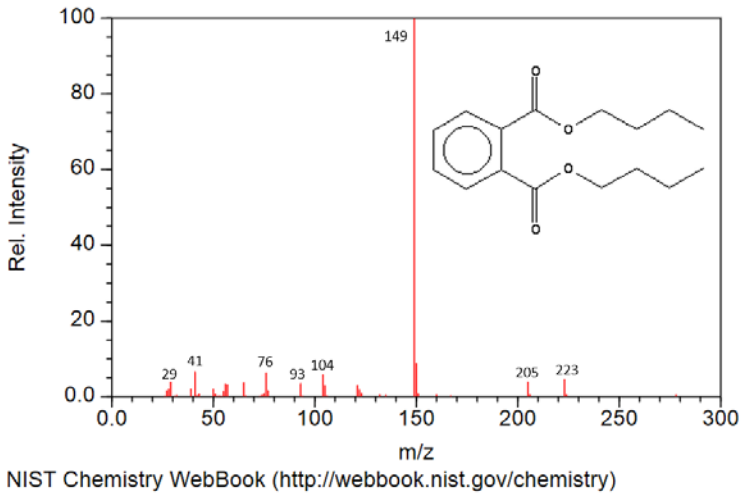

Figure 75. Mass spectrum of DBP plasticizer.

2.2.3 Cloths

2.2.3.1 Polyester (PEs)/Polyamide (PA)

In cleaning products, microfiber can be 100% polyester, or a blend of polyester and polyamide (nylon). It can be both a woven product or a non-woven product, the latter most often used in limited use or disposable cloths.
In the highest-quality fabrics for cleaning applications, the fibre is split during the manufacturing process to produce multi-stranded fibres. A cross section of the split microfiber fabric under high magnification would look like an "asterisk" (Fig. 65). The split fibres and the size of the individual filaments working in conjunction with the spaces between them that make the cloths more effective than other fabrics for cleaning purposes. The structure traps and retains the dirt and absorbs liquids.

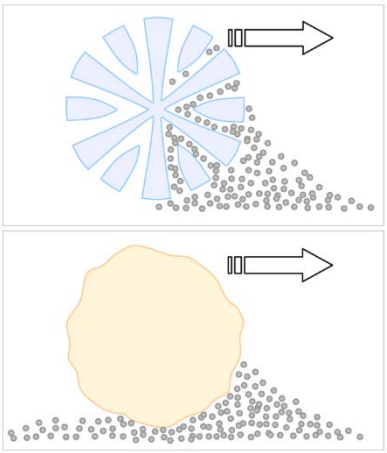

Figure 76. Schematic representation of cross sections: microfiber thread above, cotton thread below.

Unlike cotton, microfiber leaves no lint, the exception being some micro suede blends, where the surface is mechanically processed to produce a soft plush feel.
For microfiber to be most effective as a cleaning product, especially for water-soluble soiling and waxes, it should be a split microfibre. Non-split microfibre is little more than a very soft cloth. The main exception is for cloths used for facial cleansing or optical surfaces such as camera, phones and eyeglasses where 100% polyester cloths using 2µm filaments, will absorb these types of dirt without smearing.
Microfiber products used for consumer cleaning are generally constructed from split conjugated fibres of polyester and polyamide. Microfiber used for commercial cleaning products also includes many products constructed of 100% polyester microfiber.
Fabrics made with microfibers are exceptionally soft and hold their shape well. When high-quality microfiber is combined with the right knitting process, it creates an extremely effective cleaning material. This material can hold up to eight times its weight in water. Microfiber products have exceptional ability to absorb oils and are not hard enough to scratch even paintwork unless they have retained grit or hard particles from previous use.
Microfiber cleaning tools also absorb fat and grease and their electrostatic properties give them a high dust-attracting power.

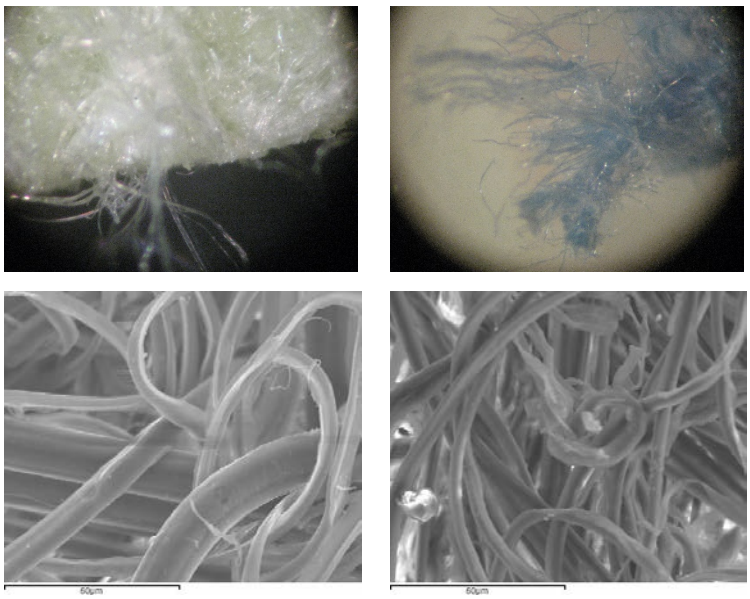

Figure 77. Stereomicroscopy (45X) and SEM-SEI (1000X) images of samples: P_Di_3 (left) and P_Vi_2 (right).

Figure 66 shows cloths samples P_Di_3 and P_Vi_2 observed by stereomicroscopy and SEM-SEI. Both type of analysis underline that are made of microscopic threads interlaced. SEM-SEI images at 1000X reveals that in the case of P_Di_3 sample, fibres have different sizes, while in P_Vi_2 are more homogeneous. Fibres networks seem to be random in both trademarks cloths.

Samples P_Di_3 and P_Vi_2 show Polyamide/Polyester (PA/Pes) polymer composition. In fact, we find both polymers signals, in particular for sample P_Vi_2: 3294mw, 3064w, 2933mw, 2860mw, 1708ms, 1632ms, 1541ms, 1473mw, 1462mw, 1407mw, 1371w, 1337mw, 1240s, 1169w, 1093ms, 1015ms, 968mw, 968ms, 845w, 793w, 722vs and 573mw cm^{-1} (Fig. 67 a). Figure 67 b shows Polyester (Pes) reference spectrum: 2934mw, 2857mw, 1721vs, 1577w, 1506mw, 1453mw, 1409ms, 1371w, 1339ms, 1265vs, 1100s, 1021ms, 973mw, 873mw, 794w and 732s cm^{-1}, while Polyamide (PA) reference spectrum is reported in Fig. 71 b: 3305s, 3075mw, 2934ms, 2863ms, 1642vs, 1542s, 1462mw, 1418mw, 1371mw, 1268mw, 1197mw, 935w and 726w cm^{-1}.

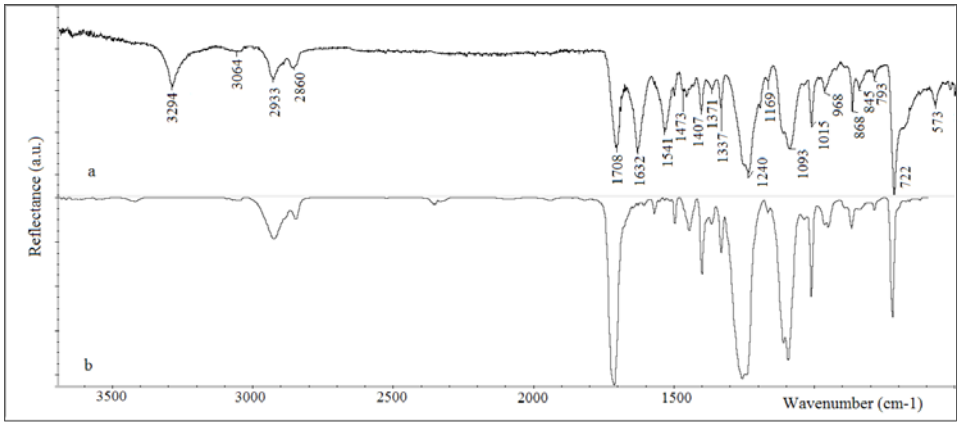

Figure 78. FTIR-ATR spectra of samples P_Vi_2 (a) and PEs polymer reference (b).

Py GC-MS chromatogram shown in Fig. 68 presents peaks of pyrolysis products of Polyester (Pes) and Polyamide (PA), as commented in previous FTIR-ATR analysis. Table 16 and 17 listed Polyamide and Polyester pyrolysis products, respectively. In addition, there is a peak at 21.45 min (1*) attributable to 1,2-ethanediol dibenzoate (Benzoflex 998) used as plasticizer [74] (Fig. 69).

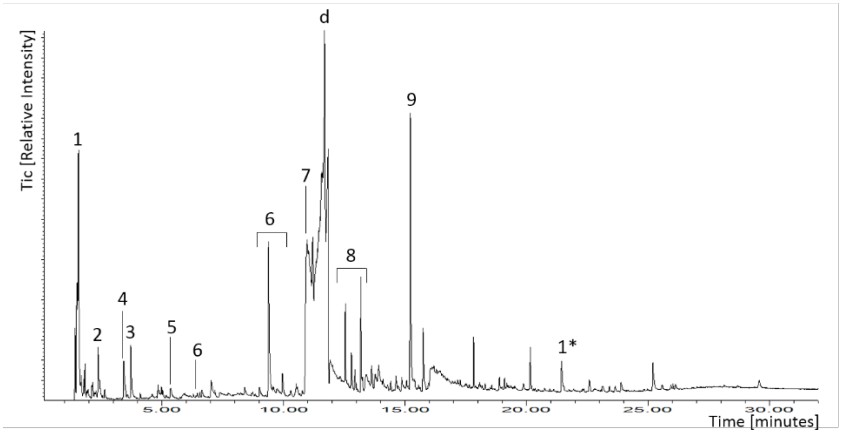

Figure 79. Py GC-MS chromatogram of sample P_Vi_2, identified as PEs/PA.

Table 16. Polyamide (PA) pyrolysis products.

Peak n°	Retention Time [min]	Assignment	Principal ions [m/z]	MW
a	3.56	Pentanenitrile	41,54,68,82,29,96,143	97
3	3.72	Cyclopentanone	55,84,41,29	84
b	5.11	Der. nitrile + n-butylether	-	-
c	5.83	Der. nitrile	-	-
d	12.03	ε-caprolactame	113,55,30,85,42,67,98	113
e	15.77	Der. nitrile	-	-
f	16.93	NA_1 $CH_3CONH(CH_2)_5CN$	-	154
g	17.27	NA_3 $CH_3(CH_2)_2CONH(CH_2)_5CN$	71,43,30,100,114,128,154	182
h	19.26	N-(5-cyanopentyl)hexanamide	114,154,43,99,55,30,71,83	210

Table 17. Polyester (PEs) pyrolysis products.

Peak n°	Retention Time [min]	Assignment	Principal ions [m/z]	MW
1	1.56	1,3 butadiene	39,54,29	54
2	2.37	Benzene	78,52,39,74,29	78
4	3.42	Toluene	91,65,39,51,89	92
5	5.35	Styrene	104,78,103,51,39,63	104
6	9.38-9.96	Der. Benzoic ac.	-	-
7	10.96	Acid Benzoic	105,122,77,51,74,38,94	122
8	12.50-13.19	Der. Benzoic ac.	-	-
9	15.23	Phthalic anhydride	104,76,50,148,74,38	148

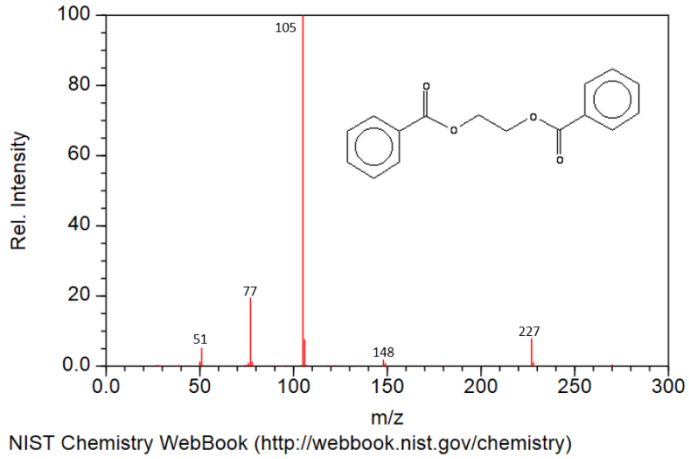

Figure 80. Mass spectrum of 1,2-ethanediol dibenzoate (Benzoflex 998), a plasticizer.

2.2.3.2 Polyurethane (PU)/Polyamide (PA)

Most of microfiber cloths are made of Polyester and Polyamide, as reported in Par. 2.2.3.1.
In the case of sample P_Sp_1, identification of polymer composition is different; in fact, it results to be Polyurethane/Polyamide fibres.
Analysis results are reported below.

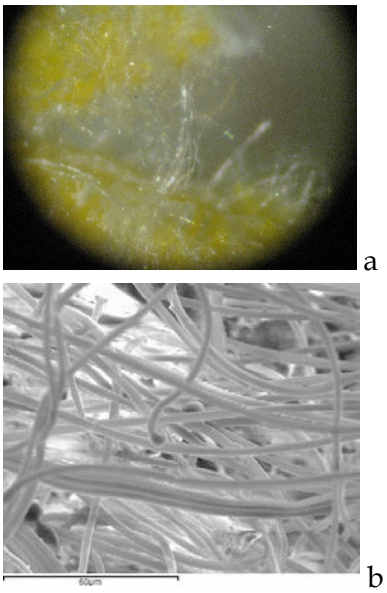

Figure 81. Stereomicroscopy (45X) and SEM-SEI (1000X) images of sample P_Sp_1.

As visible in stereomicroscopy and SEM-SEI images, cloth is made of fibres network, but more homogeneous in shape and size than that viewed above (Fig. 70 a, b). EDS spectrum of sample gives presence of Ti, confirmed by µRaman analysis, that show the presence of nanoparticles of Anatase as TiO_2 polymorph (see Fig. 36 Par.2.2.2.3).

FTIR-ATR spectrum of sample P_Sp_1 shows composition of Polyurethane/Polyamide (PU/PA) as reported in Fig. 71 a. In particular: 3293s, 3072w, 2933s, 2854s, 1729w, 1704w, 1635vs, 1536vs, 1475w, 1460w, 1437w, 1412mw, 1371mw, 1308w, 1199w, 1169w, 1103s, 956w, 872mw, 821w, 768w, 710w, 687ms, 573ms and 522mw cm^{-1}.

Reference spectra of Polyamide is shown in Fig. 71 b, while Polyurethane one in Fig. 57 b (Par. 2.2.2.6).

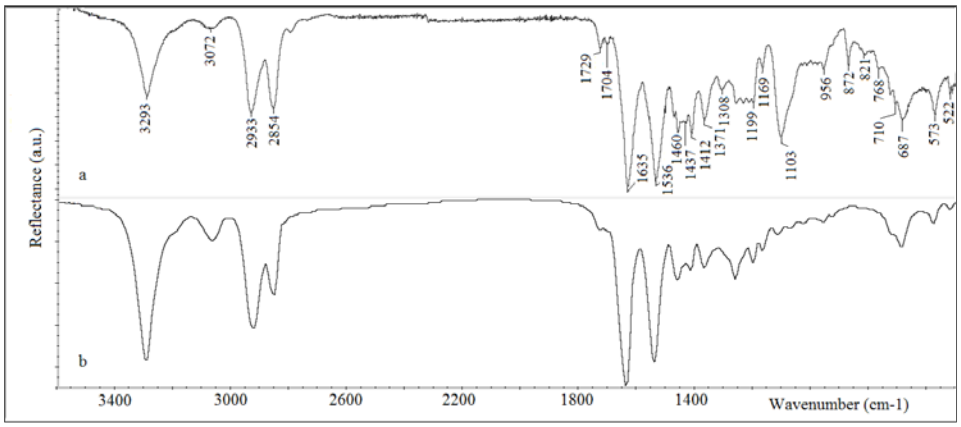

Figure 82. FTIR-ATR spectra of samples P_Sp_1 (a) and PA 6 polymer reference (b).

Py GC-MS spectrum of sample S_Sp_1 is presented below (Fig. 72); pyrolysis products of Polyurethane are listed in Table 14 (Par. 2.2.2.6), Polyamide one in Table 16 (Par. 2.2.3.1) and confirm polymer composition as PU/PA.

Py GC-MS chromatogram reveals the presence of an additive (1*), 4,4'-diaminodiphenylmethane (DDM) (Fig. 73), used as hardener for Polyurethane and in Polyamide manufacturer [75].

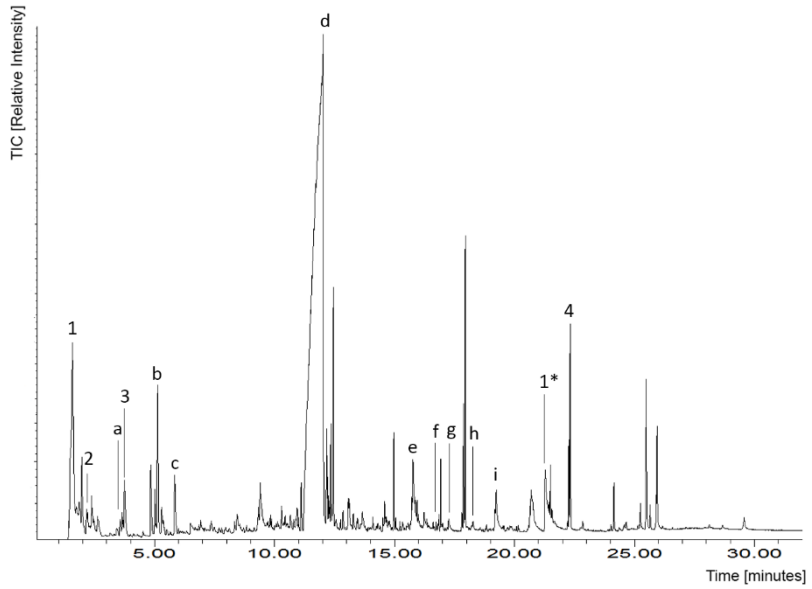

Figure 83. Py GC-MS chromatogram of sample P_Sp_1, identified as PU/PA.

Table 18. Polyurethane (PU) pyrolysis products.

Peak n°	Retention Time [min]	Assignment	Principal ions [m/z]	MW
1	1.57	1,3 butadiene	39,54,29	54
2	2.16	Tetrahydrofuran (THF)	42,72,29,53	72
3	3.74	Cyclopentanone	55,84,41,29	84
4	22.32	Der. polyurathane	-	-

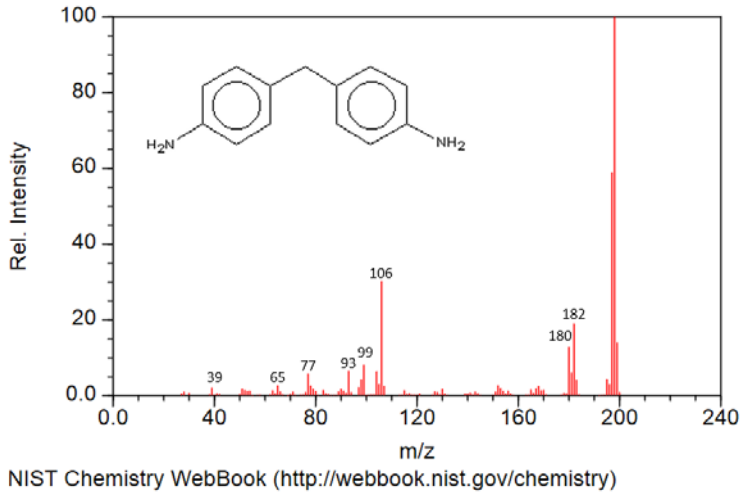

Figure 84. Mass spectrum of 4,4'-diaminodiphenylmethane (DDM) used as additive.

2.2.4 Acrylic and oil painted samples

2.2.4.1 Physico-chemical characterization

Concerning oil colours, composition declared by producer, lists the following materials:

- OIL PURO series 00: 20-35% safflower and carthame oil
  60-75% pigment
  5% excipients

Besides, pigments were identified as Ultramarine light blue 390 (PB29) and Titanium white 018 (PW6).

Py GC-MS spectrum of Ultramarine blue Puro Maimeri (Fig. 74), shows pyrolysis products corresponding to the presence of linseed oil, as confirmed by relative ratio P/S (palmitic acid/stearic acid ratio), that has a value >1 [76,77,78,79].

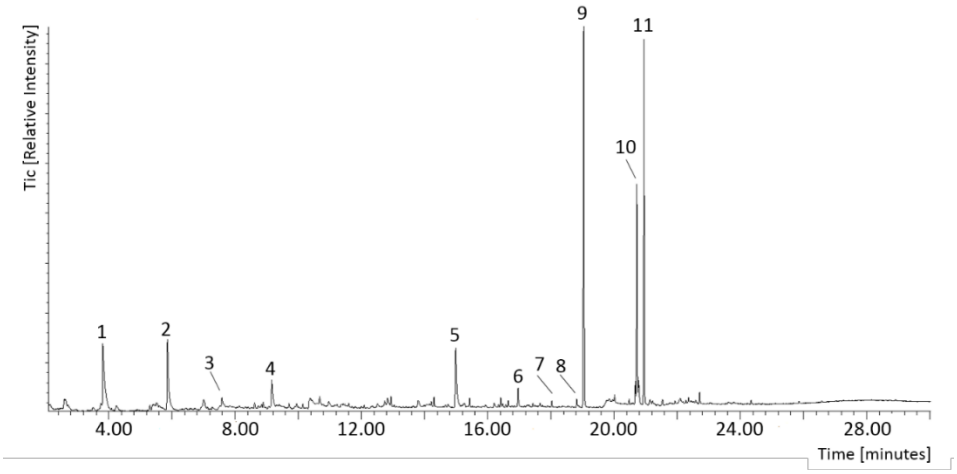

Figure 85. Py GC-MS chromatogram of oil Ultramarine blue Puro Maimeri with principal peaks numbered.

Table 19. Ultramarine blue Puro Maimeri sample, with specified assignments, number, retention time of principal peaks of Py GC-MS chromatogram.

Peak n°	Retention Time [min]	Assignment	Principal ions [m/z]	MW
1	3,81	Hexanol	56,43,41,55,31,27,39,69	102
2	5,86	Methyl hexoate	74,87,43,99,59,55,41	130
3	7,59	Methyl heptoate	74,87,43,113,59,101	144
4	9,17	Methyl octanate	74,87,43,41,127,59,115	158
5	14,99	Nonanedioic acid, mono/di methyl ester	152,55,74,83,111,59,185,124	216
6	16,93	Methyl myristate	74,87,55,43,41,143,75,199	242
7	18,03	Pentadecanoic acid, methyl ester	74,87,43,55,143,75,69	256
8	18,82	9-hexadecanoic acid, methyl ester	55,41,69,43,83,67,97,111,236	254
9	19,04	Palmitic acid, methyl ester	74,87,43,55,143,75,69,227	270
10	20,73	Oleic acid, methyl ester	55,69,74,41,87,264,222,180	296
11	20,96	Stearic acid, methyl ester	74,87,43,55,143,69,255	298

Regarding acrylic colours, producer composition declared is:
ACRYLIC BRERA series 08: 40-50% acrylic resin
20-30% pigment
30% excipients
As for oil colours, pigments were identified as, Ultramarine blue 390 (PB29) and Titanium white 018 (PW6).

As discussed in a degree thesis[6] with object, among others, the characterization of synthetic medium of commercial colours, physico-chemical characterization clarifies several points. In particular, FTIR-ATR spectra identifies an acrylic resin as medium (2952, 2926, 2870, 1724 1454, 1382, 1070 and 1153 cm^{-1}), in particular the presence of peaks at 3054 and 3022 cm^{-1} due to the presence of styrene, confirms the identification of a styrene-acrylic copolymer, p(nBMA-2EHA-Styrene) where nBMA is Poly(n-butylmethacrylate) and 2EHA is Poly(2-ethylhexylacrylate), as reported in literature [80,81,82]. The use of acrylic-styrene medium is confirmed for the complete series Brera.

µRaman spectra for Titanium white, confirm the presence of Rutile (TiO_2), while for blue one, is confirmed the presence of artificial Ultramarine [83]. SiO_2 is used as extender and the addition of surfactant, was determined after extraction with different solvents[7] of fresh colour and consequently analysed using µFTIR-ATR and UV-VIS spectroscopy [84,85].

FTIR-ATR extracted fractions in water and butilacetate, show the presence of cellulose derivative, maybe carboxymethyl cellulose (3384, 1934, 1115 and 1053 cm^{-1}), while extracted fractions in ethanol and acetone, reveal the use of polyacrylic acid derivative as thickener (1244, 1554 and 2926 cm^{-1}).

The addition of silicone oil as defoamer was confirmed and UV-VIS spectra show the presence of Tween 20 as surfactant [86].

Py GC-MS spectrum obtained from white Titanium fresh colour, is presented below (Fig. 75); it shows typical pyrolysis products of PnBMA-MMA-HMA-styrene (Poly(n-butylmethacrylate)-methylmethacrylate-hexamethylacrylate-styrene), confirming literature data [87].

Similarly, Ultramarine blue Py GC-MS spectra shows the same composition.

[6] Degree thesis in Scienze dei Beni Culturali (12/S) titled "*Studio dei colori acrilici della pittura contemporanea: dalla caratterizzazione ai materiali per la pulitura*", graduate: Daniela Caputo at University of Parma, Academic year 2009-2010.

[7] Extraction from fresh colours with isoctane, toluene, butilacetate, acetone, ethanol and water, 1:1 volume ratio, stirring for 30 min, centrifuged for 10-20 min in order to separate pigment from solvent. The latter was separated with a syringe, then filtered (with a nylon filter Whatman 0.45 µm) and a drop put on a TLC plates Silica gel aluminium and evaporated for 24h at environmental temperature.

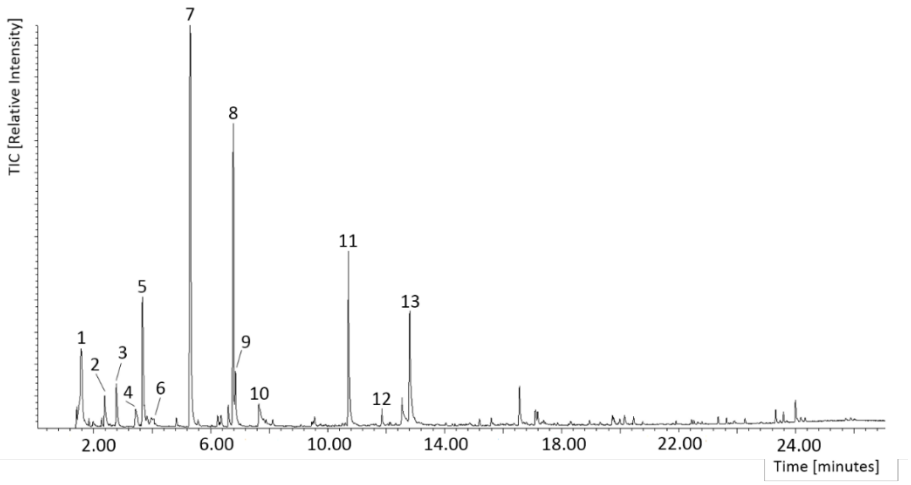

Figure 86. Py GC-MS chromatogram of acrylic Titanium white Brera Maimeri with principal peaks numbered.

Table 20. Titanium white Brera Maimeri sample, with specified assignments, number, and retention time of principal peaks of Py GC-MS chromatogram.

Peak n°	**Retention Time [min]**	**Assignment**	**Principal ions [m/z]**	**MW**
1	1,58	1-butene	41,39,28,27,55,29,28	56
2	2,37	1-butanol	56,31,41,43,27,42,55,39,26	74
3	2,78	Methyl methacrylate (MMA)	41,69,39,40,59,85	100
4	3,43	Toluene	91,65,39,63,51,50	92
5	3,67	2-Ethyl-1-hexene	70,55,41,53,112	112
6	4,07	β-methacrylic acid	41,39,40,45,69,38,42	86
7	5,31	Styrene	78,51,77,50,52,102,74	104
8	6,77	n-buthyl methacrylate (nBMA)	-	-
9	6,85	α-methyl styrene	103,78,77,91,115,51,39	118
10	7,65	2-Ethyl-1-hexanol	57,43,70,83,98,112	130
11	10,72	Ethyl hexyl acrylate (EHA)	55,70,57,41,83,56,43,112	184
12	11,86	Octil methacrylate	70,41,112,55,83,87	198
13	12,81	Propanoic acid, 2-methyl 3-hydroxy-2,4,4 trimethylpentyl ester	71,56,43,89,85,173,143	216

2.2.4.2 Evaluation of cleaning tests

Several tests were performed to evaluate the effectiveness of each product on soiled surface.
Below, Titanium white acrylic paints samples were presented, divided into different areas, related on each treatments (Fig. 76-79).

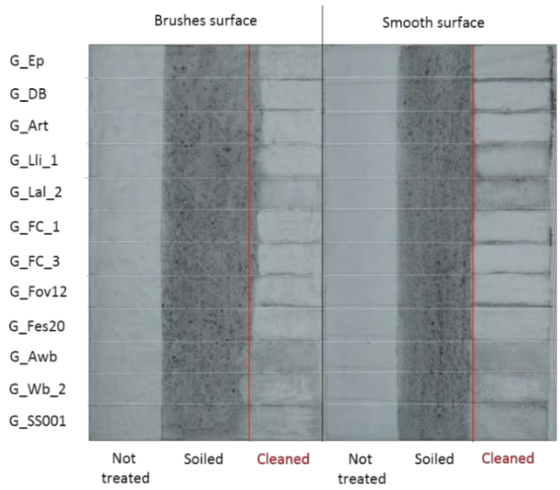

Figure 87. Titanium white acrylic paint sample 1, with highlighted some different Dry cleaning methods used (on the left), each area subdivided into three parts (not treated, soiled, cleaned on the bottom) and specifying brushes or smooth surfaces (on the top).

Figure 88. Titanium white acrylic paint sample 2, with highlighted some different Dry cleaning methods used (on the left), each area subdivided into three parts (not treated, soiled, cleaned on the bottom) and specifying brushes or smooth surfaces (on the top).

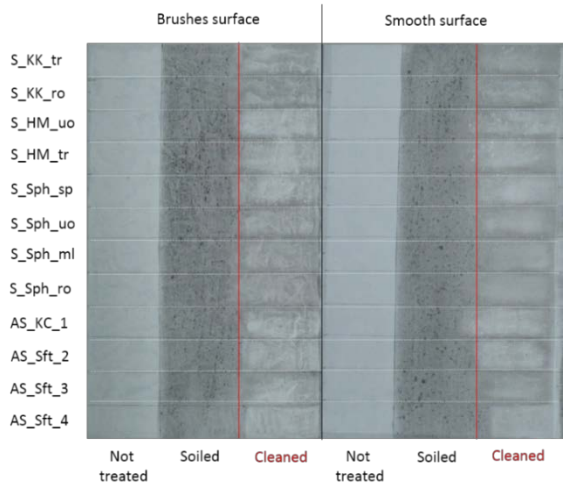

Figure 89. Titanium white acrylic paint sample 3, with highlighted some different Dry cleaning methods used (on the left), each area subdivided into three parts (not treated, soiled, cleaned on the bottom) and specifying brushes or smooth surfaces (on the top).

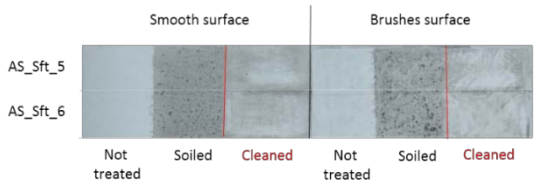

Figure 90. Titanium white acrylic paint sample 4, with highlighted two different Dry cleaning methods used (on the left), each area subdivided into three parts (not treated, soiled, cleaned on the bottom) and specifying brushes or smooth surfaces (on the top).

Macroscopic observation of samples, reveals different effectiveness on cleaning surfaces by different products; in addition, in some single area we can observe inhomogeneous cleaned surfaces.

In a similar way, also Ultramarine blue acrylic paints samples were reported (Fig. 80-83).

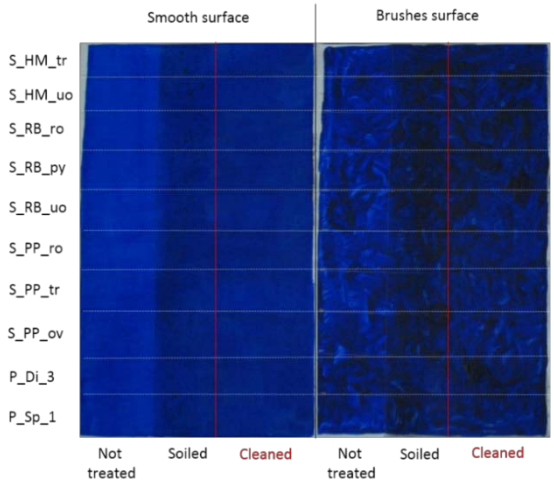

Figure 91. Ultramarine blue acrylic paint sample 1, with highlighted some different Dry cleaning methods used (on the left), each area subdivided into three parts (not treated, soiled, cleaned on the bottom) and specifying brushes or smooth surfaces (on the top).

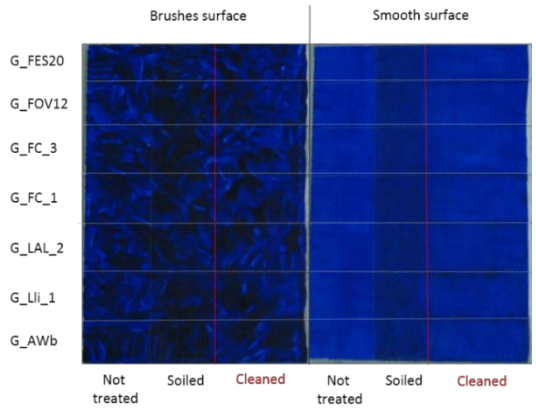

Figure 92. Ultramarine blue acrylic paint sample 2, with highlighted some different Dry cleaning methods used (on the left), each area subdivided into three parts (not treated, soiled, cleaned on the bottom) and specifying brushes or smooth surfaces (on the top).

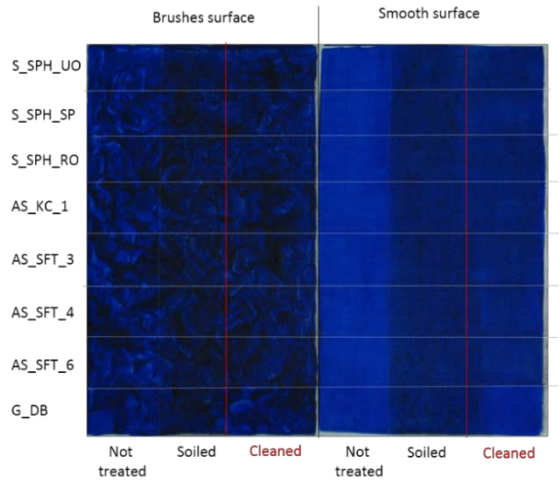

Figure 93. Ultramarine blue acrylic paint sample 3, with highlighted some different Dry cleaning methods used (on the left), each area subdivided into three parts (not treated, soiled, cleaned on the bottom) and specifying brushes or smooth surfaces (on the top).

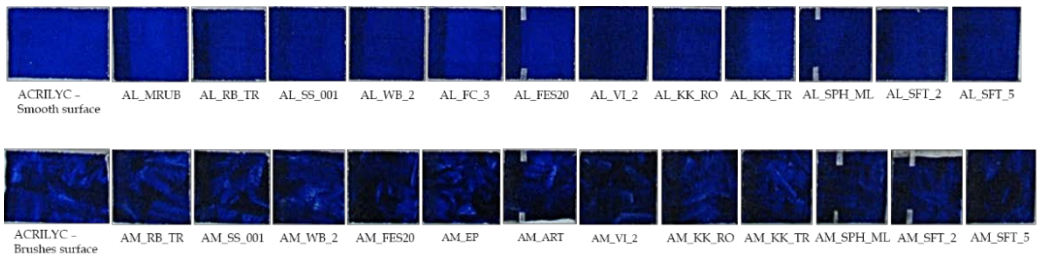

Figure 94. Ultramarine blue acrylic paint sample 4: samples not treated (on the left) and several areas cleaned with selected products.

Also in these cases, some areas show different level of cleaning referred to effectiveness and homogeneity.
In order to evaluate every single treatment, analytical results were listed below, according to colour (white or blue) and type of characterization.

Similarly as acrylic drafts, oil ones were reported divided into different treatments firstly white and blue after (Fig. 84 – 91).
Macroscopic observation of samples reveals different effectiveness on cleaning surfaces by different products, as seen for acrylic ones.
From a preliminary observation, it seems that brushes surfaces are cleaned worse than smooth one, in quite all treatments.

In general, *dry methods* appear less effective on oil drafting, probably due to chemical affinity between colours medium and constituents of artificial soiling (mineral oil, among others).

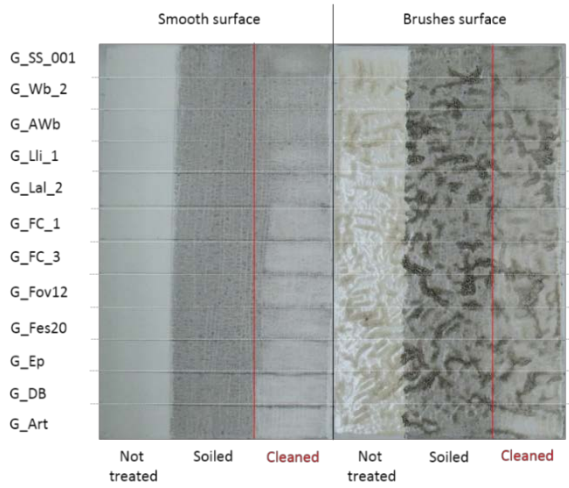

Figure 95. Titanium white oil paint sample 1, with highlighted some different Dry cleaning methods used (on the left), each area subdivided into three parts (not treated, soiled, cleaned on the bottom) and specifying brushes or smooth surfaces (on the top).

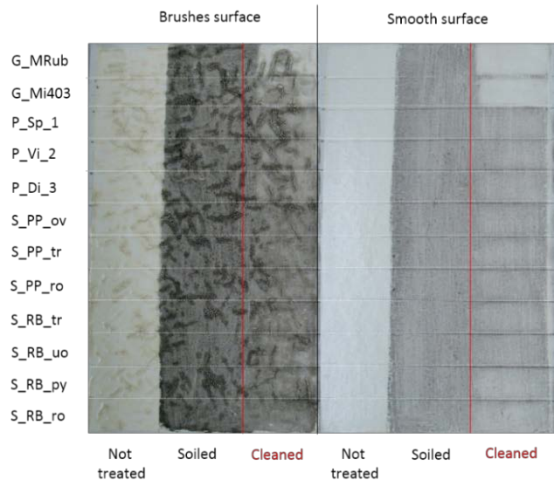

Figure 96. Titanium white oil paint sample 2, with highlighted some different Dry cleaning methods used (on the left), each area subdivided into three parts (not treated, soiled, cleaned on the bottom) and specifying brushes or smooth surfaces (on the top).

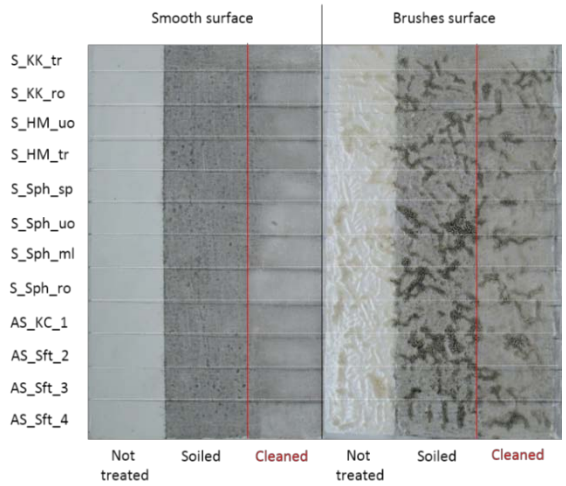

Figure 97. Titanium white oil paint sample 3, with highlighted some different Dry cleaning methods used (on the left), each area subdivided into three parts (not treated, soiled, cleaned on the bottom) and specifying brushes or smooth surfaces (on the top).

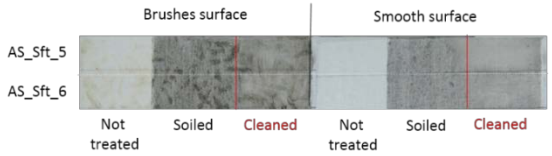

Figure 98. Titanium white oil paint sample 4, with highlighted some different Dry cleaning methods used (on the left), each area subdivided into three parts (not treated, soiled, cleaned on the bottom) and specifying brushes or smooth surfaces (on the top).

As for acrylic samples, white colour gives changes in dirty removal more evident, in some sample, but colorimetric results are fundamental once again.

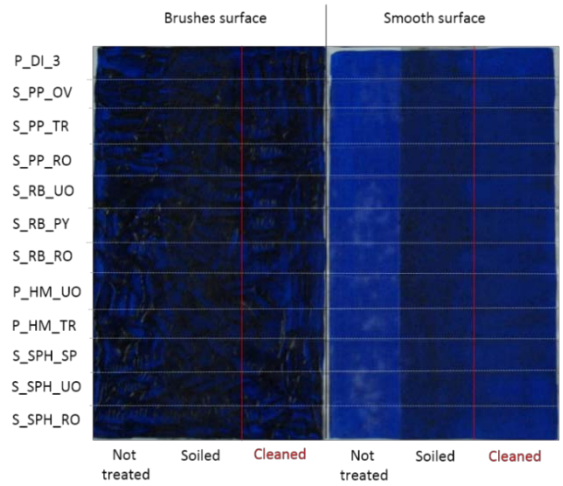

Figure 99. Ultramarine blue oil paint sample 1, with highlighted some different Dry cleaning methods used (on the left), each area subdivided into three parts (not treated, soiled, cleaned on the bottom) and specifying brushes or smooth surfaces (on the top).

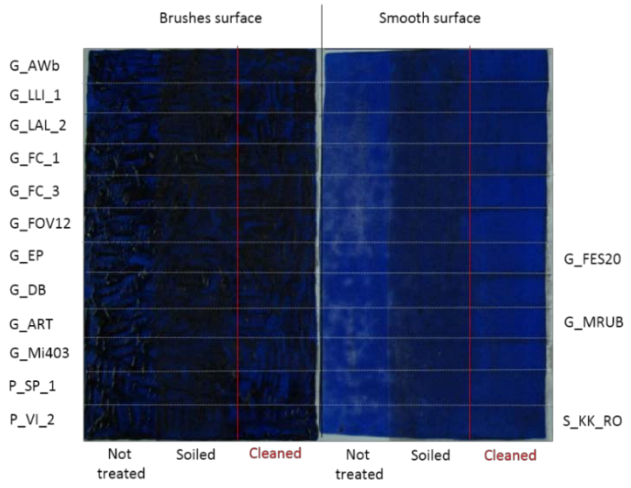

Figure 100. Ultramarine blue oil paint sample 2, with highlighted some different Dry cleaning methods used (on the left), each area subdivided into three parts (not treated, soiled, cleaned on the bottom) and specifying brushes or smooth surfaces (on the top).

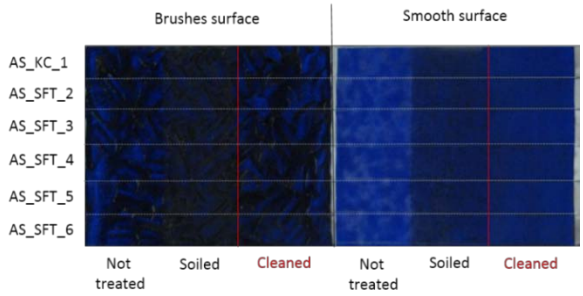

Figure 101. Ultramarine blue oil paint sample 3, with highlighted some different Dry cleaning methods used (on the left), each area subdivided into three parts (not treated, soiled, cleaned on the bottom) and specifying brushes or smooth surfaces (on the top).

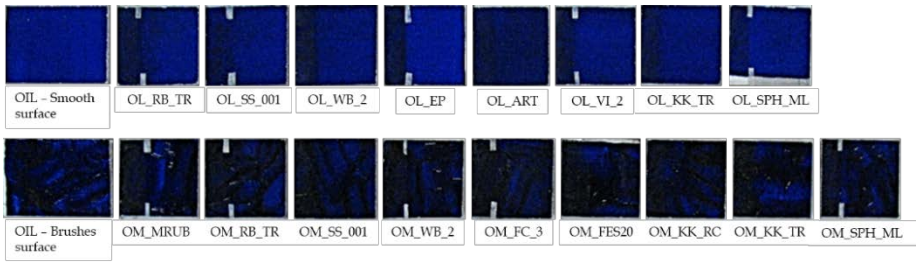

Figure 102. Ultramarine blue oil paint sample 4: samples not treated (on the left) and several areas cleaned with selected products.

2.2.4.2.1 Stereomicroscopy

The results of stereomicroscopic observation of *Dry cleaning* tests were presented, divided as type of materials: erasers, make-up sponges and art sponges and cloths. Images were also divided by colour, Titanium white firstly and then Ultramarine blue. Below, a brief explanation of the main differences among products effectiveness, that will be analyse thoroughly after.

To better compare and understand the differences among samples soiled-and-than-cleaned and surfaces not treated, stereomicroscopic images were shown, for each colour (white and blue) and technique (acrylic and oil) (Fig. 92).

Titanium white acrylic

Smooth surface Brushes surface

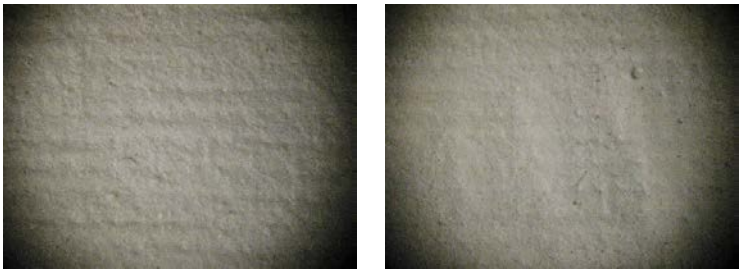

Figure 103. Stereomicroscopic images (7X) of Titanium white acrylic areas, differentiated into smooth and brushes surfaces, not treated.

Table 21 shows samples treated with erasers. It is easy to observe that some products gives better results, compared to others. In particular, G_FC_1, G_FC_3, G_FOV12, G_FES20, G_EP, G_DB, G_MRub and G_Mi403, exhibit satisfactory results from cleaning point of view. We can notice that remaining surfaces are only partially cleaned, so white colours appear greying, result due to a not completed soiling removal (for example: G_Wb_2 on brushes surfaces).
Compared to not treated samples, it seems that the better level of cleaning, is obtained when, besides soiling particles, also oily film is removed.

Table 21. Stereomicroscopic images (7X) of Titanium white acrylic samples areas, treated with erasers: on the left, a soiled not cleaned areas compared with surface cleaned on the right.

ERASERS **Name of sample**	**Smooth surface**	**Brushes surface**
G_SS_0001	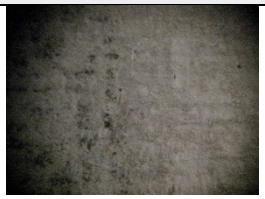	
G_Wb_2	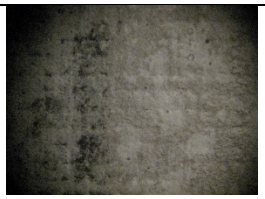	

G_Awb	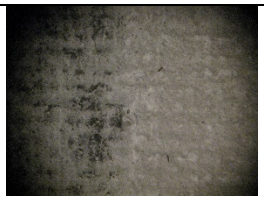	
G_Lli_1	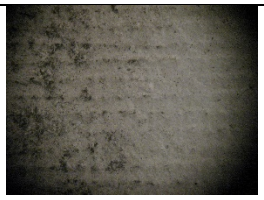	
G_Lal_2		
G_FC_1		
G_FC_3		
G_FOV12		
G_FES20		

G_Ep	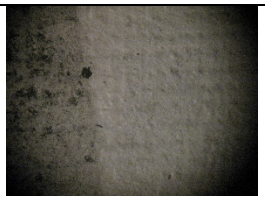	
G_DB		
G_Art		
G_Mrub	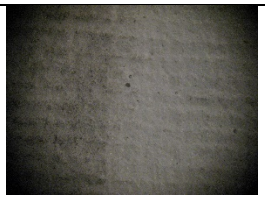	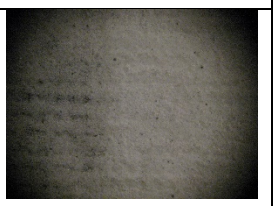
G_Mi_403	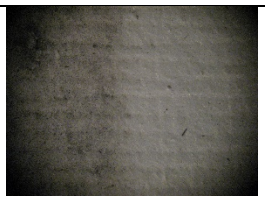	

From residues point of view, there is an important consideration to do: this type of materials are made to be "consumed"; erasers, during mechanical action, lost particles of gum, but it is quite simple to remove them with a gentle brush.
In spite of this procedure, some materials leave a great amount of particles, for example samples cleaned with G_Lli_1 and G_Lal_2, gum file dusts (Fig. 93).

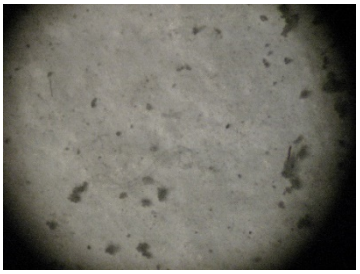

Figure 104. Detail of samples G_Lal_2 (45X), cleaned with gum file dust. We can observe the presence of gum residues as black particles.

Surfaces cleaned with sponges were listed in Table 22. It's divided into two parts, one relative to make-up type and the other to art type.
Compared to results obtained with erasers, is clear that these materials are not so effective in dirty removal.
All samples, in fact, present quite homogeneous oily greying skin, signing that sponges are not able to give complete cleaning. To catch imperceptible differences in the quality of treatment is essential to take into account colorimetric results, which will be presented in Par. 2.2.4.3.3.

Table 22. Stereomicroscopic images (7X) of Titanium white acrylic samples areas, treated with sponges (make-up and art): on the left, soiled not cleaned areas compared with surface cleaned on the right.

MAKE-UP SPONGES **Name of sample**	**Smooth surface**	**Brushes surface**
S_PP_ov	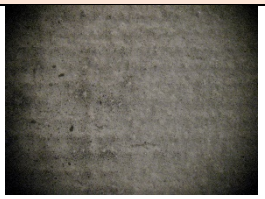	
S_PP_tr		

S_PP_ro		
S_RB_tr		
S_RB_uo	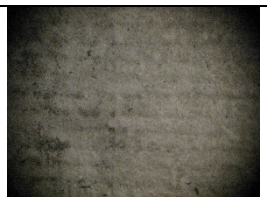	
S_RB_py	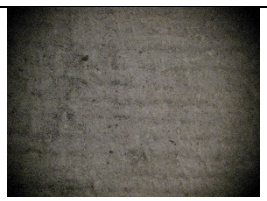	
S_RB_ro	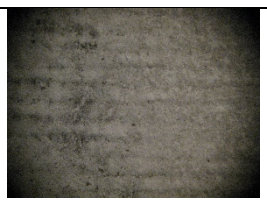	
S_KK_tr		
S_KK_ro	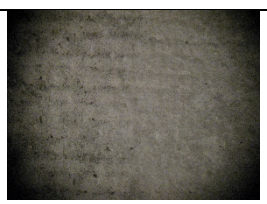	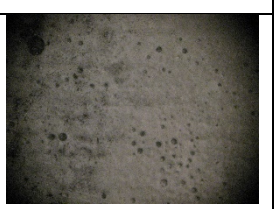

S_HM_uo		
S_HM_tr		
S_Sph_sp	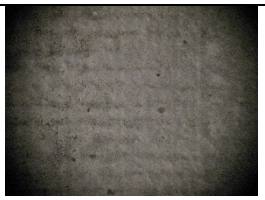	
S_Sph_uo		
S_Sph_ml	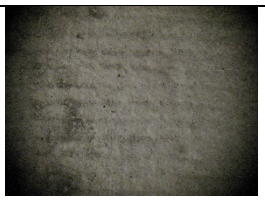	
S_Sph_ro		
ART SPONGES		
AS_kc_1	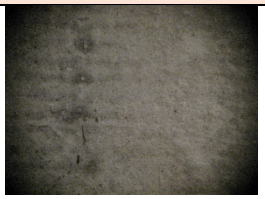	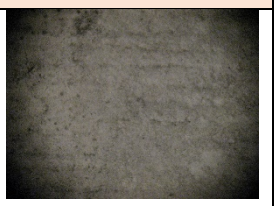

AS_sft_2		
AS_sft_3		
AS_sft_4		
AS_sft_5	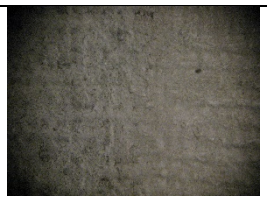	
AS_sft_6	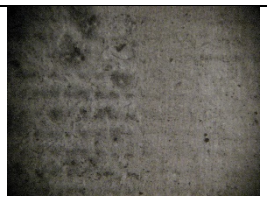	

Anyway, there is no visually perceptible difference, between make-up and art sponges, in terms of effectiveness.

Instead, some surfaces show the presence of residues of polymer, indifferently left by make-up and art treatment (Fig. 94). In fact, it is due to physico-mechanical characteristic of polymer constituent. They are soft and capable of being deformed during mechanical rubbing.

Figure 105. Detail of samples S_KK_tr (7X), cleaned with make-up sponge. We can observe the presence of polymer residues as black particles.

Finally, samples treated with cloths, are listed in Table 23. Similarly to considerations made for sponges, the effect of cleaning is not fully satisfactory. These materials, in fact are not able to remove dirty oily film completely, but only particles; probably their cleaning capacity is better if used wet.
In addition, there is no considerable difference among three trademarks, as shown in stereomicroscopic images.

Table 23. Stereomicroscopic images (7X) of Titanium white acrylic samples areas, treated with cloths: on the left, soiled not cleaned areas compared with surface cleaned on the right.

CLOTHS **Name of sample**	**Smooth surface**	**Brushes surface**
P_Sp_1	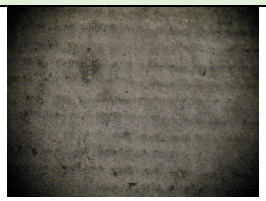	
P_Vi_2	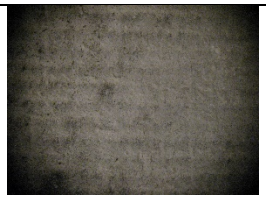	
P_Di_3	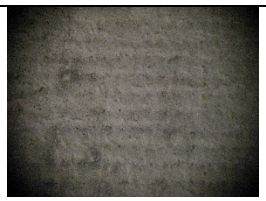	

In the case of Ultramarine blue acrylic samples, differences between cleaned and soiled-than-cleaned, are not as evident as for Titanium white one.
Obviously depending on darker colour, so also in this case, colorimetric test is indispensable to evaluate results correctly.
Figure 95 shows not treated surfaces, smooth and brushes.

Ultramarine blue acrylic

Smooth surface | Brushes surface

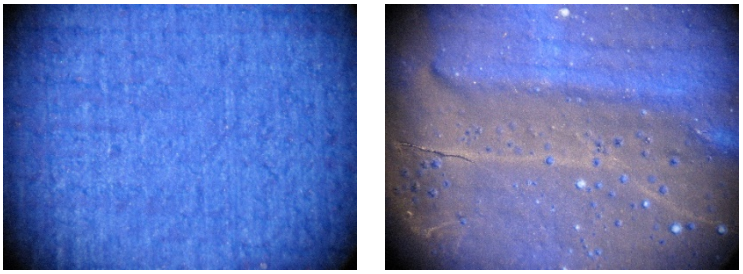

Figure 106. Stereomicroscopic images (7X) of Ultramarine blue acrylic areas, differentiated into smooth and brushes surfaces, not treated.

All the same, similarly to data obtained for white paint, we can observe that areas treated with erasers show the better level of cleaning. In particular, only in few samples are easy to see, as for example, G_Mi403, G_MRub, G_Art and G_SS001.

Table 24. Stereomicroscopic images (7X) of Ultramarine blue acrylic samples areas, treated with erasers: on the left, soiled not cleaned areas compared with surface cleaned on the right.

ERASERS **Name of sample**	**Smooth surface**	**Brushes surface**
G_SS_0001	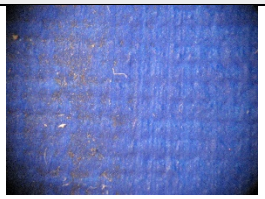	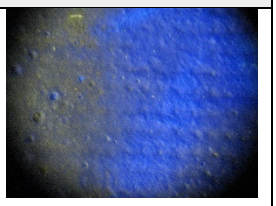
G_Wb_2		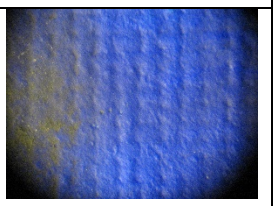

G_Awb	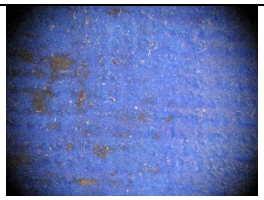	
G_Lli_1		
G_Lal_2	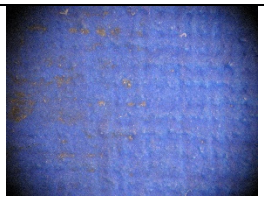	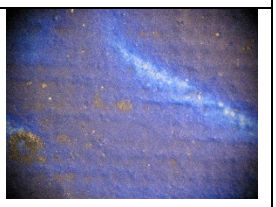
G_FC_1		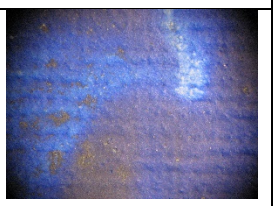
G_FC_3	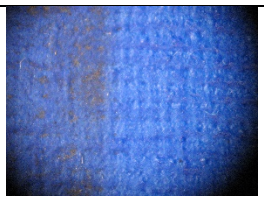	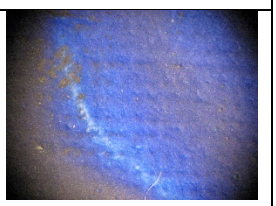
G_FOV12		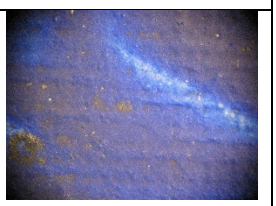
G_FES20		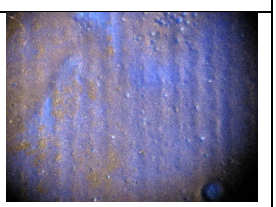

G_Ep		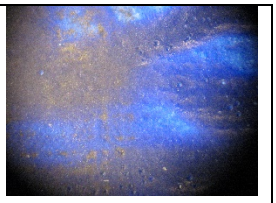
G_DB	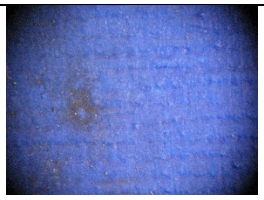	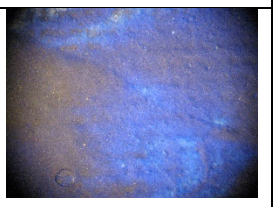
G_Art	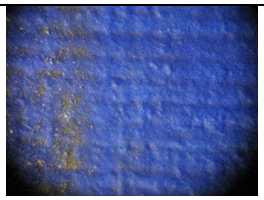	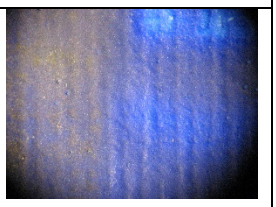
G_Mrub	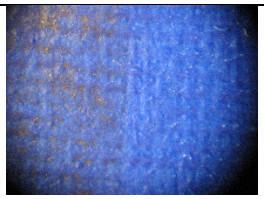	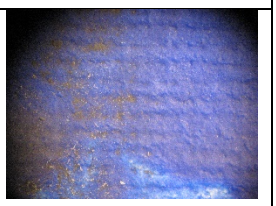
G_Mi_403	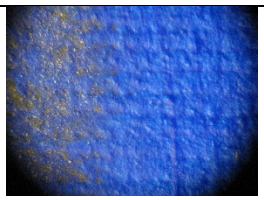	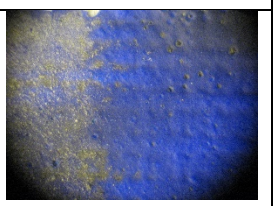

On the contrary, the presence of residues is more evident on blue surfaces: Fig. 96 reports evidences about this unavoidable effect.

On blue painting, in particular for smooth surface cleaned with Magic Rub eraser, mechanical degradation in term of abrasion and loss of colour was found, as shows in Fig. 97.

Figure 107. Detail of eraser residue on sample AL_Mi403 (45X).

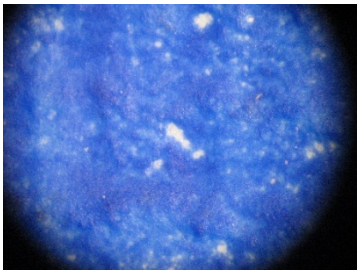

Figure 108. Particular of colour removal due to abrasion on sample AL_MRub (30X). This effect is caused by mechanical rubbing.

The difficulty of assessing the effectiveness of cleaning procedure is higher in the case of make-up and art sponges cleaning treatment, as seen for white paint.

Table 25. Stereomicroscopic images (7X) of Ultramarine blue acrylic samples areas, treated with sponges (make-up and art): on the left, soiled not cleaned areas compared with surface cleaned on the right.

MAKE-UP SPONGES **Name of sample**	**Smooth surface**	**Brushes surface**
S_PP_ov		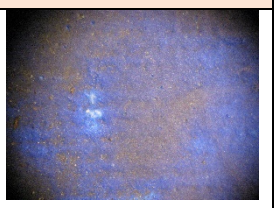
S_PP_tr		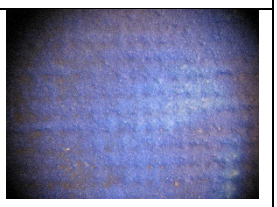
S_PP_ro	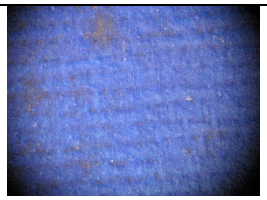	

S_RB_tr		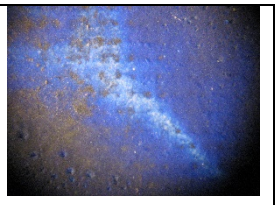
S_RB_uo	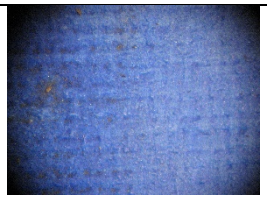	
S_RB_py	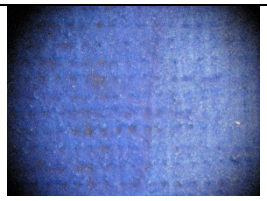	
S_RB_ro	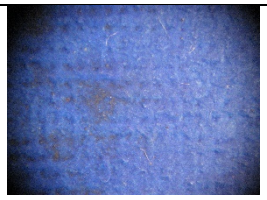	
S_KK_tr		
S_KK_ro		
S_HM_uo		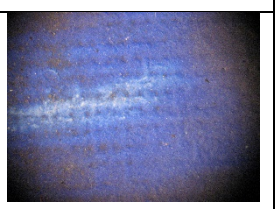

S_HM_tr	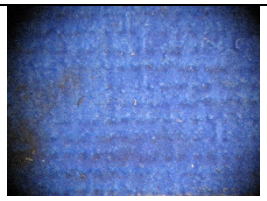	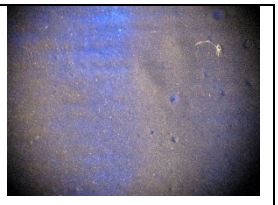
S_Sph_sp		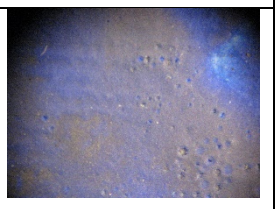
S_Sph_uo	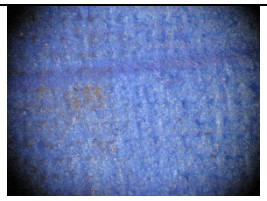	
S_Sph_ml	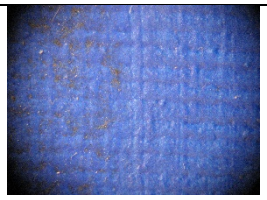	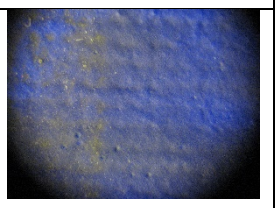
S_Sph_ro		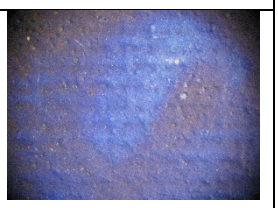
ART SPONGES		
AS_kc_1		
AS_sft_2		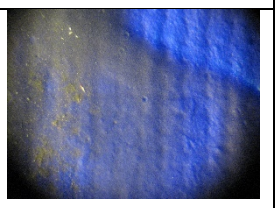

AS_sft_3		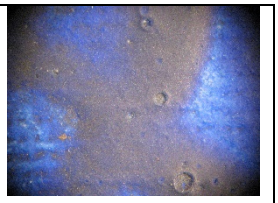
AS_sft_4		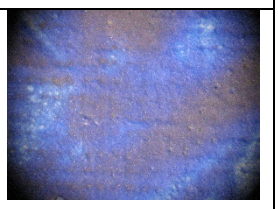
AS_sft_5		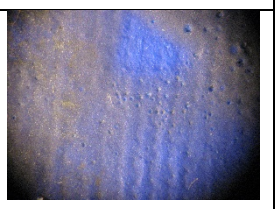
AS_sft_6		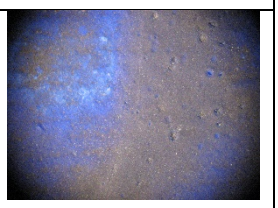

It can be stated that, both make-up and art sponges give comparable results from quality point of view (Table 24). In fact, both in smooth and brushes areas, sponges show a tendency to leave not slight amount of dirty deposits (Fig. 98).
We can find, again, the presence of polymer as residue (for example Fig. 99) and in some cases, scratches with vertical orientation, due to cleaning action (Fig. 100). This effect is not probably caused by sponge itself exclusively, but probably by the presence of particles on surfaces, drag during rubbing.

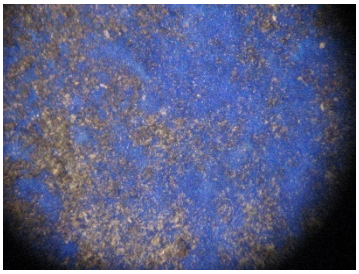

Figure 109. Detail of dirty residue on sample AL_RB_tr (30X).

Figure 110. Particular of make-up sponge residue on sample AM_RB_tr (45X).

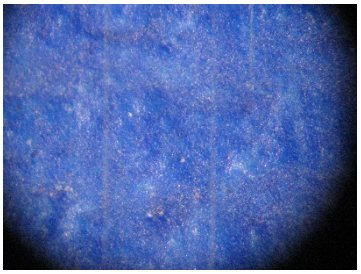

Figure 111. Detail of surface whit the evidence of scratches resulted by mechanical action of sponge on sample AL_RB_tr (30X).

For residues aspect, compared with comments made for erasers, sponges are not classified as "consumable"; mechanical stress due to rubbing cause breakup of material into smaller particles. Is to take into consideration the fact that this class of products are made for beauty and personal care, so substrate is human skin and not painted surfaces, wall, stone and so on.

The same considerations presented above can be apply to samples treated employing cloths (Table 26).

Table 26. Stereomicroscopic images (7X) of Ultramarine blue acrylic samples areas, treated with cloths: on the left, soiled not cleaned areas compared with surface cleaned on the right.

CLOTHS **Name of sample**	**Smooth surface**	**Brushes surface**
P_Sp_1	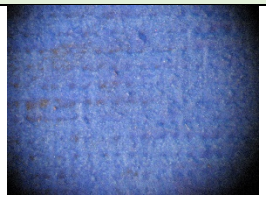	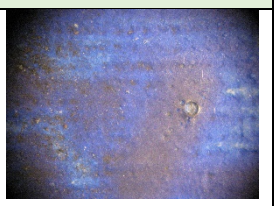
P_Vi_2	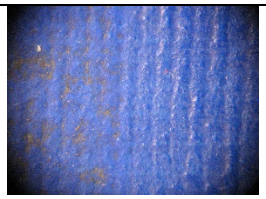	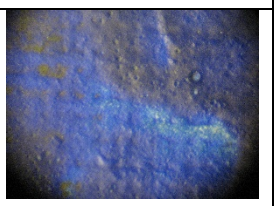

P_Di_3	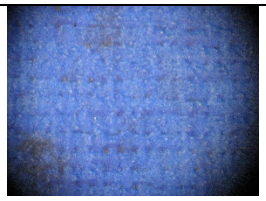	

Comparing surfaces not treated (Fig. 101) with samples soiled-than-cleaned reported in table below, is evident that cleaning gives no satisfactory results, in almost all cases of cleaning on oil film.

Titanium white oil

Smooth surface Brushes surface

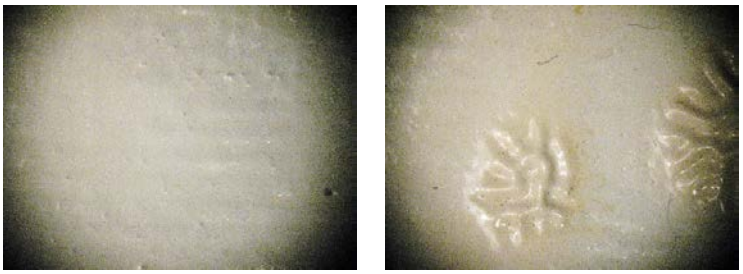

Figure 112. Stereomicroscopic images (7X) of Titanium white oil areas, differentiated into smooth and brushes surfaces, not treated.

Among erasers, only two samples show perceptible changes in soiling thinning and these are G_MRub and G_Mi403 (Table 27).

Table 27. Stereomicroscopic images (7X) of Titanium white oil samples areas, treated with erasers: on the left, soiled not cleaned areas compared with surface cleaned on the right.

ERASERS **Name of sample**	**Smooth surface**	**Brushes surface**
G_SS_0001		
G_Wb_2	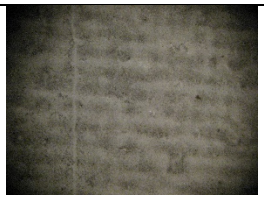	

G_Awb		
G_Lli_1	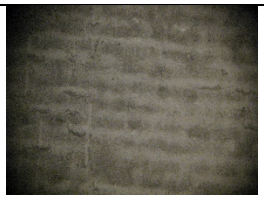	
G_Lal_2		
G_FC_1		
G_FC_3	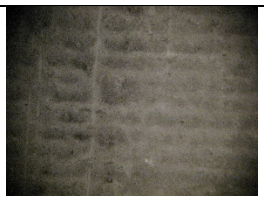	
G_FOV12	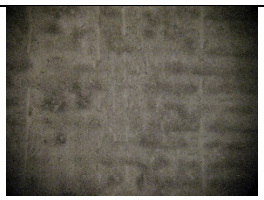	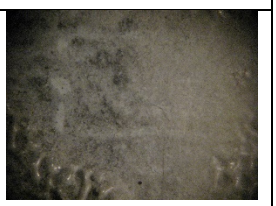
G_FES20		

G_Ep	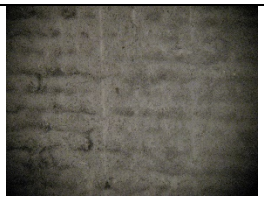	
G_DB	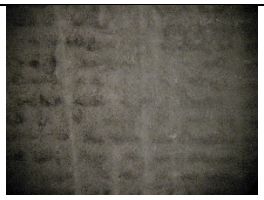	
G_Art	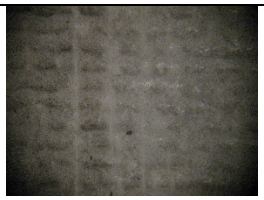	
G_Mrub		
G_Mi_403		

The same remarks could be extended to sponges (Table 28) and cloths (Table 29). Comparing two images of the same area cleaned with an art sponge, for example Soft tools_4, it is possible to notice that is inhomogeneous situation: despite surface in Fig. 102 a is considered "cleaned", there are a lot of soiling residues; Fig. 102 b represents worst result.

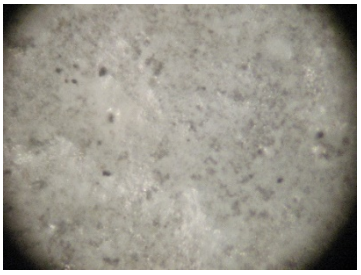
a
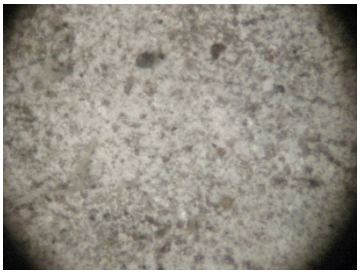
b

Figure 113. Images show the consequence of an inhomogeneous cleaning of surfaces, in sample OL_Sft_4: area in figure a present better result than one in figure b (45X).

Table 28. Stereomicroscopic images (7X) of Titanium white oil samples areas, treated with sponges (make-up and art): on the left, soiled not cleaned areas compared with surface cleaned on the right.

MAKE-UP SPONGES **Name of sample**	**Smooth surface**	**Brushes surface**
S_PP_ov		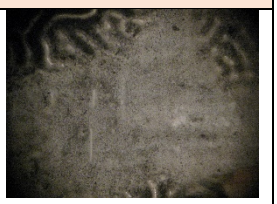
S_PP_tr		
S_PP_ro		
S_RB_tr		

S_RB_uo	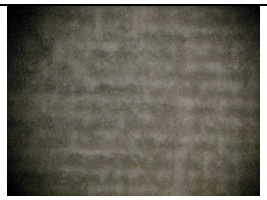	
S_RB_py		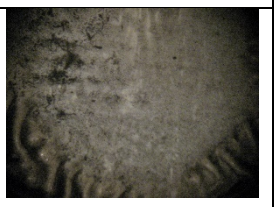
S_RB_ro	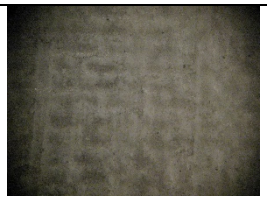	
S_KK_tr		
S_KK_ro	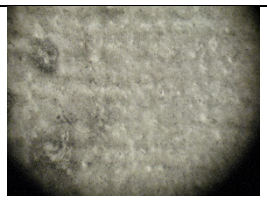	
S_HM_uo	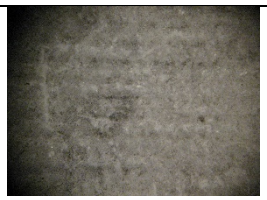	
S_HM_tr	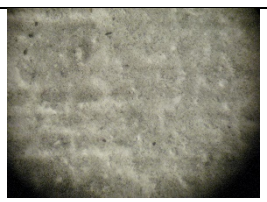	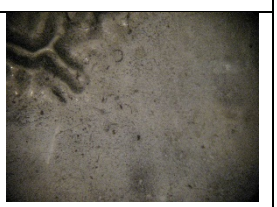

S_Sph_ml	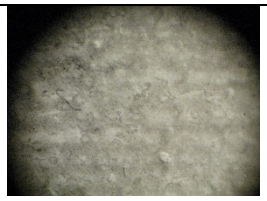	
S_Sph_sp	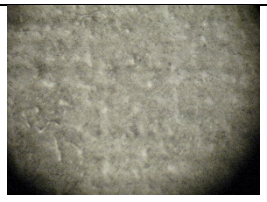	
S_Sph_ro		
S_Sph_uo		
ART SPONGES		
AS_kc_1	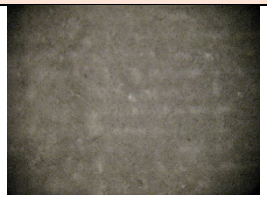	
AS_sft_2		
AS_sft_3		

AS_sft_4		
AS_sft_5		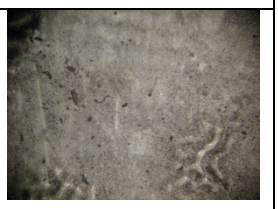
AS_sft_6	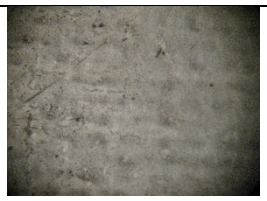	

Table 29. Stereomicroscopic images (7X) of Titanium white oil samples areas, treated with cloths: on the left, soiled not cleaned areas compared with surface cleaned on the right.

CLOTHS **Name of sample**	**Smooth surface**	**Brushes surface**
P_Sp_1	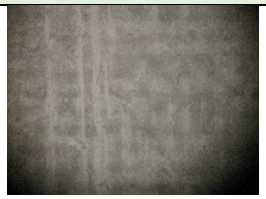	
P_Vi_2	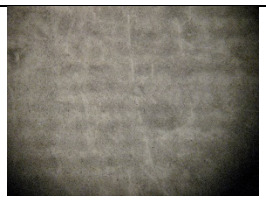	
P_Di_3		

In the case of Ultramarine blue oil drafts, evaluation of treatments is quite different; comparing not treated surfaces (Fig. 103) with treated samples, we can observe that among erasers cleaning, some results are perceptible (Table 30). In particular samples G_SS_0001, G_Wb_2 and G_MRub on brushes areas, G_FC_3 and G_Ep on smooth areas.

Ultramarine blue oil

Smooth surface Brushes surface

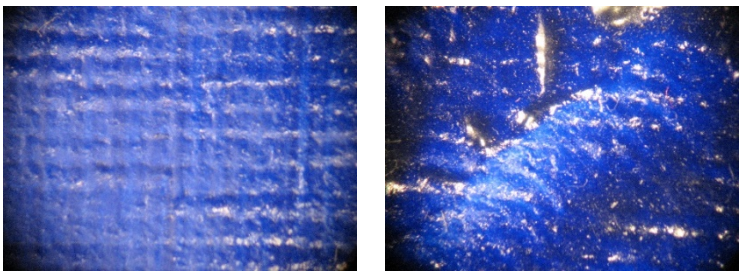

Figure 114. Stereomicroscopic images (7X) of Ultramarine blue oil areas, differentiated into smooth and brushes surfaces, not treated.

Table 30. Stereomicroscopic images (7X) of Ultramarine blue oil samples areas, treated with erasers: on the left, soiled not cleaned areas compared with surface cleaned on the right.

ERASERS **Name of sample**	**Smooth surface**	**Brushes surface**
G_SS_0001		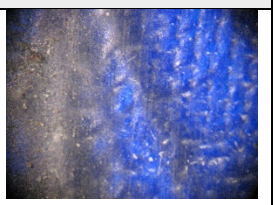
G_Wb_2		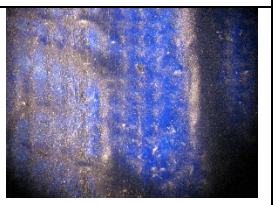
G_Awb		

G_Lli_1	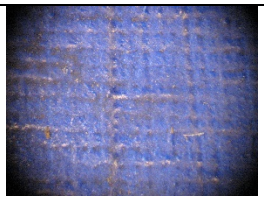	
G_Lal_2		
G_FC_1	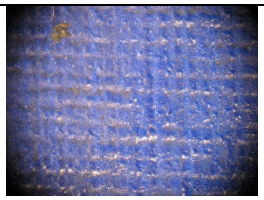	
G_FC_3	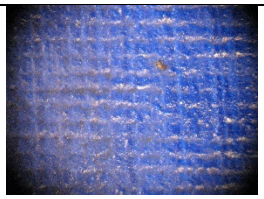	
G_FOV12		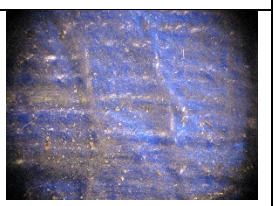
G_FES20	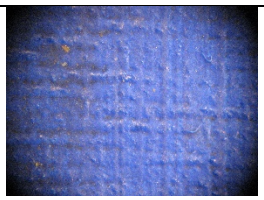	
G_Ep	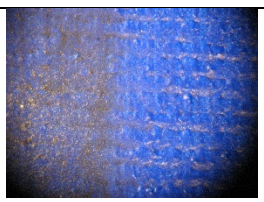	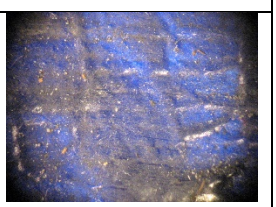

G_DB		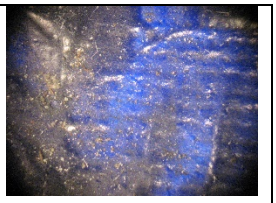
G_Art		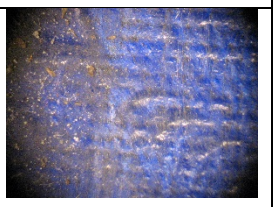
G_Mrub		
Mi_403		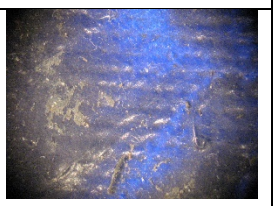

As for Ultramarine blue acrylic, residues if present are more visible. Two areas in particular are characterized by the presence of particles of polymer: samples treated with G_Wb_2 (Fig. 104) and with G_SS_0001. Personal experience in restauration, confirm tendency of these materials to breakup, leaving fragments of gum.

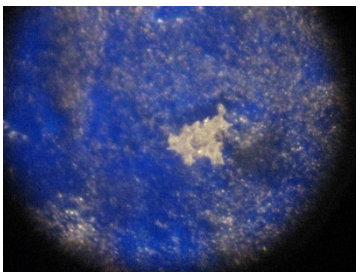

Figure 115. Particular of surface treated with G_Wb_2 characterized by the presence of a fragment of gum (45X).

Also among sponges, there are some relevant examples: areas cleaned with S_PP_ov, S_KK_tr, S_KK_ro, S_Sph_ml and AS_Sft_3 all on brushes surfaces; S_Sph_ml gives good result on smooth one too.

Table 31. Stereomicroscopic images (7X) of Ultramarine blue oil samples areas, treated with sponges (make-up and art): on the left, soiled not cleaned areas compared with surface cleaned on the right.

MAKE-UP SPONGES **Name of sample**	**Smooth surface**	**Brushes surface**
S_PP_ov		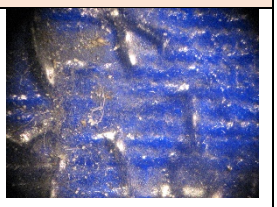
S_PP_tr	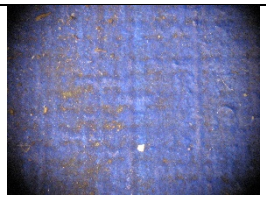	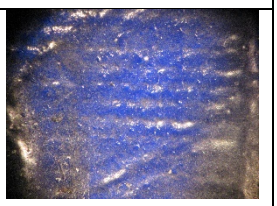
S_PP_ro	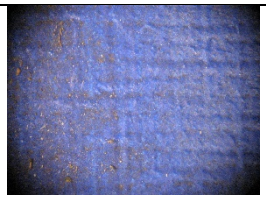	
S_RB_tr	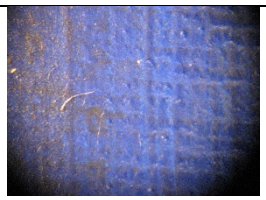	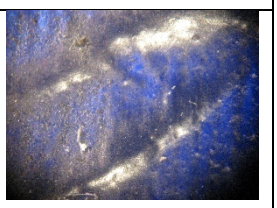
S_RB_uo		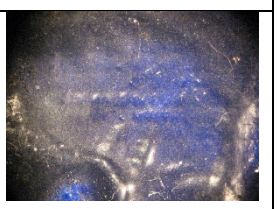

S_RB_py	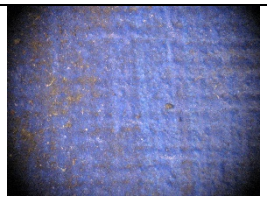	
S_RB_ro	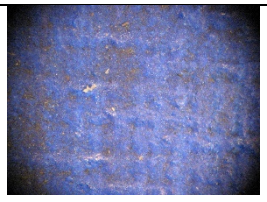	
S_KK_tr		
S_KK_ro		
S_HM_uo		
S_HM_tr	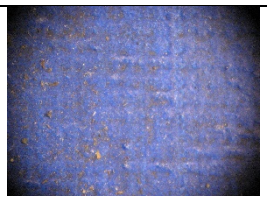	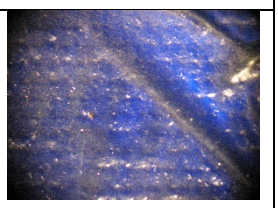
S_Sph_sp		

S_Sph_uo		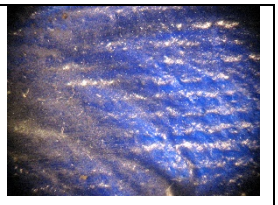
S_Sph_ml		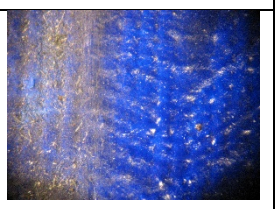
S_Sph_ro		
ART SPONGES		
AS_kc_1		
AS_sft_2		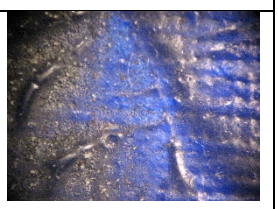
AS_sft_3	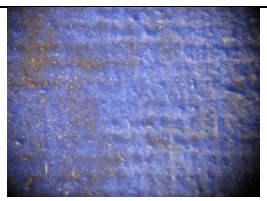	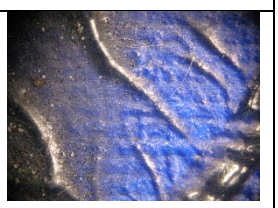
AS_sft_4	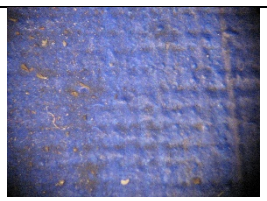	

AS_sft_5	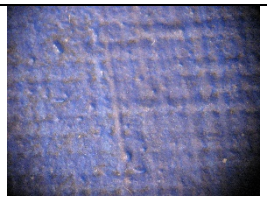	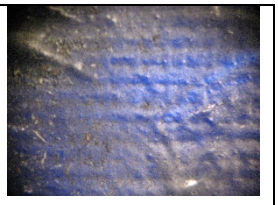
AS_sft_6	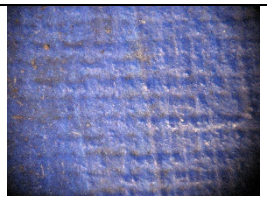	

Finally, treatment with cloths is reported in Table 32. Not peculiar observations can be made, respect to those already made for previous drafts.

Table 32. Stereomicroscopic images (7X) of Ultramarine blue oil samples areas, treated with cloths: on the left, soiled not cleaned areas compared with surface cleaned on the right.

CLOTHS **Name of sample**	**Smooth surface**	**Brushes surface**
P_Sp_1	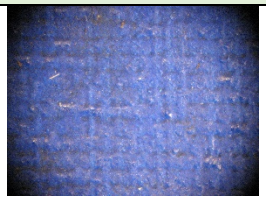	
P_Vi_2		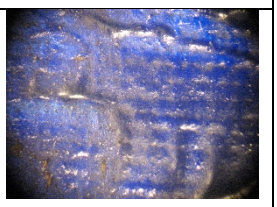
P_Di_3	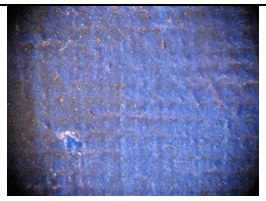	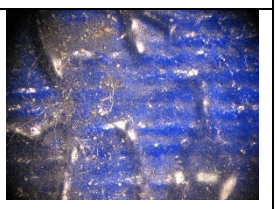

2.2.4.2.2 Environmental Scanning Electron Microscopy

A selected number of samples were observed by Environmental Electron Scanning Microscopy (ESEM), in order to evaluate changes in morphology of surfaces, not visible by stereomicroscopy observation.
In particular, firstly it was confirmed the different chemical affinity of soiling respect to acrylic and oil. Fig. 105 shows the comparison of two surfaces, once acrylic and the other oil, treated with two different products. In the image on the right, it is easy to recognize area not cleaned (left side of the photo), while in acrylic one, only few particles of dirty are visible. This behaviour can have influences on effectiveness of cleaning treatment.

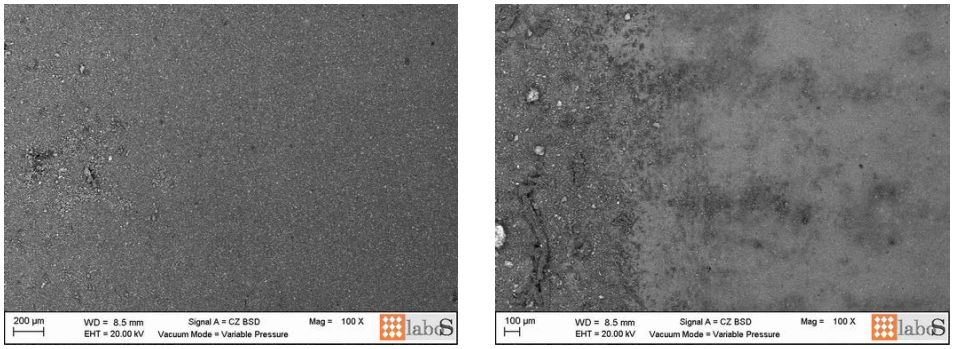

Figure 116. Comparison between surfaces of acrylic S_Sph_ml (left) and oil G_Ep (right) samples (BSD 100X): in the second one, dirty area on the left part of image is more evident than the same on S_Sph_ml.

Another remarkable aspect, not visible on stereomicroscopy revealed by scanning microscopy, is an unwanted degradation of film: some parts of colour film, collapsed under pressure caused by mechanical rubbing. Especially on brushes surfaces, where film is more thick and inhomogeneous (Fig. 106). This effect is more evident for acrylic film, because of the presence of air bubbles, originated during drying process.

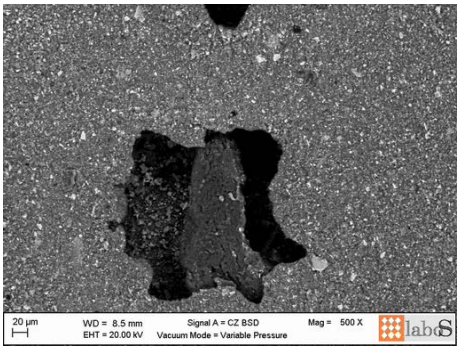

Figure 117. Detail of collapsed fragment of film colour on acrylic brushes sample treated with S_Sph_ml (BSD 500X).

ESEM images confirm again the effect of scratching of surfaces caused by some products as, for example, G_Ep shown in Fig. 107, already reported in stereomicroscopy remarks. Highest magnifications reveal biggest amount of this abrasion, respect to previous observations.

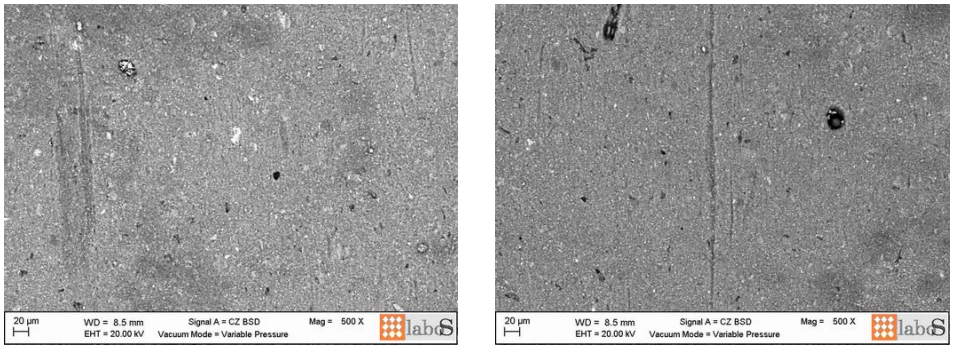

Figure 118. Surface scratched of sample cleaned with G_Ep: BSD 500X on the left and VPSE 500X on the right.

Finally, Fig. 108 reports another example of fragments of polymer left on surfaces after treatment with two different products (Eraser and make-up sponge, in particular). The image on the right is significant also to appreciate the morphology of one type of make-up sponge, at highest magnification.

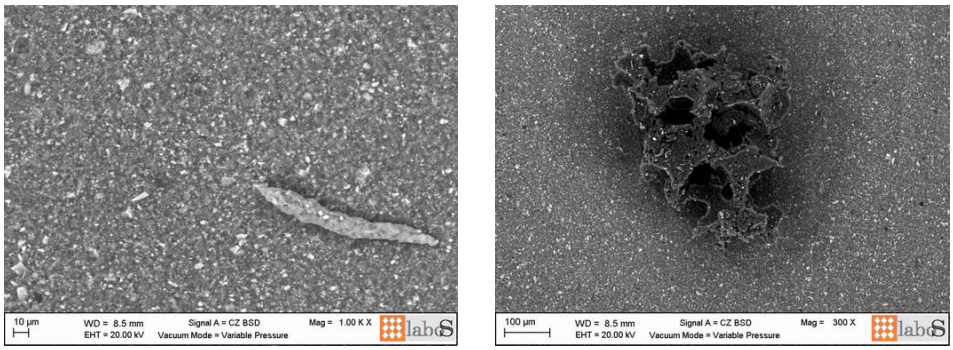

Figure 119. Details of polymer residues: on the left, sample treated with G_Fes20 (BSD 1000X) and on the right, sample treated with S_Sph_ml (VPSE 300X).

2.2.4.2.3 Colorimetric and Gloss tests

From colorimetric tests point of view, statistical analysis of data obtained is presented below.

Firstly, we can observe that, considering drafts separately with no attention to smooth or brushes surfaces, Ultramarine blue acrylic samples give the following results: 1.7% for ΔE*<2.3, 5.2% for ΔE* 2.3-5, 22.4% for ΔE* 5-10 and 70.7% for ΔE*>10

In the case of Ultramarine blue oil samples, values are: 6.7% for ΔE*<2.3, 8.3% for ΔE* 2.3-5, 23.3% for ΔE* 5-10 and 61,7% for ΔE*>10.

Comparing these values is possible to see that percentage of samples with ΔE* 5-10 and >10 is 93.1 and 85, respectively for acrylic and oil. This indicates that *dry methods* are more effective on Ultramarine blue oil draft, compared to acrylic one.

For Titanium white acrylic samples, values obtained are: 13.9% for ΔE*<2.3, 15.3% for ΔE* 2.3-5, 44.4% for ΔE* 5-10 and 26.4% for ΔE*>10.

Titanium white oil samples give the following results: 1.7% for ΔE*<2.3, 5.2% for ΔE* 2.3-5, 10.3% for ΔE* 5-10 and 82.8% for ΔE*>10 (Table 33).

Table 33. Pie charts of ΔE ranges values, related to both acrylic and oil, Ultramarine blue and Titanium white drafts, cleaned with Dry cleaning methods.*

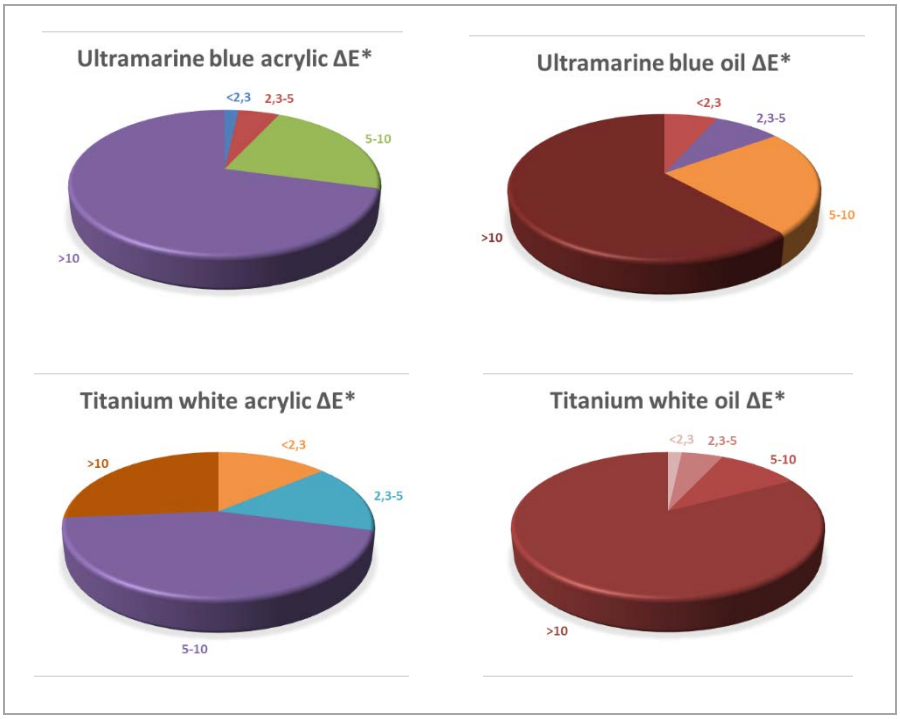

Starting from the same pie charts above, we can compare samples with same medium, but different colours; we observe that cleaning effectiveness on Ultramarine blue acrylic draft is less than the same on Titanium white acrylic one (ΔE* 5-10 and >10 of 93.1% for blue and 70.8% for white).

On the contrary, for oil drafts, blue colour gives a ΔE* 5-10 and >10 value of 85% compared to 93.1% of white one.

If we consider colorimetric data from materials point of view, is possible to underline that: 1.5% of sponges give value of ΔE*<2.3, while erasers 14.9% and cloths 0%; for values of ΔE* 2.3-5, percentages are 4.4% for sponges, 16% for erasers and 5.9% for cloths; for values of ΔE* 5-10, 24.8% is referred to sponges, 30.9% for erasers and 11.8% for cloths; finally values are 69.3% for sponges, 38.3% for erasers and 82.4% for cloths, related to ΔE*>10 (Fig. 109).

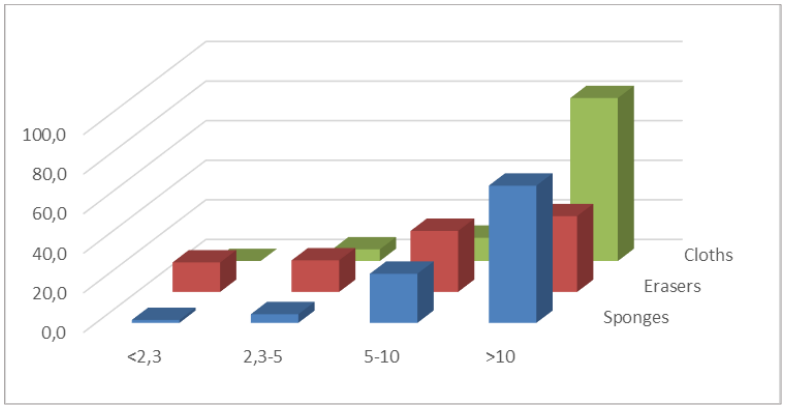

Figure 120. Histogram of ΔE ranges values respect to three classes of Dry cleaning materials. Percentages are calculated on total amount of samples (248).*

Referring to data shown above, we can observe that cleaning effectiveness that gives ΔE*<2.3 or 2.3-5, is due to treatments with erasers. Cloths, on the contrary, give worst results for major percentage of ΔE*>10, while sponges show intermediate behaviour.

Figure 110 focuses attention on effectiveness of cleaning, in the cases of smooth and brushes surfaces respectively. In particular, smooth film samples give 6.5% of ΔE*<2.3, the same value for ΔE* 2.3-5, 26.6% for ΔE* 5-10 and 60.5% for ΔE*>10.

Comparable results are obtained on brushes film surface: 6.5% for ΔE*<2.3, 11.3 for ΔE* 2.3-5, 25.8% for ΔE* 5-10 and 56.5% for ΔE*>10.

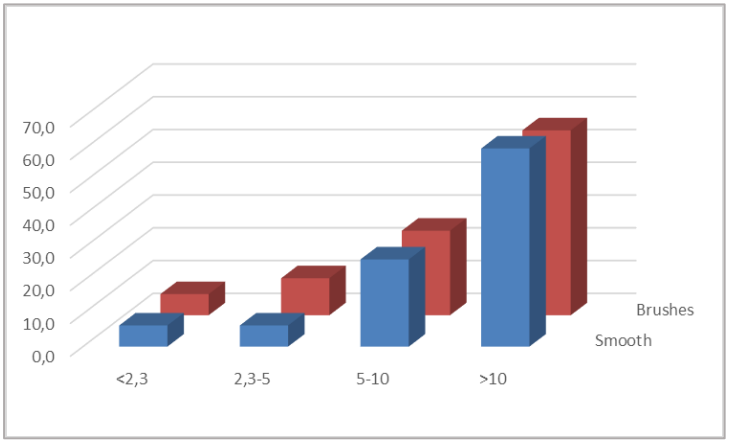

Figure 121. Histogram of ΔE ranges values respect to smooth and brushes painted surfaces. Percentages are calculated on total amount of samples (248).*

Histograms show in Fig. 111, plot percentages contributions of the different films, (smooth and brushes) on the total amount of cleaning treatments, presented on the basis of ΔE* ranges values. It's possible to confirm that data are comparable for each

draft and so, there is no difference between cleaning treatment effectiveness on smooth surface, as to brushes one.

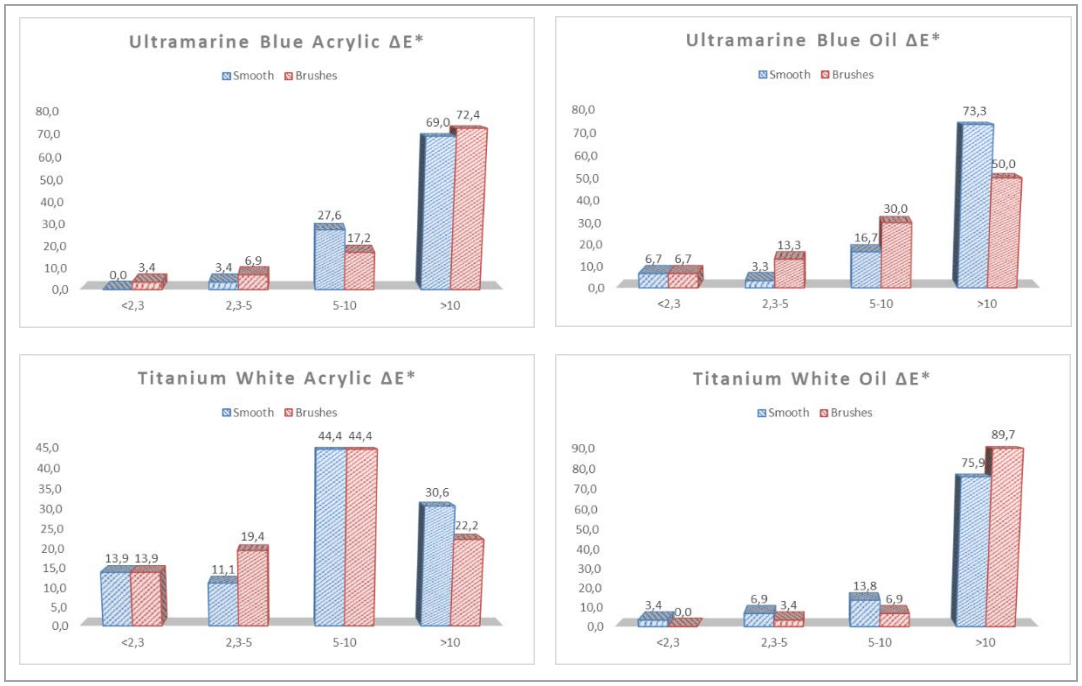

Figure 122. Histograms show, for each colour and medium, percentages given by two types of film (smooth or brushes), related on each ΔE ranges values.*

Figure 112 shows as dry methods (sponges, erasers and cloths), contribute to each ΔE* ranges values, divided into smooth and brushes surfaces.

In particular, in Ultramarine blue acrylic graph, smooth surface gives no ΔE*<2.3 values, while brushes one, gives 100% value using erasers. As for previous case, also ΔE* 2.3-5 values for smooth and brushes films, are given 100% by erasers. For smooth surface ΔE* 5-10 values are 100% obtained by erasers too, differently by brushes surface, that gives 40% by sponges and 60% by erasers. Finally, ΔE*>10 values for smooth surface are 75% by sponges, 15% by erasers and by 10% cloths, while for brushes one, 61.9% by sponges, 28.6% by erasers and 9.5% by cloths.

In Ultramarine blue oil graph, ΔE*<2.3 values are due for 100% by erasers for smooth film, while by sponges for brushes one; ΔE* 2.3-5 values are obtained for 100% by erasers for smooth surface, while for brushes one, data are 75% for sponges and 25% for cloths. In the case of ΔE* 5-10, values are 80% erasers, 20% cloths for smooth film, while 66.7%, 22.2% and 11.1% respectively for sponges, erasers and cloths, in the case of brushes one. For ΔE*>10, values are 81.8% for sponges, 13.6%

for erasers and 4.5% for cloths on smooth surface, while on brushes one, data are 40%, 53.3% and 6.7% for sponges, erasers and cloths respectively.
In Titanium white acrylic graph, 100% of values for ΔE*<2.3 is given by erasers both for smooth and brushes surfaces. For ΔE* 2.3-5, percentages are 25% for sponges and 75% for erasers on smooth surface, while 28.6% and 71.4% for sponges and erasers respectively. ΔE* 5-10 data are given by 75% and 25% thus by sponges and erasers for smooth film and 81.2% and 18.2% thus for sponges and erasers. Finally, on smooth surface, 63.6% for sponges, 18.2% for erasers and 18.2% for cloths are values for ΔE*>10 and on brushes one, 62.5% for sponges, 12.5% for erasers and 25% for cloths.
Concluding with Titanium white oil graph, 100% of values of ΔE*<2.3 on smooth surface is given by erasers. For the same ΔE* value on brushes surface, any type of dry methods gives result. For ΔE* 2.3-5, both in smooth surface than brushes one, 100% of data is obtained with erasers. Considering smooth surface and ΔE* 5-10, 25% of values is obtained with sponges, while 75% with erasers; differently on brushes surface, 100% of values is given by erasers. Finally, for ΔE*>10 on smooth surface, 68.2% is given by sponges, 22.7% by erasers and 9.1% by cloths, while 61.5% by sponges, 30.8% by erasers ad 7.7% by cloths, in the case of brushes surface.
A final consideration can be made on general effectiveness of dry methods: 6.5% of treatments give ΔE*<2.3, 8.9% ΔE*2.3-5, 26.2% ΔE* 5-10 and 58.5% ΔE*>10. These values indicate that surface *dry cleaning*, is not resolutive of cleaning operation on this type of artificial soiling.

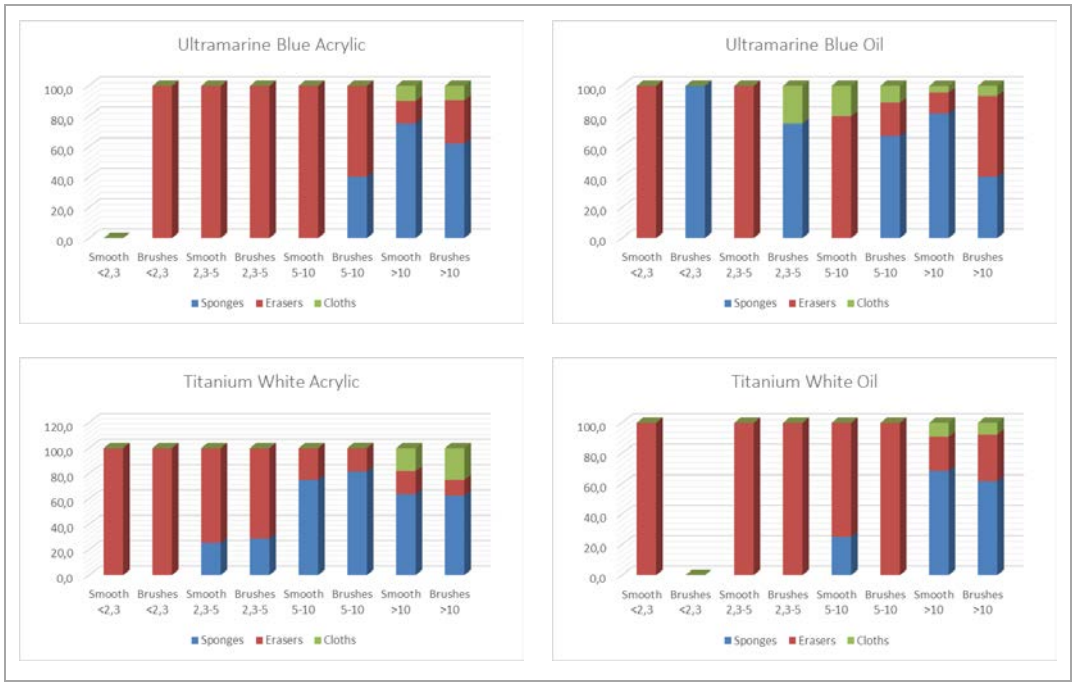

Figure 123. Histograms show percentages contribution of sponges, erasers and cloths, on the total amount of samples, divided as ΔE ranges values and smooth and brushes surfaces.*

Considering gloss test, data obtained are different related to type of treatments, colour and medium.

In fact, ΔUG% is higher in acrylic drafts, than in oil ones; there is no difference between colours white or blue. Discriminating factor is chemical composition of medium. Not treated oil film is glossier than acrylic one, therefore, changing in gloss factor is more detectable on acrylic matt film than that oil one.

Among *dry cleaning* methods tested, erasers and cloths give worst results; in fact they caused gloss increase of, respectively, +6.4% and 6.7%. On the contrary, samples treated with sponges, give moderate decrease of UG% factor. This result shows that artificial soiling oily component is partially removed during treatments.

2.3 Examples of applications of *Dry Cleaning* methods on real works of art

As explained in Introduction section, *Dry Cleaning* methods find their first application on paper conservation. Only during the last years, restorers try to

transfer this experience on different supports. This is the case of examples of surface cleaning reported below.

The first case study regards the application of some dry methods on a XV century wooden architectonic decoration, located in the Castle of Trabia, in Palermo, Sicily [88].

In particular, they are polychrome wooden shelves in a poor state of conservation (Fig. 113). The main reasons for degradation can be attributed, in addition to factors related to the technique, also to loss of functionality and consequently to preservation in an unsuitable environment where they remained stacked for decades.

Figure 124. Pictures of shelves covered with a thick soiling layer.

Firstly, cleaning tests were performed to find better method to use (controlled suction with polyester filter, brushes with soft bristles of different sizes and fat emulsions), but all were ineffective or dangerous for surfaces integrity.

The disappointing results obtained by traditional methods, prompted to test the *dry cleaning* methods, in particular: make-up sponges (PU and SBR) and white Wishab (Fig. 114).

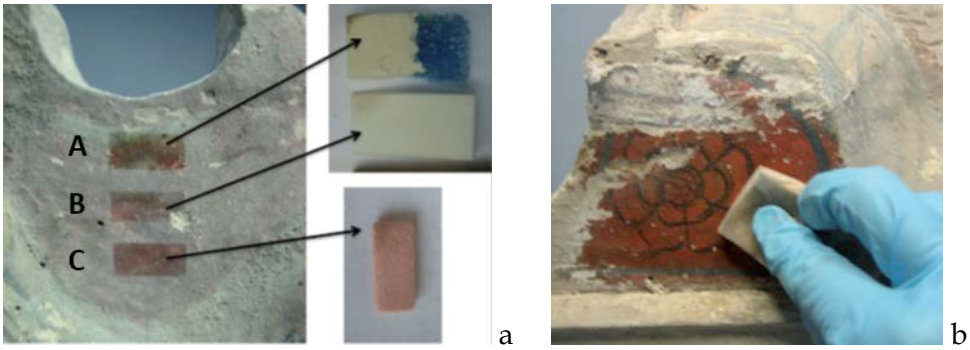

a b

Figure 125. a: Cleaning test with white Wishab (A), white PU make-up sponge (B) and pink SBR make-up sponge (C); b: particular of cleaning test with white PU make-up sponge.

Finally, representatives areas treated with dry methods were observed with optical and stereomicroscopy and SEM-EDS, before and after treatments, in order to evaluate effectiveness and respect of surfaces in term of abrasion and residues, confirming the validity of method.

The second case presented is about a conservation project on two wall paintings, Moani Haghighi "Senza titolo" (1996) and Emilio Tadini "Città" (1995) [89], part of the Mapp collection, a contemporary museum born in 1995 as restoration project of the former psychiatric hospital Paolo Pini in Milan.

Despite the young age of the works, some of these were in conservative precarious situations. The causes stem from several factors, primarily environmental: many works are open air and then directly exposed to climatic influences, such as changes in temperature and humidity, the solar irradiance, the rains and contaminants. Furthermore, some of them have been compromised by accidental or human damage: seepage of water, vandalism or maintenance work in buildings that were not considered as "substrate" of works of art.

Another critical is due to the very nature of the techniques used in contemporary materials or synthetic colours of which little is known on their behaviour over time. Often were used products borrowed from sectors not belonging to the sphere of art, where the concept of life has certainly not the same claim of "eternity".

Conservative project on paintings presented above, has taken into account new products and new systems of intervention, *dry cleaning*, in order to deal with more respect and selectivity of the refund of the surfaces, without compromise constituent materials.

Concerning Haghighi painting "*Senza Titolo*", the pictorial involving all elements of the wall, making them an integral part of the work as juxtaposed volumes (Fig. 115). The artist has concealed support materials with a uniform layer of white wall paint on which has triggered with acrylics.

Figure 126. Particular of Moani Haghighi "Senza Titolo" (1996), after restoration.

Damage were caused by a seepage of water from the roof that had washed out part of the surface, exposing the underlying materials, the wood of the door had brought to the surface brown tannins gore and the crystals of sulfates were solidified below white wall paint.

The peculiarities of the degradation and of the constituent materials, have conditioned the choices of products and the succession of work phases.

The delicacy of acrylic paint, sensitive both to the aqueous treatments, both to the apolar one, made preferable, where possible, the use of methods that would provide single mechanical removal of surface deposits, without the use of solvents.

Three types of products were chosen: white Wishab, Smoke Sponge and make-up sponges.

Considering the graphite drawing of Emilio Tadini "*Città*" (1995) (Fig. 116) it is arranged on either side of a fireplace. Again the elements present on the wall at the time of construction, such as applique mushroom for the lighting of the room, were been exploited by the artist to translate them into integral elements of the work.

Once again, with greater invasiveness, maintenance operations of the room did not take into account the interaction with the artwork.

Figure 127. Particular of graphite drawing of Emilio Tadini "Ciità" (1995) during cleaning tests.

It was necessary to differentiate cleaning according to the different degrees of dirt to be removed, by choosing different products.
Smoke sponge, used to clean white wall, was able to effectively clean the film of dirt deposited. Areas adjacent to the pencil marks were cleaned with a dry make-up sponge, because they could be passed even gently on graphite, without removal. The same sponges, used slightly moistened, allow effective cleaning action.
The uniformity of contact surface, combined with excellent ductility and smoothness, make make-up sponges a good substitute for traditional cotton swabs as support for aqueous solutions.
For halos residue was used a rubber Maped Epure type and to finish off areas adjacent to the pencil marks an elastomer in stick ø 2.3 mm brand Tombow Mono type zero have been used, supported by a pencil leads mines with expulsion snap.
Finally, also in these cases representatives areas treated with dry methods were observed with optical and stereomicroscopy and SEM-EDS, before and after treatments, in order to evaluate effectiveness and respect of surfaces in term of abrasion and residues, confirming the validity of methods.
The latter example regards a modern outside wall painting located in contemporary museum Mapp, as presented above.
Painting titled "*Sopra/Sotto*" was realized by Bernard Zimmer in 1995 [90], directly on the wall with synthetic colours acrylic base in aqueous medium: the abstract form and colour of the composition occupies a vertical height almost the entire

surface of the wall, using as background and pictorial component of the painting the same white paint of the exterior wall (Fig. 117). The colour is coated with a protective transparent acrylic drafting, waterproof and non-breathable, applied by a roller on the coloured surface, roughly following the morphology of the representation.

Figure 128. Image of wall painting "Sopra/Sotto"(1995), Bernard Zimmer, Mapp, Milano.

The pictorial surface, with not homogeneous degree of cohesion and amount of atmospheric particles deposited, needed a differentiated cleaning intervention. The inconsistent distribution of the protective and the different behaviour of the pigments in respect of the binder, responded differently to the products used for cleaning and the application methods.

Established the peculiarities of different backgrounds, cleaning tests specific for each of them were performed.

Among dry methods, three types of products have been selected: white Wishab, a SBR make-up sponge and Smoke Sponge rubber. Each pattern and products were used in two modes of application: for rubbing and "dabbing".

In general the tests by rubbing have shown a greater cleaning capacity than that "by dabbing", but for the most delicate parts, material and optical integrity of the surface were not guaranteed.

The Smoke sponge, as already mentioned, for applicability of the method and degree of cleaning obtained was preferred for the cleaning of both the white background, already partially washed away by rain, because it easier to obtain a

uniform cleaning. To contour coloured areas the sponge was sectioned into smaller chunks, proceeding, as for the rest, by dabbing.
Make-up sponges proved to be the most suitable for the colours that are not covered by the protective or for those areas, especially on the dark, where hairline cracks paint required cleaning action more delicate.

Studies presented show various but limited conservation cases, certainly not complete. For this reason, application on several works of art can improve knowledge about these materials and their optimal application.

2.4 Conclusions

The study about composition and chemical properties of materials for conservation is of paramount importance to improve knowledge and made restorers able to make well-reasoned decisions.
The aim of *Dry Cleaning* project was to characterize and apply different products for cleaning treatment on modern acrylic and unvarnished oil paints.
Major conclusions are about chemical characterization and application too.
The first consideration is about the presence of additives, both as inorganic fillers, and as antioxidants (BHT, BKF,…) and plasticizers (in particular phthalates). In fact, they could be released on surfaces after treatments and caused unwanted interactions with pictorial material.
Fillers were added to improve physico-mechanical properties of polymeric dough, but in some cases, not only inert compounds are present. In particular, this is the case of make-up sponges, in which nanoparticles of TiO_2 as Rutile and Anatase polymorphs are detectable. Therefore, the major problem rising by presence of residues containing TiO_2 is due to its well-known photocatalytic activity that could interfere with chromatic paintings conservation, in particular on organic dies.
Antioxidants and plasticizers, instead, were added respectively, to contrast oxidation phenomenon especially if natural rubber is present in polymeric dough, and to improve elastic properties, especially in erasers.
For this reason, restorers and conservators should choose among few products with no additives. However, often, manufacturer's formulations may change and provided product information may not be adequate.
Considering each class of compounds, it is possible to observe that, among products that can be classified as similar, there are several differences, not only from chemical point of view. The most significant example regards make-up sponges: in fact,

different polymers were identified, also in the same trademark but with various shapes, and characterized by very variable porosity. Not only between two different polymer, as expected, but also among sponges with the same chemical composition. This is probably due to extrusion properties depending on the final form.

This variability influences cleaning results: products with closed and fine porosity have higher effectiveness than more opened and less compact ones. Therefore, the latter have no mechanical resistance on rubbing, leaving great amounts of residues on surfaces. In particular, from this point of view, Polyurathane and Styrene-butadiene/natural rubber sponges are preferable to Acrylonytrile-butadiene-styrene ones.

After applications on painted samples, several considerations can be made about cleaning effectiveness on oil or acrylic, respects of surfaces, both in term of residues and of increasing of gloss factor or superficial abrasion or loss of colour.

Considering colorimetric data, it is possible to highlight that effectiveness of treatment on acrylic painting is better than that on oil painting. As discussed, this could be due to higher chemical affinity between artificial soiling oily medium and colours one. On the contrary, on acrylic film, soiling is not strongly bounded as so easily removable. Not significant differences are detectable between white or blue colours.

In general, erasers give better results on cleaning treatment, while sponges a middle result and, finally cloths the worst one.

In term of residues and respect of surfaces, cloths give highest results, while sponges left particles of polymer due to mechanical crumbling, while erasers cause, both abrasion and loss of colour.

Mechanical action due to "rubbing" products on surface, can cause not only morphology alterations, but also gloss factor increase. In particular, this effect is more significant on acrylic surface, because film is matt, while oil surface is glossy. For this reason the slightest variation in gloss factor are better detectable in the first case. Cloths and erasers treatments cause not negligible gloss factor increase, compared to sponges. This is probably due to higher compactness and hardness of the first two classes, compared to softness of sponges.

To better evaluate dry methods characteristics, diagrams were carried out, followings six (or five) parameters: **T** (topography integrity), **Cp** (cleaning power), **R** (absence of residues e.g. crumbs), **Cr** (clearance of residues e.g. crumbs), **G** (gloss integrity) and **ΔE** (conservation of original colorimetric parameters).

Multiple criteria should be taken in account to determine a successful dry cleaning treatment. Moreover, they should be considered in balance with each other to

achieve an optimum cleaning result, showing the best possible cleaning for the optimum preservation of the paint layer integrity.
Diagrams were carried out for most representative materials and they are presented below divided into erasers (fig. 118), sponges (Fig.119) and cloths (Fig.120).

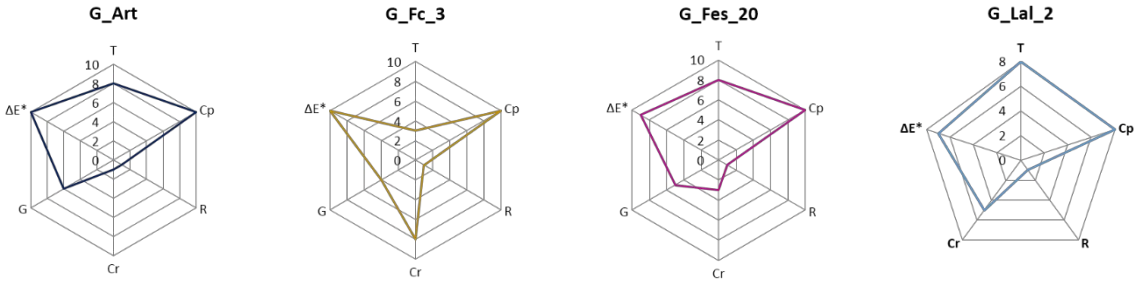

Figure 129. Examples of five and six points diagrams of erasers.

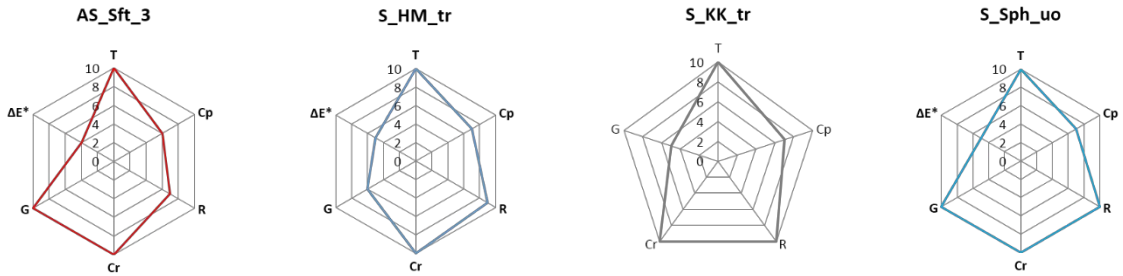

Figure 130. Examples of five and six points diagrams of art and make-up sponges.

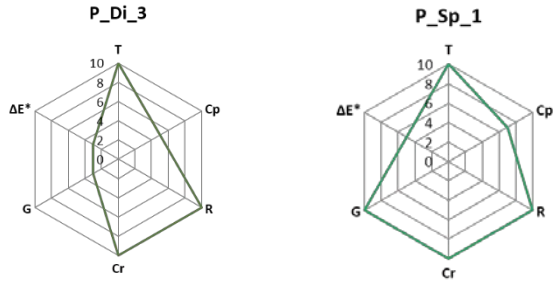

Figure 131. Examples of five and six points diagrams of cloths.

Diagrams give a visual representation of quality and effectiveness of each materials: bigger is area enclosed between the colored straight lines, better is the general evaluation of that product. For example, sample G_FC_3 has performed worse than S_Sph_uo or P_Sp_1 ones.
On the basis of this preliminary study, several investigations could be made; among these, for example, a study about interactions between products containing TiO_2

and substrates: the well-known photocatalytic action of these nanoparticles, can alter colours matter, if present as residues? Are these residues actually available? On the other hand, additives as antioxidants and plasticizers can be left on surfaces after treatment, an evaluation and characterizations of chemical products could be essential.

Studies on behaviour during ageing of these polymers. Residues can be chemically activated? Alternatively, the use of these materials to support solvents (if compatible) or aqueous solution in *Semi-humid cleaning* method.

Finally, a study about the increase of painted surface temperature due to mechanical action, using thermocromatic colours or a study about selectivity of dry methods on organic and inorganic fractions that make soiling.

Concluding, *Dry cleaning* method shows advantages and disadvantages in cleaning procedures: on incoherent soiling, as dust or particulate not bonded on artistic surfaces, it is possible to consider that as a complete treatment. On the contrary, on "hard" soiling considered, for example, in this study, effectiveness of dirt removal cannot be considered exhaustive and so proves to be most suitable for a previous operation on artworks, followed, if possible, by traditional solvent or aqueous cleaning treatment.

3. Conclusions

The projects presented are part of one of the most important conservative procedures applied on work of art: the cleaning treatment.
In particular, the first one concerns the application of chelating agents solutions on inorganic substrates, in order to remove calcium patinas present as decay products due to interaction between artistic support with environment.
Study about ability of two solutions of chelating agents, in particular ethylenediaminetetraacetic acid trisodium salt dihydrate and tribasic sodium citrate dihydrate at pH 8.35 and 8.60 respectively, to solubilize calcium salts, i.e. calcium carbonate, calcium sulfate dihydrate and calcium oxalate monohydrate, has been presented.
EDTA trisodium dihydrate solution shows higher effectiveness than that of tribasic sodium citrate dihydrate on all three salts, as expected comparing stability complex constants. In addition, it seems to have not selectivity among three salts, whose solubility depends only to the solubility products.
This evidence confirms what restorers observe during treatments with EDTA sodium salts, i.e. it is not possible to control its chelating activity, especially in the form of EDTA tetrasodium. It means that it is not guarantee that the action is only superficial and not dangerous for the integrity of the support.
Analytical determination of calcium concentrations in solutions, confirms the highest solubility of calcium sulfate dihydrate, followed by calcium carbonate and then by calcium oxalate monohydrate.
In the case of solution of tribasic sodium citrate dihydrate, results are different. It exerts its chelating ability less than EDTA trisodium dihydrate, as seen above; moreover, it seems to be almost completely ineffective on calcium oxalate monohydrate, while the reaction with calcium sulfate dihydrate causes the formation of an unexpected sparingly soluble sodium calcium double citrate ($NaCaC_6H_5O_7$), which has been characterized by physico-chemical analyses.
This result has important impact in conservation practice: the treatment of plaster surfaces with sodium citrate in the presence of calcium sulfate (either derived from degradation of plaster via sulfatation or as constituent material) can lead to the formation of this sparingly soluble salt resulting in a permanent compositional and morphological modification of the substrate.
The *Dry Cleaning* treatment, on the contrary, is defined as *surface cleaning* thanks to the completely absence of solvents or aqueous solutions.
This characteristic is essential in treatments on sensitive surfaces as paper, unvarnished oil, acrylic film or contemporary works of art, in general.

In particular, this method can be used both as complete treatment on incoherent soiling as dust or powder and as preventive approach on more bounded soiling, as presented in this study.
A selection among products available in the Italian large-scale retail trade was made, classified into erasers, sponges and cloths.
Complete analytical characterization was carried out in order to have the most complete knowledge about them and they were applied on painted samples and on real works of art too.
Polymers and additives identification is of paramount importance to choose products respectful of artistic substrate and that can guarantee no side effects after use. For example, among results obtained, Magic Rub eraser reveals polyvinyl-chloride rubber (PVC) composition, rich in plasticizers as phthalates, whose contact with surfaces may give rise to dangerous alterations on conservative point of view. In addition, erasers PVC free, so made of copolymer styrene-ethylene-butadiene-styrene rubber (SEBS) or vulcanized oils (Factice), for example, contains inorganic compounds, i.e. calcium carbonate, that can cause abrasion or mechanical stress to surface. Sponges are more softness and suitable to be applied on more substantial brushstrokes matter or with adhesion problems, but reveal the presence of antioxidants, above all into styrene-butadiene rubber/natural rubber (SBR/NR) or, in few cases, of nanoparticles of TiO_2 as filler, both in Anatase and Rutile polymorphs.
Among sponges class, make-up one give various polymer composition (polyurethane, styrene-butadiene rubber, natural rubber, acrylonitrile-butadiene rubber, acrylonitrile-butadiene-styrene rubber), showing compositional variability too high to be completely classified. Among different trademarks, as expected, but also among different shapes of the same trademark, composition changes.
Cloths characterzation, on the other hand, confirms what producers declare, showing compositional constancy.
In term of effectiveness, the best results in cleaning treatment, is given by erasers, followed by make-up and art sponges and the latter, cloths.
Colorimetric data prove that, on "hard" soiling considered in this study, effectiveness of dirt removal of dry methods cannot be considered complete.
In some cases, rubbing action on surfaces causes abrasion, scratches and loss of colour, besides gloss factor increase, in particular on acrylic film.
In addition, erasers and sponges leaves residues, i.e. crumbs, on surface, given by mechanical crumbling of materials. Cloths give better results with no residues left.

Macroscopic crumbs can be gently removed with a soft brush, but additives contained into microscopic fragments can persist on surface. For this reason is of paramount importance clarify chemical properties of these plasticizers or antioxidants and if they are really available and able to interact with support.
This preliminary study focuses attention on chemical composition of materials, but a large survey of applications and control of parameters to validate the method is required.
Concluding, the two studies presented have the objective to highlights the importance of scientific approach on conservation practices. A good cognisance on physico-chemical properties can help restorers and conservators to make better choices and plan more suitable conservative project, in full compliance of work of art.

References

[1] A.A. Ramadan, Journal of Cultural Heritage, "*Chemical cleaning of soiled deposits and encrustations on archaeological glass: A diagnostic and practical study*", (2013), Volume 14, Issue 2, pp. 97-108. DOI: 10.1016/j.culher.2012.03.010

[2] P. Gaspar, C. Hubbard, D. McPhail, A. Cummings, Journal of Cultural Heritage, "*A topographical assessment and comparison of conservation cleaning treatments*", (2003), Volume 4, Supplement 1. DOI: 10.1016/S1296-2074(02)01211-6

[3] M. Rizzi, M. Matteini, OPD Restauro, "*Solvent action of Bi- and Tetra-sodic EDTA towards gypsum and calcium oxalate in the cleaning of calcareous artefacts*", (1999), Volume 11, pp. 235-240.
http://www.opificiodellepietredure.it/index.php?it/389/opd-restauro-n-11-1999

[4] D. Benedetti, E. Bontempi, R. Pedrazzani, A. Zacco and L.E. Depero, Phase Transitions, "*Transformation in calcium carbonate stones: some examples*", (2008), Volume 81 (2-3), pp. 155-178. DOI: 10.1080/01411590701514342.

[5] G. Montana, L. Randazzo, I.A. Oddo, M. Valenza, Environmental Geology, "*The growth of "black crusts" on calcareous building stones in Palermo (Sicily): a first appraisal of anthropogenic and natural sulphur sources*", (2008), Volume 56, pp. 367–380. DOI: 10.1007/s00254-007-1175-y.

[6] A. Duran, M.D Robador, J.L. Perez-Rodriguez, International Journal of Architectural Heritage, "*Degradation of Two Historic Buildings in Northern Spain by Formation of Oxalate and Sulphate-Based Compounds*", (2012), Volume 6, Issue 3, pp. 342-358. DOI: 10.1080/15583058.2010.551447

[7] F. Cariati, R. Rampazzi, L. Toniolo, A. Pozzi, Studies in Conservation, "*Calcium oxalate films on stone surfaces: Experimental assessment of the chemical formation*", (2000), Volume 45:3, pp. 180-188.

[8] J.L. Perez-Rodriguez, A. Duran, M.A. Centeno, J.M. Martinez-Blanes, M.D. Robador, Thermochimica Acta, "*Thermal analysis of monument patina containing*

hydrated calcium oxalates", (2011), Volume 512, Issues 1–2, Pages 5-12. DOI: 10.1016/j.tca.2010.08.015

[9] L. Rampazzi, A. Andreotti, I. Bonaduce, M.P. Colombini, C. Colombo, L. Toniolo, Talanta, "*Analytical investigation of calcium oxalate films on marble monuments*",(2004), Volume 63, Issue 4, Pages 967-977. DOI: 10.1016/j.talanta.2004.01.005

[10] A. Bralia, M. Matteini, A. Moles, G. Sabatini, Atti del Convegno Internazionale "Le pellicole ad ossalati: origine e significato nella conservazione delle opere d'arte. Milano, Ottobre 1989. Centro CNR, Gino Bozza" in Milan, "*La sintesi degli ossalati di calcio nell'interpretazione delle patine presenti sui marmi esposti all'aperto. Risultati preliminari*", (1989), pp. 75–84.

[11] B. Doherty, M. Pamplona, C. Miliani, M. Matteini, A. Sgamellotti, B. Brunetti, Journal of Cultural Heritage, "*Durability of the artificial calcium oxalate protective on two Florentine monuments*", (2007), Volume 8, Issue 2, pp. 186–192. DOI: 10.1016/j.culher.2006.12.002

[12] B. Doherty, M. Pamplona, R. Selvaggi, C. Miliani, M. Matteini, A. Sgamellotti, B. Brunetti, Applied Surface Science, "*Efficiency and resistance of the artificial oxalate protection treatment on marble against chemical weathering*", (2007), Volume 253, Issue 10, pp. 4477-4484. DOI: 10.1016/j.apsusc.2006.09.056

[13] E. Beltrami, M. Berzioli, M. Cagna, A. Casoli, V.E. Selva Bonino, QUADERNO N.10/CESMAR7, "*La pulitura dei dipinti murali: uno studio di applicabilità di sistemi tradizionali e sistemi addensati con gel acquosi di poliacrilato*", (2012), il Prato ed., Padova.

[14] R.M. Smith, A.E. Martell, R.J. Motekaitis, *NIST Critically Selected Stability Constants of Metal Complexes Database*, (2007), Gaithersburg, MD, USA.

[15] J. Fan, P.O. Schwille, A. Schmiedl, E. Fink, M. Manoharan, Arzneimittel-Forschung-drug research, "*Calcium oxalate crystallization in undiluted postprandial urine of healthy male volunteers as influenced by citrate*", (2001), Volume 51(10), pp. 848-857.

[16] U. Herrmann, P.O. Schwille, A. Schmiedl, J. Fan, M. Manoharan, Biomedicine & Pharmacotherapy, "*Acute effects of calcium sodium citrate supplementation of a test meal on mineral homeostasis, oxalate, and calcium oxalate crystallization in the urine of healthy humans - preliminary results in patients with idiopathic calcium urolithiasis*", (1999), Volume 53(5/6), pp. 264-273. DOI: 10.1016/S0753-3322(99)80097-3

[17] Y. Ito, S. Tsurufuji, M. Shikita, S. Ishibashi, Chemical & Pharmaceutical Bulletin, "*Detoxication and excretion of radioactive strontium. IV. Effect of sodium calcium citrate and the mode of action of citrate*", (1958), Volume 6, pp. 287-90, Retrieved from http://www.biomedsearch.com/nih/Detoxication-excretion-radioactive-strontium-IV/13573487.html

[18] CAS Registry Number: 14076-65-4.

[19] B. Ormsby, T. Learner, M. Schilling, J. Druzik, H. Khanjian, D. Carson, G. Foster, M. Sloan, "*The Effects of Surface Cleaning on Acrylic Emulsion Paintings – A Preliminary Investigation*", In Oberflächenreinigung; Materialien und Methoden, (2006), VDR Schriftenreihe 2, Ed. Cornelia Weyer, Theiss Verlag, Stuttgart, pp. 135-149.

[20] B. Ormsby, P. Smithen, "*A scientific evaluation of surface cleaning acrylic emulsion paintings*", ICOM Committee For Conservation, Vol II, (2008), 15th Triennial Conference New Delhi: 22-26 September 2008, Allied Publishers. ISBN: 8184243464, 9788184243468

[21] B. Ormsby, T. Learner, "*The effects of wet surface cleaning treatments on acrylic emulsion artist's paints – a review of recent scientific research*", (2009), Reviews in Conservation, Number 10.

[22] L. Mills, A. Burnstock, S. de Groot, L. Megens, M. Bisschoff, H. van Keulen, F. Duarte, K.J. van den Berg, "*Water Sensitivity of Modern Artists' Oil Paints*" in preprints ICOM Committee for Conservation, Vol. II, (2008), 15th Triennial Meeting New Delhi: 22-26 September 2008, Allied Publishers Pvt. Ltd. pp.651-659.

[23] A. Burnstock, K.J. Van den Berg, S. de Groot, L. Wijnberg, "*An Investigation of Water-Sensitive Oil Paints in 20th Century Paintings*", In Reprints of the Modern

Paints Uncovered conference, London 2006, (2008), ed. T. Learner, Los Angeles: Getty, pp. 177-188.

[24] R. Morrison, A. Bagley-Young, A. Burnstock, K.J. van den Berg, H. van Keulen. "*An investigation of parameters for the use of citrate solutions for surface cleaning unvarnished paintings*", Studies in Conservation 52 (2007), pp. 255-270. DOI: http://dx.doi.org/10.1179/sic.2007.52.4.255

[25] J.S. Tsang, D. Erhardt, "*Current Research on the Effects of Solvents and Gelled and Aqueous Cleaning Systems on Oil Paint Films*", Journal of the American Institute for Conservation, (1992), Volume 31 Issue 1, pp. 87-94. ISSN: 0197-1360 1945-2330

[26] A. Phenix, K. Sutherland, "*The cleaning of paintings: effects of organic solvents on oil paint films*", Studies in Conservation, (2001), Volume 46 Issue Supplement-1 pp. 47-60. DOI: http://dx.doi.org/10.1179/sic.2001.46.Supplement-1.47

[27] L. Owen, R. Ploeger, A. Murray, "*The effects of water exposure on surface characteristics of acrylic emulsion paints*", (2009), Journal of the Canadianassociation for conservation, Volume 29.

[28] B. Ormsby, E. Kampasakali, C. Miliani, T. Learner, "*An FTIR-based exploration of the effects of wet cleaning treatments on artists' acrylic emulsion paint films*", e-Preservation Science, (2009), Volume 6, pp.186-195. ISSN: 1581-9280 1854-3928. morana-rtd.com

[29] R. Ploeger, D. Scalarone, O. Chiantore, "*The characterization of commercial artists' alkyd paints*", Journal of Cultural Heritage, (2008), Volume 9, Issue 4, pp. 412-419. DOI: http://dx.doi.org/10.1016/j.culher.2008.01.007

[30] T. Learner, "*Analysis of Modern Paints*", Research in conservation (2004), Getty Publications. ISBN: 0892367792, 9780892367795

[31] M. Daudin-Schotte, M. Bisschoff, I. Joosten, H. van Keulen, K.J. van den Berg, "*Dry Cleaning Approaches for Unvarnished Paint Surfaces*", Smithsonian contributions to museum conservation, (2013), Number 3.

[32] M. Daudin-Schotte, M. Bisschoff, I. Joosten, H. van Keulen, K.J. van den Berg, "*Dry Cleaning Approaches for Unvarnished Paint Surfaces, New Insights into the Cleaning of Paintings*", Proceedings from the Cleaning 2010 International Conference, Smithsonian Institution Scholarly Press, (2013), Valencia, 26-28 May 2010, Smithsonian Institute, pp. 209-219. ISSN: 1949-2359 1949-2367

[33] B.V. Mendes, K.J. van den Berg, L. Megens, I. Joosten, M. Daudin, "*New Approaches to Surface Cleaning of Contemporary Unvarnished Oil Paintings - Moist Sponges and Cloths*", in Issues in Contemporary Oil Paint, (2014), Proceedings from the ICOP Symposium, 28 and 29 March 2013, Amersfoort, The Netherlands; Springer Ed.

[34] J. Cowan, S. Guild, "*Dry methods for surface cleaning paper*", Technical Bulletin No. 11, Department of Canadian Heritage, Canadian Conservation Institute, (2001), ISBN: 0-662-30077-7

[35] E. Estabrook, "*Consideration of the effect of erasers on cotton fabric,* JAIC 28, (1989), pp.79-96.

[36] P. Sterlini, "*Surface cleaning products and their effect on paper*", in Paper Conservation News, no 76, pp.3-7, (1995).

[37] M. Daudin-Schotte, H. Van Keulen, K.J. Van der Berg, "*Analisi e applicazione di materiali per la pulitura a secco di superfici dipinte non verniciate – Analysis and application of dry cleaning materials on unvarnished paint surfaces RCE Project from 2006 to 2009*", Quaderno Cesmar7 n°12, (2014), Il Prato Ed. ISBN:978-88-6336-235-0

[38] G. Antonioli, F. Fermi, C. Oleari, R. Reverberi, "*Spectrophotometric Scanner for imaging of paintings and other works of art*", (2004), CGIV, pp.219-224.

[39] G. Sharma, *Digital Color Imaging Handbook (1.7.2 ed.),* (2003), CRC Press, ISBN 0-8493-0900-X.

[40] R.B. Simpson, "*Rubber basics*", Rapra Technology LTD, (2002), ISBN: 1-85957-307-x

[41] S. Tsuge, H. Ohtani, C. Watanabe, "*Pyrolysis-GC/MS data book of Synthetic polymers*", Elsevier, (2011), ISBN: 978-0-444-53892-5

[42] P. Larkin, "*Infrared and Raman Spectroscopy. Principles and spectral interpretation*", Elsevier, (2010).

[43] R.C Wolbers, "*The use of a synthetic soiling mixture as a means for evaluating the efficacy of aqueous cleaning materials on painted surfaces*", Conservation, restauration des Biens Culturels: revue de l'ARAAFU, (1992)

[44] A.R. Khataee, M.B. Kasiri, "*Photocatalytic degradation of organic dyes in the presence of nanostructured titanium dioxide: Influence of the chemical structure of dyes*", Journal of Molecular Catalysis A: Chemical, Volume 328, Issues 1–2, 3, (2010), Pages 8-26, ISSN 1381-1169, http://dx.doi.org/10.1016/j.molcata.2010.05.023.

[45] L. Bergamonti, I. Alfieri, A. Lorenzi, A. Montenero, G. Predieri, G. Barone, P. Mazzoleni, S. Pasquale, P.P. Lottici, "*Nanocrystalline TiO2 by sol–gel: Characterisation and photocatalytic activity on Modica and Comiso stones*", Applied Surface Science, Volume 282, (2013), pp.165-173, ISSN 0169-4332, http://dx.doi.org/10.1016/j.apsusc.2013.05.095.

[46] L. Bergamonti et al., "*Synthesis and characterization of nanocrystalline TiO2 with application as photoactive coating on stones*", Environmental Science and Pollution Research, (2014), Volume 21, Issue 23.

[47] L. Bergamonti et al., "*Characterization and photocatalytic activity of TiO2 by sol–gel in acid and basic environments*", Journal of Sol-Gel Science and Technology, (2014), DOI: 10.1007/s10971-014-3498-y

[48] K. Gorna, M. Hund, M. Vučak, F. Gröhn, G. Wegner, "*Amorphous calcium carbonate in form of spherical nanosized particles and its application as fillers for polymers*", Materials Science and Engineering: A, Volume 477, Issues 1–2, (2008), pp. 217-225, ISSN 0921-5093, http://dx.doi.org/10.1016/j.msea.2007.05.045.

[49] S. Kwon, K. J Kim, H. Kim, P. P Kundu, T. J Kim, Y. K Lee, B. H Lee, S. Choe, "*Tensile property and interfacial dewetting in the calcite filled HDPE, LDPE, and LLDPE composites*", Polymer, Volume 43, Issue 25, (2002), pp. 6901-6909, ISSN 0032-3861, http://dx.doi.org/10.1016/S0032-3861(02)00399-3.

[50] M.A. Osman, A. Atallah, "*Effect of the particle size on the viscoelastic properties of filled polyethylene*" Polymer, Volume 47, Issue 7, (2006), pp. 2357-2368, ISSN 0032-3861, http://dx.doi.org/10.1016/j.polymer.2006.01.085.

[51] M. and I. Ash, "*Handbook of preservatives*", Synopse Information Resources Inc, SIR, (2004), ISBN: 1-890595-66-7

[52] A. Nersasian, D.E. Andersen, "*The structure of polysulphonated polyethylene*", Journal of Applied Polymer Science, Vol.4, Issue 10, pp.74-78, (1960).

[53] D. Messadi, J.M Vergnaud, "*Quick identification and analysis of plasticizers in PVC by programmed-temperature gas chromatography using the best stationary phases*", Journal of Applied Polymer Science, Volume 24, Issue 5, pp.1215-1225, (1979), DOI: 10.1002/app.1979.070240507

[54] R. Navarro, M. Pérez Perrino, M. Gómez Tardajos, H. Reinecke, "*Phthalate Plasticizers Covalently Bound to PVC: Plasticization with Suppressed Migration*", Macromolecules, 2010, 43 (5), pp 2377–2381, DOI: 10.1021/ma902740t

[55] A. Marcilla, S. García, J.C. García-Quesada, "*Study of the migration of PVC plasticizers*", Journal of Analytical and Applied Pyrolysis, Volume 71, Issue 2, (2004), pp. 457-463, ISSN 0165-2370, http://dx.doi.org/10.1016/S0165-2370(03)00131-1.

[56] S.M. Erhan, R. Kleiman, "*Factice from oil mixtures*", Journal of the American Oil Chemists' Society, (1993), Volume 70, Issue 3, pp 309-311.

[57] M. E. Cain, K. F. Gazeley, I. R. Gelling, P. M. Lewis, "*The Chemistry and Technology of Rubber-Bound and Related Novel Antioxidants*", Rubber Chemistry and Technology, (1972), Vol. 45, No. 1, pp. 204-221

[58] D.K. Setua, S.K. De, "*Scanning electron microscopy studies on mechanism of tear fracture of styrene-butadiene rubber*", Journal of Materials Science, (1983), Volume 18, Issue 3, pp 847-852

[59] J. Diez1, R. Bellas, C. Ramírez, A. Rodríguez, "*Effect of organoclay reinforcement on the curing characteristics and technological properties of SBR sulphur vulcanizates*",

Journal of Applied Polymer Science, Volume 118, Issue 1, pp. 566–573, (2010), DOI: 10.1002/app.32431

[60] W. Salgueiro, A. Marzocca, A. Somoza, G. Consolati, S. Cerveny, F. Quasso, S. Goyanes, "*Dependence of the network structure of cured styrene butadiene rubber on the sulphur content*", Polymer, Volume 45, Issue 17, (2004), pp. 6037-6044, ISSN 0032-3861, http://dx.doi.org/10.1016/j.polymer.2004.05.008.

[61] N. Minagawa, J.L. White, "*The influence of titanium dioxide on the rheological and extrusion properties of polymer melts*", Journal of Applied Polymer Science, Volume 20, Issue 2, pp. 501–523, (1976), DOI: 10.1002/app.1976.070200222

[62] C.B. Ng, L.S. Schadler, R.W. Siegel, "*Synthesis and mechanical properties of TiO_2-epoxy nanocomposites*", Nanostructured Materials, Volume 12, Issues 1–4, 1999, pp.507-510, ISSN 0965-9773, http://dx.doi.org/10.1016/S0965-9773(99)00170-1.

[63] W. Bahloul, V. Bounor-Legaré, L. David, P. Cassagnau, "*Morphology and viscoelasticity of PP/TiO_2 nanocomposites prepared by in situ sol–gel method*", Journal of Polymer Science Part B: Polymer Physics, Volume 48, Issue 11, pp. 1213–1222, (2010), DOI: 10.1002/polb.22012

[64] S. Chakravarty, P.K. Chatterjee, A.K. Sircar, "*Sulfur group analysis in unaccelerated vulcanization of natural rubber*", Journal of Applied Polymer Science, Volume 9, Issue 4, pp. 1395–1417, (1965), DOI: 10.1002/app.1965.070090417

[65] R. L. Sibley, "*Organic Sulfides as Vulcanizing Agents of Rubber*", Rubber Chemistry and Technology, (1951), Vol. 24, No. 1, pp. 211-223, DOI: http://dx.doi.org/10.5254/1.3543041

[66] M.J. Fernandez-Berridi, N. Gonzalez, A. Mugica, C. Bernicot, "*Pyrolysis-FTIR and TGA techniques as tools in the characterization of blends of natural rubber and SBR*", Thermochimica Acta 444, (2006), pp.65-70.

[67] S. Chakraborty, S. Bandyopadhyay, R. Ameta, R. Mukhopadhyay, A.S. Deuri, "*Application of FTIR in characterization of acrylonitrile-butadiene rubber (nitrile rubber)*", Polymer Testing, Volume 26, Issue 1, (2007), pp. 38-41, ISSN 0142-9418, http://dx.doi.org/10.1016/j.polymertesting.2006.08.004.

[68] D.M. Kulich, S.K. Gaggar, V. Lowry, R. Stepien, "*Acrylonitrile–Butadiene–Styrene Polymers*", Encyclopedia Of Polymer Science and Technology, DOI: 10.1002/0471440264.pst011

[69] D.M. Kulich, S.K. Gaggar, V. Lowry, R. Stepien, "*Acrylonitrile–Butadiene–Styrene (ABS) Polymers*", Kirk-Othmer Encyclopedia of Chemical Technology, DOI: 10.1002/0471238961.01021911211209.a01.pub2

[70] Technical sheet "*Antioxidant BHT, 2,6-di-tert-butyl-para-cresol (butylated hydroxytoluene),* Akrochem Corporation Rubber Chemicals.

[71] E. Delebecq, J.P. Pascault, B. Boutevin, F. Ganachaud, (2013), "*On the Versatility of Urethane/Urea Bonds: Reversibility, Blocked Isocyanate, and Non-Isocyanate Urethane*". Chemical Reviews 113: 80–118. DOI: 10.1021/cr300195n.

[72] T. Whelan, "*Polymer Technology Dictionary*", Springer Science & Business Media, (1994), ISBN: 0412581809, 9780412581809

[73] P. Bahadur, N.V. Sastry, "*Principles of Polymer Science*", Alpha Science International, (2005), ISBN: 184265246X, 9781842652466

[74] R.O. Ebewele, "*Polymer Science and Technology*", CRC Press, (2010), ISBN: 1420057804, 9781420057805

[75] S. Thomas, C. Sinturel, R. Thomas, "*Micro and Nanostructured Epoxy / Rubber Blends*", John Wiley & Sons, (2014), ISBN: 3527666893, 9783527666898

[76] J.S. Mills, "*The Gas Chromatographic Examination of Paint Media. Part I. Fatty Acid Composition and Identification of Dried Oil Films*", Studies in Conservation, 11(2), pp. 92–107, DOI: http://dx.doi.org/10.1179/sic.1966.011

[77] E. Manzano, L.R. Rodriguez-Simón, N. Navas, R. Checa-Moreno, M. Romero-Gámez, L.F. Capitan-Vallvey, "*Study of the GC–MS determination of the palmitic–stearic acid ratio for the characterisation of drying oil in painting: La Encarnación by Alonso Cano as a case study*", Talanta, Volume 84, Issue 4, (2011), pp. 1148-1154, ISSN 0039-9140, http://dx.doi.org/10.1016/j.talanta.2011.03.012.

[78] M.P. Colombini, A. Andreotti, I. Bonaduce, F. Modugno, E. Ribechini "*Analytical Strategies for Characterizing Organic Paint Media Using Gas Chromatography/Mass Spectrometry*", Acc. Chem. Res., 2010, 43 (6), pp 715–727, DOI: 10.1021/ar900185f

[79] J. Peris-Vicente, U. Baumer, H. Stege, K. Lutzenberger, J.V. Gimeno Adelantado, "*Characterization of Commercial Synthetic Resins by Pyrolysis-Gas Chromatography/Mass Spectrometry: Application to Modern Art and Conservation*", Anal. Chem., 2009, 81 (8), pp 3180–3187, DOI: 10.1021/ac900149p

[80] T.J.S. Learner, "*Analysis of Modern Paints,* (2005), Research in Conservation, GCI Publication, ISBN 978-0-89236-779-2.

[81] M.T. Doménech-Carbò, A. Doménech-Carbò, J.V. Gimeno-Adelantado, F. Bosch-Reig, "*Identification of synthetic resins used in work of art by Fourier Transform Infrared Spectroscopy*", (2001), Applied Spectroscopy Vol. 55, Number 12.

[82] M.R. Derrick, D. Stulik, J.M. Landry, "*Infrared Specrtoscopy in Conservation Science*", (1999), The Getty Conservation Institute, Los Angeles.

[83] N.C. Scherrer, Z. Stefan, D. Francoise, F. Annette, K. Renate, "*Synthetic organic pigments of the 20th and 21thcentury relevant to artist's paints: Raman spectra reference collection",* (2009), Spectrochimica Acta Par A 73, pp.505-524.

[84] S.Q. Lomax, T. Learner, "*A review of the classes, structures and methods of analysis of synthetic organic pigments*", (2006), JAIC 45, pp.107-125.

[85] D. Scalarone, O. Chiantore, "*Separation techniques for the analysis of artists' acrylic emulsion paints*", (2204), J. Sep. Sci. 27, pp.263-274.

[86] A.C. Hellgren, P. Weissenborn, K. Holmberg, "*Surfactants in water-borne paints*", (1999), Progress in organic Coating, Number 35, pp. 79-87.

[87] E. Jablonski, T. Learner, J. Hayes, M. Golden, "*Conservation concerns for acrylic emulsion paints*", (2003), Reviews in Conservation number 4.

[88] A. Giordano, A.Casoli, V. E. Selva Bonino, "*Il metodo Dry Cleaning per la pulitura delle opere d'arte: il caso studio delle mensole lignee policrome del castello di Trabia*", Progetto Restauro, Il Prato Casa Editrice, Saonara, Padova 2014, 68, 42-48.

[89] D. Riggiardi, A. Casoli, V.E. Selva Bonino, "*La Pulitura a Secco di due opere murali contemporanee: Moani Haghighi "Senza Titolo" ed Emilio Tadini "Città*", Progetto Restauro, Il Prato Casa Editrice, Saonara, Padova 2014, 68, 32-41.

[90] D. Riggiardi, E. Isella, "*Dry Cleaning e consolidamento: due ricerche applicate su un'opera ad acrilico su muro nel cantiere scuola dell'Accademia di Brera nel parco del Mapp*", Atti del Congresso Annuale IGIIC - 23/25 ottobre 2014 - Accademia di Belle Arti di Brera, Milano.

- webbook.nist.gov/chemistry/
- www.britannica.com
- www.sigmaaldrich.com
- www.specialchem4polymers.com
- www.sciencedirect.com
- https://apps.webofknowledge.com
- https://scifinder.cas.org

Acknowledgments

I would like to thanks so many people and Institutions for their contribution to realization of this thesis.

Firstly, from the Department of Chemistry of University of Parma, Prof. Antonella Casoli who allow me to carry out this project during PhD period.
Very special thanks to Prof. Giovanni Predieri and Prof. Matteo Tegoni who supported with precious spurs and comprehension my research and me. Without their suggestions, I hardly would have reached these levels in experimentation.
From Department of Physics of University of Parma, Prof. Pier Paolo Lottici, who gave me the possibility to improve my analysis.

I am also grateful to Prof. Oscar Chiantore, from Department of Chemistry of University of Turin and Dr. Chiara Riedo and Dr. Dafne Cimino, for their fundamental contribute to chemical characterization of materials and for their sincere friendship. I found in them valid researchers and reliable professional.

Thanks to Dr. Paola Croveri from Centro Conservazione e Restauro La Venaria Reale (Turin), a very helpful person, who gave me support in environmental electron microscopy materials characterization.

I would like also to express my gratitude to Association Cesmar7, in particular Dr. Ilaria Saccani, Mr. Davide Riggiardi, Dr. Michela Berzioli and Mr. Erminio Signorini, who encourage me during all PhD period and cooperated concretely for realization of project.

A special thanks to Dr. Elisa Isella from Academy of Brera (Milan) and Experimental stations for the industry INNOVHUB, Experimental Station for Paper, Pulp and Paper Cartoons Division-Milan, the first one who allow to test method on real works of art and the possibility to disclose study and results; the second one for its precious analytical support.

Finally, I would also like to thank Dr. Laura Bergamonti for its friendship and daily encouragement, Mr. Beppe Foroni, for its irreplaceable work, Dr. Monica Maffini, Dr. Beatrice Bonati and Dr. Monica Mattarozzi.

Last but not least, my family and friends who have never doubted my abilities.

Appendix I

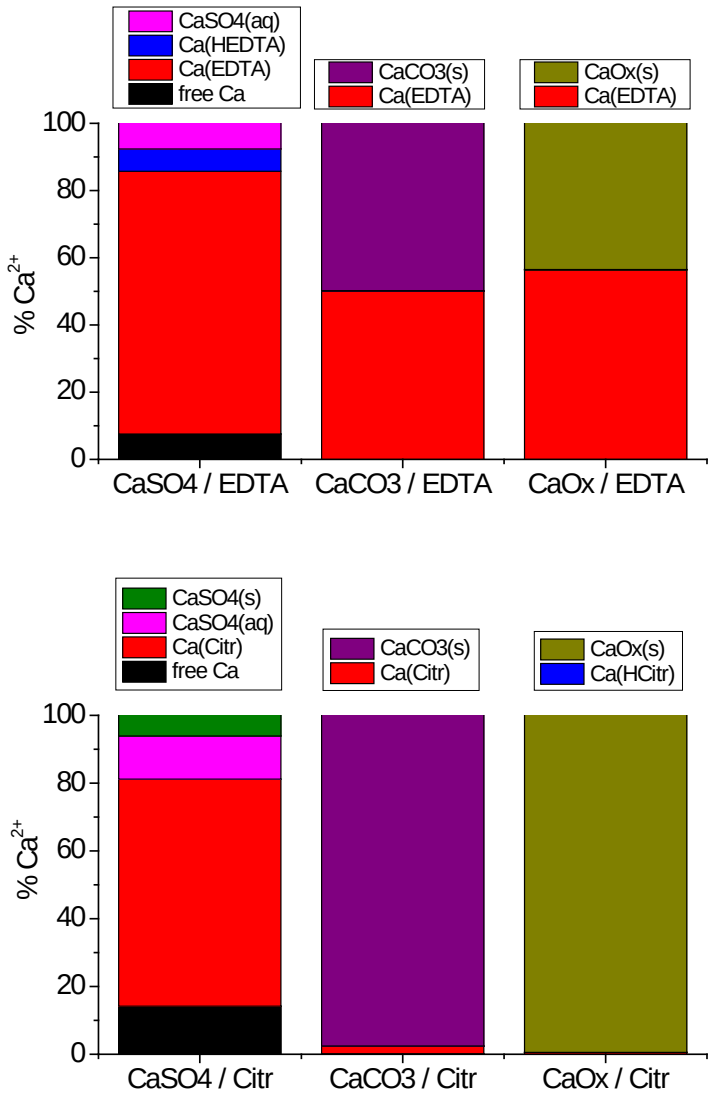

Figure S1. Distribution of Ca^{2+} (% total Ca^{2+}, charges omitted) for the systems containing the solid calcium salts treated with a 0.1 M solution of $Na_3HEDTA \cdot 2H_2O$ (above) or $Na_3Citr \cdot 2H_2O$ (below). Total concentrations used in the calculations have been obtained by considering the total amount of components in 50 mL of solution, and are as follows: $C_{Ca} = C_{sulfate} = 0.116$ M (calcium sulfate); $C_{Ca} = C_{carbonate} = 0.200$ M (calcium carbonate); $C_{Ca} = C_{oxalate} = 0.137$ M (calcium oxalate); $C_{EDTA} = 0.1$ M or $C_{Citr} = 0.1$ M, $C_{Na} = 0.3$ M. The calculations were carried out at pH values reported in Tables 4 and 5. The percentage of the species in these histograms refer to the total

moles of Ca^{2+} present in each system. Because this amount is different for the three salts (*i.e.* the moles of total calcium is different for the three salts) the histograms cannot be compared directly for different salts. However, they can be directly compared for the same salt with the two different chelators.

Table S1. Logarithms of protonation constants of $EDTA^{4-}$ and citrate ions, and logarithms of formation constants of their complexes with Na^+ and Ca^{2+}. Data taken from NIST Critically selected stability constants database v. 7.0 [14].

Species	log β	Species	log β
$HEDTA^{3-}$	8.86[a]	$HCitr^{2-}$	5.56[a]
H_2EDTA^{2-}	14.96[a]	H_2Citr^-	9.91[e]
H_3EDTA^-	17.65[b]	H_3Citr	12.81[e]
H_4EDTA	19.65[b]		
$[Ca(EDTA)]^{2-}$	10.47[c]	$[Ca(Citr)]^-$	2.71[a]
$[Ca(HEDTA)]^-$	13.57[d]	$[Ca(HCitr)]$	7.63[e]
$[Na(EDTA)]^{3-}$	1.77[c]	$[Na(Citr)]^{2-}$	0.75[d]

a) μ = 0.5 M; Na^+ as background
b) μ = 0.1 M
c) μ = 0.5 M; NR_4^+ as background
d) μ = 0.1 M; NR_4^+ as background
e) μ = 0.5 M

Table S2. Logarithms of protonation constants of sulfate, oxalate and carbonate ions, and logarithms of formation constants of their complexes with Na^+ and Ca^{2+}. Data taken from NIST Critically selected stability constants database v. 7.0 [14].

Species	log β
$[CaSO_4]_{(aq)}$	1.19[a]
$[NaSO_4]^-$	0.4[b]
HCO_3^-	9.61[c]
H_2CO_3	15.61[b]
$[CaCO_3]_{(aq)}$	2.21[d]
$[Ca(HCO_3)]^+$	11.82[d]
$[NaCO_3]^-$	0.63[e]
HOx^-	3.62[f]
$[CaOx]_{(aq)}$	3.19[g]
$[NaOx]^-$	0.5[h]

a) μ = 0.5 M; $NaClO_4$ as background
b) μ = 0.5 M
c) μ = 0.5 M; NaCl as background
d) μ = 0.7 M; NaCl as background
e) μ = 0.7 M
f) μ = 0.5 M; Na^+ as background
g) μ = 0.0 M

Table S3. Logarithms of solubility products (K_{sp}) of calcium salts with sulfate, oxalate and carbonate ions used in the calculations. Data taken from NIST Critically selected stability constants database v. 7.0 [14].

Species	log K_{sp}
$CaSO_{4(s)}$	-3.02[a]
$CaCO_{3(s,\ calcite)}$	-7.03[b]
$CaOx_{(s)}$	-7.86[c]

a) μ = 0.5 M; $NaClO_4$ as background
b) μ = 0.5 M; NaCl as background; calcite
c) μ = 0.1 M

Appendix II

Table I: Erasers

Cleaning product (year of purchase) Manufacturer Supplier	**Name of sample**	**Photo**	**Composition according to supplier /manufacturer**	**Composition* analysed by: (1) Py GC-MS, (2) FTIR-ATR**	**Additives: (1) Antioxidants, (2) Plasticizers, (3) Filler**	**Residues on paint surface (i.e. crumbs)**	**Cleaning results. Potential hazards: intact paint layer 0-10 abrasion intact paint layer 0-10 polishing**
Vulcanized gum (Smoke Sponge) (2013) - CTS	**G_SS_0001**		Vulcanized natural rubber	(1) NR (2) n.d	(1) BHT (2) n.d (3) Calcite	Few particles (0-10 per cm^2) Antioxidant to be expected	cleaning results 8 abrasion 1 polishing 4
Vulcanized gum (Smoke Sponge) (2013) - CTS	**G_SS_0003**		Vulcanized natural rubber	(1) NR (2) n.d	(1) BHT (2) n.d (3) Calcite	Not tested	Not tested
Wishab (white) (2013) Akapad Antares	**G_Wb_2**		Special filled vulcanized latex	(1) SEBS (2) SBR	(1) BHT, BKF (2) n.d (3) n.d	Many particles (>50 per cm^2) difficult to remove Antioxidants to be expected	cleaning results 8 abrasion 2 polishing 6
Akawipe (white powder) (2013) Akachemie Antares	**G_Awb**		Sulfur-free and chlorine-free cross-linked castor oil	(1) CSPE (2) CSPE+PVC ?	(1) n.d (2) n.d (3) n.d	Many particles (>50 per cm^2) difficult to remove	cleaning results 5 abrasion 1 polishing 2
Gum file dust (2013) Made in USA by Lineco CTS	**G_Lli_1**		Finely powdered gum eraser in a soft fabric cover	(1) CSPE (2) CSPE+Factice	(1) n.d (2) n.d (3) n.d	Many particles (>50 per cm^2) difficult to remove	cleaning results 5 abrasion 1 polishing 2

Gum file dust (2013) Made in USA by Alvin & Company, INC. CTS	**G_Lal_2**		Finely powdered gum eraser in a soft fabric cover	(1) CSPE (2) CSPE+Factice	(1) n.d (2) n.d (3) TiO_2-Rutile	Many particles (>50 per cm^2) difficult to remove	cleaning results 5 abrasion 1 polishing 2
PVC free gum 2 (2013) Made in Malaysia Faber Castell	**G_FC_1**		No information	(1) SEBS (2) SBR	(1) n.d (2) n.d (3) Calcite	Several particles (10-50 per cm^2)	cleaning results 10 abrasion 6 polishing 8
PVC free sleeve mini eraser (2013) Made in Malaysia Faber Castell	**G_FC_2**		No information	(1) SEBS (2) SBR	(1) n.d (2) n.d (3) Calcite	Not tested	Not treated
PVC free gum (2013) Made in Malaysia Faber Castell	**G_FC_3**		No information	(1) SEBS (2) SBR	(1) n.d (2) n.d (3) Calcite	Several particles (10-50 per cm^2)	cleaning results 10 abrasion 6 polishing 8
Factis OV12 (2013) Made in Spain -	**G_FOV12**		No information	(1) Factice (2) Vegetables oils	(1) n.d (2) n.d (3) Calcite	Several particles (0-10 per cm^2)	cleaning results 10 abrasion 6 polishing 8
Factis extra soft ES20 (2013) Made in Spain -	**G_FES20**		No information	(1) Factice (2) Vegetables oils	(1) n.d (2) n.d (3) Calcite	Several particles (0-10 per cm^2)	cleaning results 10 abrasion 6 polishing 8
Epure (2013) - Maped	**G_Ep**		White vinyl eraser	(1) Factice (2) Vegetables oils	(1) n.d (2) n.d (3) TiO_2-Rutile, Calcite	Several particles (0-10 per cm^2)	cleaning results 10 abrasion 6 polishing 7

Dick Blick Gum Erasers (2013) - -	**G_DB**		Vulcanized oils	(1) CSPE (2) CSPE+Factice	(1) n.d (2) n.d (3) n.d	Several particles (0-10 per cm^2) difficult to remove	cleaning results 8 abrasion 4 polishing 3
Design Artgum eraser (2013) - Prismacolor	**G_Art**		Vulcanized oils	(1) CSPE (2) CSPE+Factice	(1) n.d (2) n.d (3) n.d	Sveral particles (0-10 per cm^2) difficult to remove	cleaning results 8 abrasion 4 polishing 3
Magic Rub (2013) Made in USA Prismacolor	**G_Mrub**		No information	(1) PVC (2) PVC+Phthalates	(1) n.d (2) Phthalates (3) n.d	Several particles (10-50 per cm^2) Plasticizer to be expected	cleaning results 10 abrasion 8 polishing 9
Milan 403 Gigante (2014) Made in Spain -	**Mi_403**		Synthetic natural rubber	(1) CSPE (2) CSPE	(1) n.d (2) n.d (3) n.d	Several particles (0-10 per cm^2)	cleaning results 8 abrasion 3 polishing 6

Table II: Sponges

Cleaning product (year of purchase) Manufacturer Supplier	**Name of sample**	**Photo**	**Composition according to supplier /manufacturer**	**Composition analysed by: (1) Py GC-MS, (2) FTIR-ATR**	**Additives: (1) Antioxidants, (2) Plasticizers, (3) Filler**	**Residues on paint surface (i.e. crumbs)**	**Cleaning results. Potential hazards: intact paint layer 0-10 abrasion intact paint layer 0-10 polishing**
Oval Make-up sponge (2013) Made in China Pro Professional style & care (C.G.A. Caldara s.r.l)	**S_PP_ov**		Latex	(1) SBR/NR (2) SBR/NR	(1) BKF (2) DIOIP (3) n.d	Few particles (0-10 per cm^2) Antioxidant and plasticizer to be expected	cleaning results 7 abrasion 1 polishing 1
Triangle Make-up sponge (2013) Made in China Pro Professional style & care (C.G.A. Caldara s.r.l)	**S_PP_tr**		Latex	(1) SBR/NR (2) SBR/NR	(1) BHT (2) n.d (3) n.d	Few particles (0-10 per cm^2) Antioxidant to be expected	cleaning results 7 abrasion 1 polishing 1
Round Make-up sponge pcs.2 (2013) Made in China Pro Professional style & care (C.G.A. Caldara s.r.l)	**S_PP_ro**		Latex	(1) SBR/NR (2) SBR/NR	(1) n.d (2) n.d (3) n.d	Few particles (0-10 per cm^2)	cleaning results 7 abrasion 1 polishing 1
Triangle Make-up sponge (2013) Made in China Royal Beauty (Golden Group s.r.l.)	**S_RB_tr**		No information	(1) SBR/NR (2) SBR/NR	(1) BHT (2) DIOIP (3) TiO_2-Anatase	Few particles (0-10 per cm^2) Antioxidant and plasticizer to be expected	cleaning results 7 abrasion 1 polishing 1

Egg make-up sponge (2013) Made in China Royal Beauty (Golden Group s.r.l.)	**S_RB_uo**		No information	(1) SBR/NR (2) SBR/NR	(1) BHT (2) n.d (3) n.d	Few particles (0-10 per cm^2) Antioxidant to be expected	cleaning results 7 abrasion 1 polishing 1
Pink make-up sponge (2013) Made in China Royal Beauty (Golden Group s.r.l.)	**S_RB_py**		No information	(1) SBR/NR (2) SBR/NR	(1) BHT (2) n.d (3) n.d	Few particles (0-10 per cm^2) Antioxidant to be expected	cleaning results 7 abrasion 1 polishing 1
Round make-up sponge (2013) Made in China Royal Beauty (Golden Group s.r.l.)	**S_RB_ro**		No information	(1) SBR/NR (2) SBR/NR	(1) BHT (2) n.d (3) n.d	Few particles (0-10 per cm^2) Antioxidant to be expected	cleaning results 7 abrasion 1 polishing 1
Triangle make-up sponge (2013) Made in UK Kiko make-up	**S_KK_tr**		No information	(1) PU (2) PU	(1) n.d (2) n.d (3) n.d	Few particles (0-10 per cm^2)	cleaning results 7 abrasion 1 polishing 1
Round make-up sponge (2013) Made in Japan Kiko make up	**S_KK_ro**		No information	(1) SBR/NR (2) SBR/NR	(1) n.d (2) DEHA (3) TiO_2-Anatase	Few particles (0-10 per cm^2) Plasticizer to be expected	cleaning results 7 abrasion 1 polishing 1
Egg make-up sponge (2013) Made in China H&M	**S_HM_uo**		No information	(1) SBR (2) SBR	(1) n.d (2) n.d (3) TiO_2-Rutile	Few particles (0-10 per cm^2)	cleaning results 7 abrasion 1 polishing 1
Triangle make-up sponge (2013) Made in China H&M	**S_HM_tr**		No information	(1) SBR/NR (2) SBR/NR	(1) BHT (2) n.d (3) TiO_2-Anatase	Few particles (0-10 per cm^2) Antioxidant to be expected	cleaning results 7 abrasion 1 polishing 1

Wedges make-up sponge (2013) Made in Korea Sephora	**S_Sph_sp**	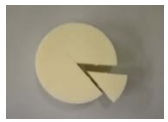	No information	(1) SBR/NR (2) SBR/NR	(1) BHT (2) n.d (3) TiO_2-Rutile	Few particles (0-10 per cm^2) Antioxidant to be expected	cleaning results 7 abrasion 1 polishing 1
Egg make-up sponge (2013) Made in Korea Sephora	**S_Sph_uo**		No information	(1) NBR (2) NBR	(1) BHT, BKF, SWP (2) DIOIP (3) n.d	Few particles (0-10 per cm^2) Antioxidants and plasticizer to be expected	cleaning results 7 abrasion 1 polishing 1
Half-moon make-up sponge (2013) Made in Malaysia Sephora	**S_Sph_ml**		No information	(1) NBR (2) NBR	(1) BHT, BKF, SWP (2) DIOIP (3) n.d	Few particles (0-10 per cm^2) Antioxidants and plasticizer to be expected	cleaning results 7 abrasion 1 polishing 1
Round make-up sponge (2013) Made in Malaysia Sephora	**S_Sph_ro**		No information	(1) NBR (2) NBR	(1) BHT, BKF, SWP (2) DIOIP (3) n.d	Few particles (0-10 per cm^2) Antioxidants and plasticizer to be expected	cleaning results 7 abrasion 1 polishing 1
ART SPONGE							
Sofft art knives e covers (2014) Made in China Colorfin LLC	**AS_kc_1**		No information	(1) ABS (2) SBR/NBR	(1) BHT (2) n.d (3) n.d	Few particles (0-10 per cm^2) Antioxidant to be expected	cleaning results 5 abrasion 3 polishing 2
Sofft art sponge - sponge bars (2014) Made in China Colorfin LLC	**AS_sft_2**		No information	(1) SBR/NR (2) SBR/NR	(1) BHT (2) n.d (3) n.d	Few particles (0-10 per cm^2) Antioxidant to be expected	cleaning results 6 abrasion 2 polishing 1
Sofft art sponge slice (2014) Made in China Colorfin LLC	**AS_sft_3**		No information	(1) ABS (2) SBR/NBR	(1) BHT (2) n.d (3) n.d	Few particles (0-10 per cm^2) Antioxidant to be expected	cleaning results 6 abrasion 2 polishing 1

Sofft art applicators mini (2014) Made in China Colorfin LLC	**AS_sft_4**		No information	(1) NR (2) n.d	(1) BHT (2) n.d (3) n.d	Few particles (0-10 per cm^2) Antioxidant to be expected	cleaning results 5 abrasion 3 polishing 1
Sofft art sponge - big oval (2014) Made in China Colorfin LLC	**AS_sft_5**		No information	(1) ABS (2) SBR/NBR	(1) BHT (2) n.d (3) n.d	Few particles (0-10 per cm^2) Antioxidant to be expected	cleaning results 6 abrasion 2 polishing 1
Sofft art applicators heads (2014) Made in China Colorfin LLC	**AS_sft_6**		No information	(1) NR (2) n.d	(1) BHT (2) n.d (3) n.d	Few particles (0-10 per cm^2) Antioxidant to be expected	cleaning results 5 abrasion 3 polishing 2
Suction block (2013) Made in Germany Saugwunder	**S_SB**		Polyvinyl acetate (PVA)	(1) PVA (2) PVA	(1) n.d (2) DIBP, DBP (3) n.d	Not tested	Not tested

Table III: Cloths

Cleaning product (year of purchase) Manufacturer Supplier	**Name of sample**	**Photo**	**Composition according to supplier /manufacturer**	**Composition analysed by: (1) Py GC-MS, (2) FTIR-ATR**	**Additives: (1) Antioxidants, (2) Plasticizers, (3) Filler**	**Residues on paint surface (i.e. crumbs)**	**Cleaning results. Potential hazards: intact paint layer 0-10 abrasion intact paint layer 0-10 polishing**
Yellow "effect deer" microfibre cloth (2013) Made in Corea Mapa Spontex	**P_Sp_1**		Nylon Poliuretano	(1) PU/PA (2) PU/PA	(1) n.d (2) DDM (3) TiO_2-Anatase	No particles Additive to be expected	cleaning results 5 abrasion 0 polishing 8
Light blue microfibre cloth plus (2013) Made in France Freudenberg Vileda	**P_Vi_2**		70% Poliestere 30%Poliammide 0,01% Argento	(1) PEs/PA (2) PEs/PA	(1) n.d (2) Benzoflex 998 (3) n.d	No particles Plasticizer to be expected	cleaning results 4 abrasion 0 polishing 8
Green Ultrafibra cloth (2013) Dianex	**P_Di_3**		50%Poliammide 50% Poliestere	(1) PEs/PA (2) PEs/PA	(1) n.d (2) Benzoflex 998 (3) n.d	No particles Plasticizer to be expected	cleaning results 5 abrasion 0 polishing 8

* NR: natural rubber, SEBS: styrene-ethylene-butadiene-styrene rubber, SBR: styrene-butadiene rubber, CSPE: chlorosulphonated polyethylene, PVC: polyvinyl chloride, Factice: vulcanized oils, PU: polyurethane rubber, NBR: acrylonitrile-butadiene rubber, ABS: acrylonitrile-butadiene-styrene rubber, PVA: polyvinyl acetate, PA: polyamide, PEs: polyester.